

UNCLASSIFIED

AD NUMBER
AD911303
NEW LIMITATION CHANGE
TO Approved for public release, distribution unlimited
FROM Distribution authorized to U.S. Gov't. agencies only; Test and Evaluation; JUN 1973. Other requests shall be referred to Commanding General, U.S. Army Electronics Command, Attn: AMSEL-VL-N-S, Fort Monmouth, NJ 07703.
AUTHORITY
USAEC ltr, 5 Oct 1973

THIS PAGE IS UNCLASSIFIED

AD

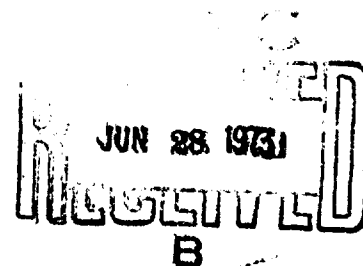


Research and Development Technical Report
ECOM-0230-F

**AUTOMATIC POLHODE DAMPING
INVESTIGATION
FOR
MICRO ELECTROSTATIC GYRO
FINAL REPORT**

By
John C. Wauer

June 1973



DISTRIBUTION STATEMENT

Distribution limited to U.S. Government agencies only.
Test and evaluation, June 1973. Other requests for this
document must be referred to Commanding General
U.S. Army Electronics Command, Attn: AMSEL-VL-
N-S, Ft. Monmouth, N.J. 07703.

ECOM

UNITED STATES ARMY ELECTRONICS COMMAND • FORT MONMOUTH, N.J.

Contract DAAB07-72-C-0230
Rockwell International
Autonetics Division
3370 Miraloma Avenue, Anaheim, Calif 92803

AD 911 303

ECOM-0230-F
June 1973

AUTOMATIC POLHODE DAMPING INVESTIGATION FOR MICRO ELECTROSTATIC GYRO

Final Technical Report For Period
1 July 1972 - 23 May 1973

Contract No. DAAB07-72-C-0230

DISTRIBUTION STATEMENT

Distribution limited to U.S. Government agencies only.
Test and evaluation, June 1973. Other requests for this
document must be referred to Commanding General
U.S. Army Electronics Command, Attn: AMSEL-VL,
NS, Ft. Monmouth, N.J. 07703.

Prepared By

John C. Wauer

Rockwell International

Autonetics Division

3370 Miraloma Avenue, Anaheim, Calif 92803

For

UNITED STATES ARMY ELECTRONICS COMMAND

Fort Monmouth, New Jersey

NOTICE

The findings in this report are not to be construed as an official Department of the Army position, unless so designated by other authorized documents.

Mention of any trade names or manufacturers in this report shall not be construed as advertising nor as an official indorsement of approval of such products or companies by the United States Government.

PATENT APPLICATION

A patent application has been filed in the U.S. Patent Office based upon subject matter included herein or related hereto, and the Secrecy Order appended hereto has been issued thereon pursuant to the Invention Secrecy Act of 1951 (Public Law 256, 66 Stat. 3). Further dissemination of said subject matter is prohibited except in strict compliance with said order.

DEPARTMENT OF COMMERCE
United States Patent Office
Washington

Serial No. Filed: Division
For:
Applicant:
Assignee:

DEPARTMENT OF COMMERCE
United States Patent Office
Washington

Serial No. Filed: Division:

SECRECY ORDER

NOTICE: — To the applicant above named, his heirs, and any and all his assignees, attorneys and agents, herein-after designated principals:

You are hereby notified that your application as above identified has been found to contain subject matter, the unauthorized disclosure of which might be detrimental to the public safety or defense, and you are ordered in nowise to publish or disclose the invention or any material information with respect thereto, including hitherto unpublished details of the subject matter of said application, in any way to any person not cognizant of the invention prior to the date of the order, including any employee of the principals, but to keep the same secret except by written permission first obtained of the Commissioner of Patents, under the penalties of Public Law 256, approved February 1, 1952, 66 Stat. 3.

Any other application which contains any significant part of the subject matter of the above identified application falls within the scope of this order. If such other application does not stand under a secrecy order, it and the common subject matter should be brought to the attention of the Patent Office, Division 70.

If prior to the issuance of the secrecy order any significant part of the subject matter has been revealed to any person, the principals shall promptly inform such person of the secrecy order and the penalties for improper disclosure set out in Public Law 256, 66 Stat. 3.

This order should not be construed in any way to mean that the Government has adopted or contemplates adoption of the alleged invention disclosed in this application; nor is it any indication of the value of such invention.

PERMIT A

An order of secrecy having been issued in the above-entitled application by the Commissioner of Patents, the principals as designated in said order are authorized to disclose the subject matter to any person of the classes hereinafter specified if such person is known to the principal disclosing to be connected directly in an official capacity with the subject matter, provided that all reasonable safeguards are taken to otherwise protect the invention from unauthorized disclosure. The specified classes are:

- (a) Any officer or employee of any department, independent agency, or bureau of the Government of the United States.
- (b) Any person designated specifically by the head of any department, independent agency or bureau of the Government of the United States, or by his duly authorized subordinate, as a proper individual to receive the disclosure of the above indicated application for use in the prosecution of the war.

The principals under the secrecy order are further authorized to disclose the subject matter of this application to the minimum necessary number of persons of known loyalty and discretion, employed by or working with the principals or their licensees and whose duties involve cooperation in the development, manufacture or use of the subject matter by or for the Government of the United States, provided such persons are advised of the issuance of the secrecy order.

The provisions of this permit do not in any way lessen responsibility for the security of the subject matter as imposed by any Government contract or the provisions of the existing laws relating to espionage and national security.

Assistant Commissioner

DISPOSITION INSTRUCTIONS

Destroy this report when it is no longer needed.
Do not return it to the originator.

ABSTRACT

A computer program for automatically damping the polhode motion of the Micro-Electrostatically Suspended Gyro (MESG) is presented. Test results are presented that demonstrate successful automatic polhode damping on two gyros. The fundamental characteristics of polhode motion of the MESG rotor are summarized. The techniques for monitoring polhode motion using Mass Unbalance Modulation (MUM) are described. The polhode torquing equation is derived and the spin motor control electronics that implement the torquing equation are described.

CONTENTS

	<u>Page</u>
Section I. Introduction	1
Section II. Definition of Problem	2
Section III. Torquing Equation	16
Section IV. Control Laws	18
Section V. Automatic Damping	22
Section VI. Automatic Damping Simulation	31
Section VII. Spin Motor Control Electronics	38
Section VIII. Test Results	46
Section IX. Conclusions	70
References	139

APPENDIX

	<u>Page</u>
A. MUM Signal with Electrostatic Suspension Forcing at Rotor Frequency . . .	72
B. Fourier Analysis Phase Tracking	75
C. Automatic Damping Mechanization	87
D. Automatic Damping Subroutine Listings	119

ILLUSTRATIONS

Figure		Page
1.	Polhode Patterns	3
2.	Polhode Frequency vs Polhode Latitude for $\theta_s = 45$ Deg and $T_A = 2.83$ Sec	6
3.	Conformal Mapping of the Surface of the Sphere Onto the Infinite Plane ($\theta_s = 45$ Deg)	7
4.	Polhode Trajectories at 10-Deg Intervals in $-A$, $+C$, and $+A$ Families and 40-Deg Trajectory in $-C$ Family ($\theta_s = 45$ Deg)	8
5.	MUM Vector Directions in $+A$ and $+C$ Families ($\theta_s = 45$ Deg, $T_A = 2.83$ Sec)	9
6.	Five Representative Polhode Trajectories and Locus of Unity MUM Magnitude ($\theta_s = 45$ Deg)	10
7.	MUM Magnitude Time Histories Over One Polhode Period for Five Polhode Trajectories of Figure 6 ($\theta_s = 45$ Deg, $T_A = 2.83$ Sec)	11
8.	MAX and MIN MUM Magnitude (45 Deg Separating Polhode, 0.03, 0.07 Pendulosity on A and B Axes Respectively)	12
9.	Difference Between High and Low Maxima, Δ Max (45 Deg Separating Polhode, 0.03, 0.07 Pendulosity on A and B Axes Respectively).	13
10.	Peak to Peak MUM Magnitude (45 Deg Separating Polhode, 0.03, 0.07 Pendulosity on A and B Axes Respectively)	14
11.	Angle Between MUM Vector and Trajectory Normal at Min and Max Points in $+C$ and $+A$ Families (45 Deg Separating Polhode, 0.03, 0.07 Pendulosity on A and B Axes Respectively)	15
12.	$+C$ Transition Control Law Torque Vectors ($\theta_s = 45$ deg, $T_A = 2.83$ sec)	19
13.	MUM Vectors in the Neighborhood of the $+C$ Axis	20
14.	Normal Control Law Torque Efficiency vs Polhode Phase for Several Polhode Latitudes (45 Deg separating Polhode).	22
15.	Average Torque Efficiency vs Polhode Latitude	22
16.	System Block Diagram	24
17.	Automatic Polhode Damping Block Diagram	26
18.	MUM Magnitude Time Histories Over One Polhode Period ($\theta_s = 45$ deg, $T_A = 2.83$ sec)	28
19.	Automatic Polhode Damping Starting 1 Deg Away From $+C$ Axis (45 Deg separating polhode, 1 percent pendulosity on A and B, 2.83 sec ANhd polhode period, 0.123 rad/sec max torque).	32
20.	Initial Trajectory of Automatic Polhode Damping Starting 1 Deg Away From $+C$ Axis	32
21.	Final Trajectory of Automatic Polhode Damping Starting 1 Deg Away From $+C$ Axis	33
22.	Automatic Polhode Damping Starting 3 Deg Away From $-A$ Axis (45 deg separating polhode, 1 percent pendulosity on A and B, 2.83 sec ANhd polhode period, 0.123 rad/sec max torque).	33
23.	Initial Trajectory of Automatic Polhode Damping Starting 3 Deg Away From $-A$ Axis	35

ILLUSTRATIONS (Cont)

Figure		Page
24.	Final Trajectory of Automatic Polhode Damping Starting 3 Deg Away From -A Axis	35
25.	Functional Block Diagram of Spin Motor Control Electronics.	39
26.	Spin Motor Controller Module Block Diagram	40
27.	Spin Motor Timing Module Block Diagram	42
28.	Spin Motor Power Amplifier Functional Block Diagram.	44
29.	Simplified Spin Motor Control Electronics	45
30.	Polhode Motion Residual of Run 2, Gyro 59 (Filter Time Constant = 0.8 sec, PPF = 0.0002)	47
31.	Polhode Motion Residual of Run 2, Gyro 59 (Filter Time Constant = 0.05 sec, PPF = 0.0002)	48
32.	Small Angle Recorder MUM Magnitude Plot with Torque Pulses Applied at the Arrows.	49
33.	Small Angle Recorder Plot of Run 1, Gyro 54	56
34.	Small Angle Recorder Plot of Run 2, Gyro 59	57
35.	Small Angle Recorder Plot of Run 3, Gyro 59	58
36.	Small Angle Recorder Plot of Run 4, Gyro 59	59
37.	Small Angle Recorder Plot of Run 5, Gyro 68	60
38.	Small Angle Recorder Plot of Run 6, Gyro 68	61
39.	Small Angle Recorder Plot of Run 7, Gyro 68	62
40.	Small Angle Recorder Plot of Run 8, Gyro 68	63
41.	Small Angle Recorder Plot of Run 9, Gyro 68	64
42.	Small Angle Recorder Plot of Run 10, Gyro 68	65
43.	Polhode Motion Residual of Run 3, Gyro 59.	66
44.	Polhode Motion Residual of Run 8, Gyro 68.	67
45.	Polhode Motion Residual of Run 9, Gyro 68.	68
46.	Polhode Motion Residual of Run 10, Gyro 68.	69
A-1.	Rotor Geometry.	73
A-2.	Suspension Forcing vs Rotor Frequency	76
B-1.	Average MUM Magnitude for Pendulosity on -A Axis of 1 Percent ($\theta_s = 45$ deg)	78
B-2.	First Harmonic Cosine of MUM Magnitude for Pendulosity on -A Axis of 1 Percent ($\theta_s = 45$ deg)	78
B-3.	Minus Second Harmonic Cosine of MUM Magnitude for Pendulosity on -A Axis of 1 Percent ($\theta_s = 45$ deg)	79
B-4.	Average MUM Magnitude for Pendulosity on -A, -B Axes of 1 and 10 Percent, Respectively ($\theta_s = 45$ deg)	79
B-5.	First Harmonic Cosine of MUM Magnitude for Pendulosity on -A, -B Axes of 1 and 10 Percent, Respectively ($\theta_s = 45$ deg)	80
B-6.	Minus First Harmonic Sine of MUM Magnitude for Pendulosity on -A, -B Axes of 1 and 10 Percent ($\theta_s = 45$ deg)	80
B-7.	Minus Second Harmonic Cosine of MUM Magnitude for Pendulosity on -A, -B Axes of 1 and 10 Percent, Respectively ($\theta_s = 45$ deg)	81
B-8.	Minus Second Harmonic Sine of MUM Magnitude for Pendulosity on -A, -B of 1 and 10 Percent, Respectively ($\theta_s = 45$ deg).	81

ILLUSTRATIONS (Cont)

Figure		Page
B-9.	Phase Locked Loop Block Diagram	82
B-10.	Torque Efficiency	84
B-11.	Polhode Frequency (f_{NEW}) vs Previous Polhode Frequency (f_{OLD}) for Torquing Rate of 0.01 Rad/Sec ($\theta_S = 45$ deg, $T_A = 2.83$ sec)	85
B-12.	Change in Polhode Frequency vs Previous Polhode Frequency (f_{OLD}) for Torquing Rate of 0.01 Rad/Sec ($\theta_S = 45$ deg, $T_A = 2.83$ sec)	85
B-13.	Phase Error Without Frequency Prediction for Torquing Rate of 0.01 Rad/Sec ($\theta_S = 45$ deg, $T_A = 2.83$ sec)	86
B-14.	Frequency Prediction Phase Error Sensitivity to Normalized A Axis Polhode Period ($\Delta T_A/T_A$). ($\theta_S = 45$ deg, $T_A = 2.83$ sec, Torque = 0.01 rad/sec)	87
B-15.	Frequency Prediction Phase Error Sensitivity to Separating Polhode Latitude ($\theta_S = 45$ deg, $T_A = 2.83$ sec, Torque = 0.01 rad/sec)	88
B-16.	Frequency Prediction Phase Error Sensitivity to Normalized Torque Magnitude ($\Delta \text{Torque}/\text{Torque}$). ($\theta_S = 45$ deg, $T_A = 2.83$ sec, Torque = 0.01 rad/sec)	88
C-1.	Angle Between MUM Vector and Trajectory Normal at Min, Max and 90° Max Points in +C and +A Families	96
C-2.	Extrapolation Frequency vs Polhode Frequency	97
C-3.	Phase Tracking Flow Diagram	98
C-4.	Identification 1 Flow Diagram	104
C-5.	NMIN Switching Logic	106
C-6.	Identification 2 Flow Diagram	107
C-7.	Peak-to-Peak MUM Magnitude in ANbhd (45 deg separating polhode, 1 percent pendulosity on A and B)	111
C-8.	Geometry of Peak-to-Peak MUM Amplitude in ANbhd	111
C-9.	Terminal Control Input-Output Relationship	116

TABLES

<u>Table</u>	<u>Page</u>
1. Sign Convention	27
2. Table of Events During Automatic Polhode Damping Starting 1 Deg Away From C Axis	34
3. Table of Events During Automatic Polhode Damping Starting 3 Deg	36
4. Polhode Parameters - Gyro 59, V Series Rotor	50
5. Automatic Damping Parameters Gyro 59 - V Series Rotor	51
6. Test Summary	53

SECTION I

INTRODUCTION

Polhode damping is a necessary function in the operation of a Micro-Electrostatically Suspended Gyro (MESG) since it is the technique to force the spherical rotor to spin about its axis of maximum inertia. Furthermore, it must always spin in the same direction about the axis of maximum inertia. The primary design goals of automatic polhode damping are reliability, low cost, and minimum time. The polhode damping logic is performed in the digital computer used for navigation. Therefore, low cost is directly related to low computer requirements. It is particularly important to minimize computer memory requirements. The minimum time requirement is related to fast reaction applications of the MICRON system. The rotor must be suspended, spun up, thermally stabilized, and polhode damped before the alignment and navigation functions can begin.

Polhode damping has been successfully accomplished as is reported in Section VIII. A detailed description of the automatic damping program is given in Appendices C and D. Two important features of the mechanization are its resilience and that no calibration of individual gyros is required. The program has demonstrated its ability to recover from major errors similar to out of specification hardware operation and successfully damp. Two gyros were automatically damped. The automatic damping parameters were entirely based on one of the gyros. The other gyro has never been calibrated.

SECTION II

DEFINITION OF THE PROBLEM

Polhode motion occurs in any freely rotating rigid body with unequal moments of inertia. A polhode is the path which is traced out by the spin axis on the body when viewed in body-fixed coordinates. The motion of the spin axis with respect to inertial space is the herpolhode.

The component of the spin vector along the angular momentum vector of the body is a constant irrespective of polhode motion if no external torques are applied to the body. For a nearly symmetric body, such as the MESG rotor, the herpolhode is very small so that the spin vector is essentially inertially fixed. The polhode motion is not small and the spin vector may move drastically with respect to the MESG rotor principal axes.

For a constant energy system there are two stable axes of rotation for which there is no polhode motion as shown in Figure 1. These are the principal axes with the largest and smallest moments of inertia. Any practical system dissipates energy due to non-perfect body rigidity or external influences. For this reason, only rotation about the axis with the largest moment of inertia is both stable and without polhode motion.

The equations describing polhode motion are derived in Ref 1. The results will be briefly summarized here.

If the three principal moments of inertia of the rotor are A, B, C where

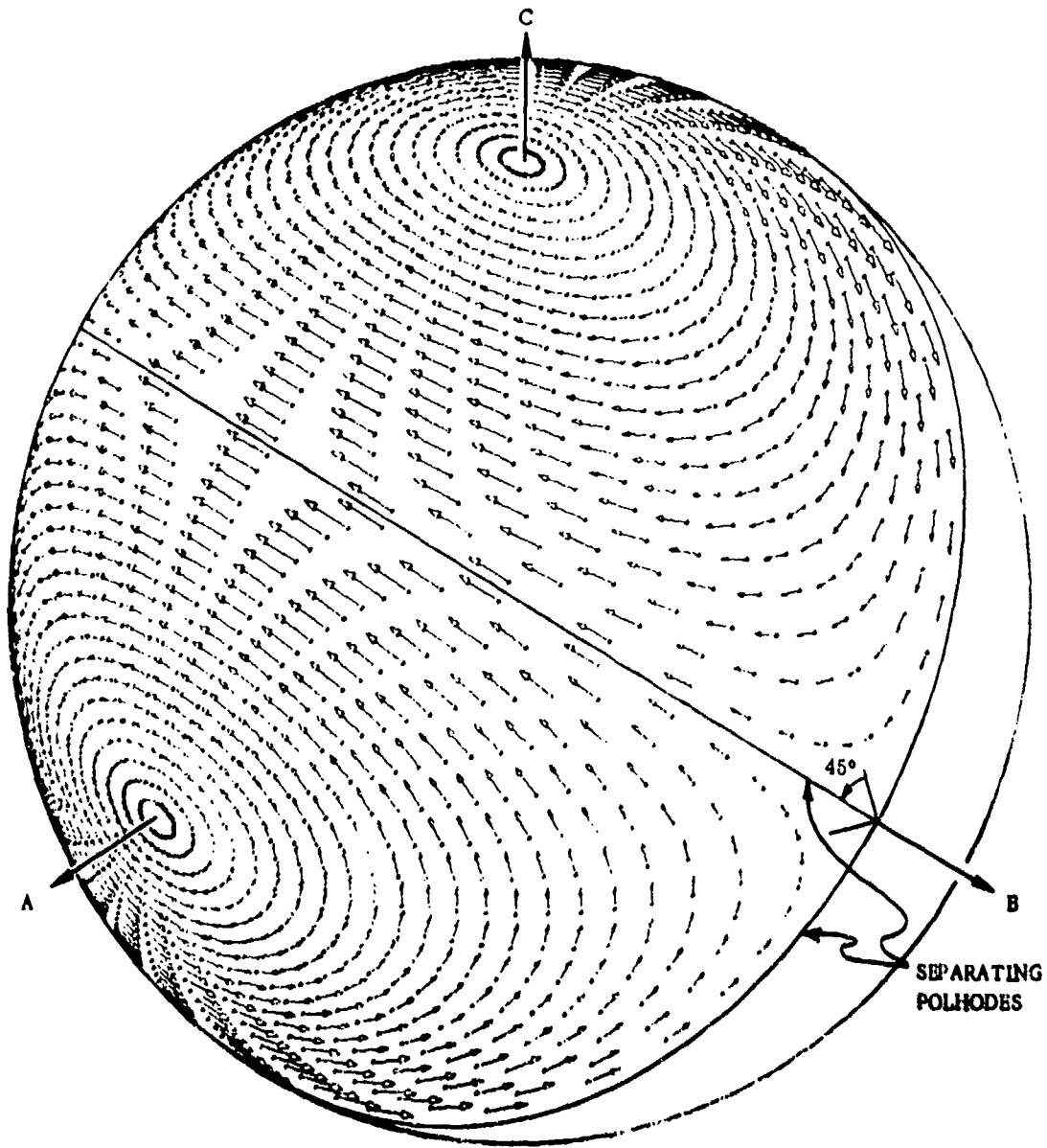
$$A > B > C \quad (1)$$

then

$$\begin{aligned} \dot{\omega}_A &= \left(\frac{B-C}{A}\right) \omega_B \omega_C + Q_A/A \\ \dot{\omega}_B &= -\left(\frac{A-C}{B}\right) \omega_C \omega_A + Q_B/B \\ \dot{\omega}_C &= \left(\frac{A-B}{C}\right) \omega_A \omega_B + Q_C/C \end{aligned} \quad (2)$$

where $(\omega_A, \omega_B, \omega_C)$ is the spin vector in body coordinates, the spin vector length is the angular rate of the rotor in rad/sec and (Q_A, Q_B, Q_C) is the applied torque vector.

The solution to Eq (2) cannot be expressed as an explicit function of time in closed form since it involves elliptic integrals. Solutions not explicitly containing time are derived in Ref 1. For the case of no torque driving functions the solutions are closed trajectories. The trajectories either enclose the A axes or the C axes depending on the initial conditions. Therefore, the trajectories are classed as A family trajectories or C family trajectories, respectively.



- A ■ AXIS OF LARGEST MOMENT OF INERTIA
- B ■ AXIS OF INTERMEDIATE MOMENT OF INERTIA
- C ■ AXIS OF SMALLEST MOMENT OF INERTIA

Figure 1. Polhode Patterns

The trajectory that divides the A and C families is called the separating polhode. It is defined by the equation

$$\left(\frac{A-B}{C}\right) \omega_A^2 = \left(\frac{B-C}{A}\right) \omega_C^2 \quad (3)$$

A spherical coordinate system will be used to uniquely define each polhode trajectory. The +A axis will be used as the north pole. Latitude is measured from the C-B plane toward the A axis and longitude is measured in the C-B plane with the +C axis at zero longitude. Each polhode trajectory is uniquely defined by its latitude at either 0 or 180-deg longitude and so this number will be used to identify the polhodes.

The latitude number for the separating polhodes is

$$\begin{aligned} \theta_S &= \tan^{-1} \left(\frac{\omega_A}{\omega_C} \right) \\ &= \tan^{-1} \left[\left(\frac{B-C}{A} \right) / \left(\frac{A-B}{C} \right) \right]^{1/2} \end{aligned} \quad (4)$$

The latitude ranges for each of the four polhode families are:

Family	Latitude	Longitude
+A	($+\theta_S$, 90 deg)	0 deg
-A	($-\theta_S$, -90 deg)	0 deg
+C	(0 deg, $+\theta_S$)	0 deg
-C	(0 deg, $+\theta_S$)	180 deg

Polhode motion is periodic since the trajectories are closed. The period is a function of polhode latitude and the A or C family. For the A family the period is

$$T = \left[\left(\frac{A-C}{B} \right) \left(\frac{A-B}{C} \right) \right]^{-1/2} \frac{1}{\omega_0 \sin \theta} \int_0^{2\pi} \frac{d\sigma}{\left[1 - \left(\frac{\tan \theta_S}{\tan \theta} \right)^2 \sin^2 \sigma \right]^{1/2}} \quad (5)$$

where θ is polhode latitude and ω_0 angular rate of the rotor at the 0 or 180-deg longitude point in the trajectory. The period for the limiting case in which the polhode latitude approaches 90 deg is

$$T_A = \left[\left(\frac{A-C}{B} \right) \left(\frac{A-B}{C} \right) \right]^{-1/2} \frac{2\pi}{\omega_0} \quad (6)$$

Therefore, the frequency of polhode motion in the A family can be written in terms of two rotor parameters, T_A and θ_S , as

$$F = 2\pi \frac{\sin \theta}{T_A} \bigg/ \int_0^{2\pi} \frac{d\sigma}{\left[1 - \left(\frac{\tan \theta_S}{\tan \theta} \sin \sigma\right)^2\right]^{1/2}} \quad (7)$$

The frequency of polhode motion in the C family is

$$F = 2\pi \frac{\cos \theta \tan \theta_S}{T_A} \bigg/ \int_0^{2\pi} \frac{d\sigma}{\left[1 - \left(\frac{\tan \theta}{\tan \theta_S} \sin \sigma\right)^2\right]^{1/2}} \quad (8)$$

The period for the limiting case in which the polhode latitude approaches zero is

$$T_C = T_A \tan \theta_S \quad (9)$$

Polhode frequency as a function of polhode latitude is plotted in Figure 2 for $\theta_S = 45$ deg and $T_A = 2.83$ sec. The slope of the frequency curve is infinite at 45-deg latitude and the frequency is zero at that latitude.

Rotors currently in use in the MESG have values of $\left(\frac{A-B}{C}\right)$ and $\left(\frac{B-C}{A}\right)$ in the range of $(10^{-4}, 0.5 \times 10^{-4})$ with θ_S very close to 45 deg and T_A in the range 3-6 sec. Rotor speed, ω_0 , is 2500 Hz. The third degree of freedom in the differential Eq (2) which is $\frac{A-C}{B}$ can be approximated by

$$\left(\frac{A-C}{B}\right) \approx \left(\frac{A-B}{C}\right) + \left(\frac{B-C}{A}\right) \quad (10)$$

Solving the right-hand side of Eq (10) for $\frac{A-C}{B}$ using a second order approximation gives

$$\left(\frac{A-C}{B}\right) = \left[\left(\frac{A-B}{C}\right) + \left(\frac{B-C}{A}\right)\right] \left[1 - \left(\frac{A-B}{C}\right) \left(\frac{B-C}{A}\right)\right] \quad (11)$$

and therefore Eq (10) is accurate to 2×10^{-12} . In a practical sense, there are only two degrees of freedom defining the polhode motion in this application. Those degrees of freedom can be expressed as T_A and θ_S defined above.

Conformal mapping will be used to transform polhode motions on the surface of a sphere onto the infinite plane. The spin vector, $(\omega_A, \omega_B, \omega_C)$, in rotor coordinates is mapped into the U, V plane by

$$\begin{aligned} U &= \frac{\xi_A}{1 + \xi_C} \\ V &= \frac{\xi_B}{1 + \xi_C} \end{aligned} \quad (12)$$

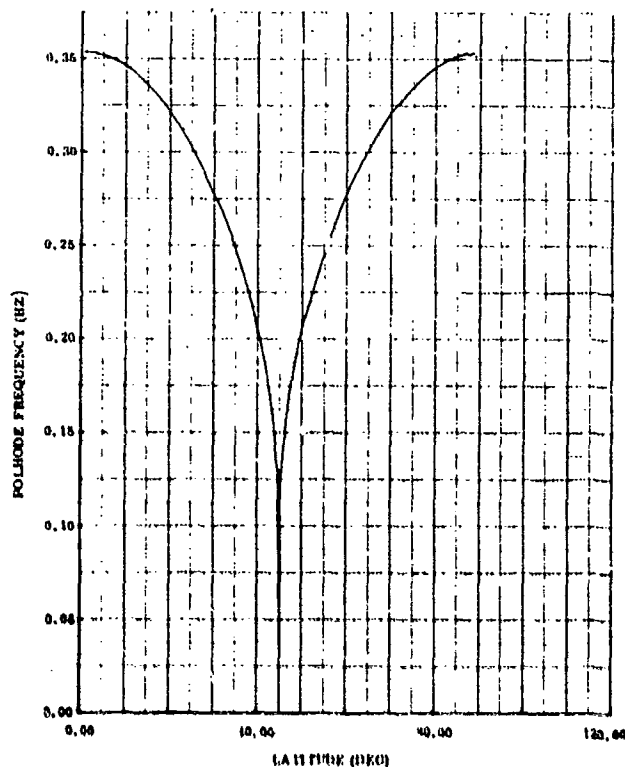


Figure 2. Polhode Frequency vs Polhode Latitude for $\theta_s = 45$ Deg and $T_A = 2.83$ Sec

$$\text{where } |\omega| = (\omega_A^2 + \omega_Y^2 + \omega_Z^2)^{1/2}$$

$$\xi_A = \omega_A / |\omega|$$

$$\xi_B = \omega_B / |\omega|$$

$$\xi_C = \omega_C / |\omega|$$

(13)

This transformation has the property that great circles are mapped into circles in the U, V plane. Great circles through the C axis are mapped into straight lines through the origin. Figure 3 shows the important great circles which will be used as the grid for polhode plots. The great circles in the A-B, B-C, and C-A planes are shown as well as the two great circles defining the separating polhodes ($\theta_s = 45$ deg). The areas enclosed by the separating polhode lines represent from left to right the -A, +C, and +A families. The -C family is represented by the area outside of both separating polhode circles in the U, V plane.

An important property of conformal mapping is that the angle between two intersecting lines on the sphere is preserved when the two lines are transformed on the U, V plane.

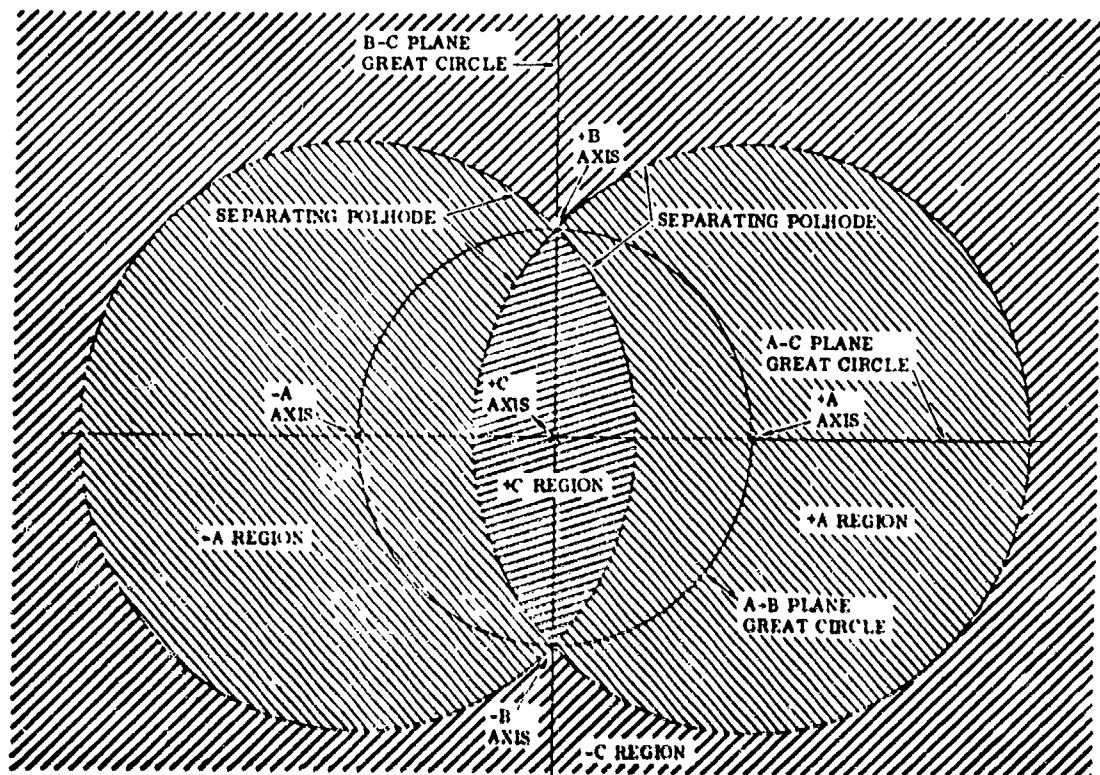


Figure 3. Conformal Mapping of the Surface of the Sphere Onto the Infinite Plane ($\theta_s = 45 \text{ Deg}$)

Figure 4 shows polhode trajectories in the +A and +C families at 10-deg latitude intervals and one trajectory in the -C family at 40-deg latitude. The distortion introduced by the transformation of points distant from +C axis should be recognized. On the sphere these trajectories are approximately elliptical in shape. The direction of motion on each trajectory is shown by arrows. As a memory aid, the right-hand rule defines the direction of motion in the A families and the left-hand rule defines the direction of motion in the C families.

The attitude readout mechanism of the MESG for navigation function is mass unbalance modulation (MUM) produced by intentionally shifting the mass center of the spherical rotor approximately along the -C axis from the geometric center. The pendulosity vector is defined as the vector from the geometric center to the mass center and is approximately 16 $\mu\text{in.}$ long. The rotor will spin about the mass center assuming there is no forcing by the electrostatic suspension at rotor frequency. The spherical rotor will appear to wobble at rotor frequency with amplitude equal to the component of pendulosity orthogonal to the spin vector. This component of pendulosity is called the MUM vector (with direction reversed).

Forcing by the electrostatic suspension at rotor frequency is not negligible except at the notch frequency of 2430 hz or below 400 hz as shown in Figure A-2 of Appendix A. When damping is performed at rotor frequency of 2000 hz the MUM vector is 50 percent larger than at 2430 hz. The equations relating MUM vector to pendulosity vector and suspension gain and phase are given in Appendix A. For zero gain the MUM equation of Appendix A reduces to:

$$\text{MUM} = \left| -\mathbf{P} + \frac{\mathbf{P} \cdot \boldsymbol{\omega}}{\boldsymbol{\omega} \cdot \boldsymbol{\omega}} \boldsymbol{\omega} \right| / |\mathbf{P}| \quad (14)$$

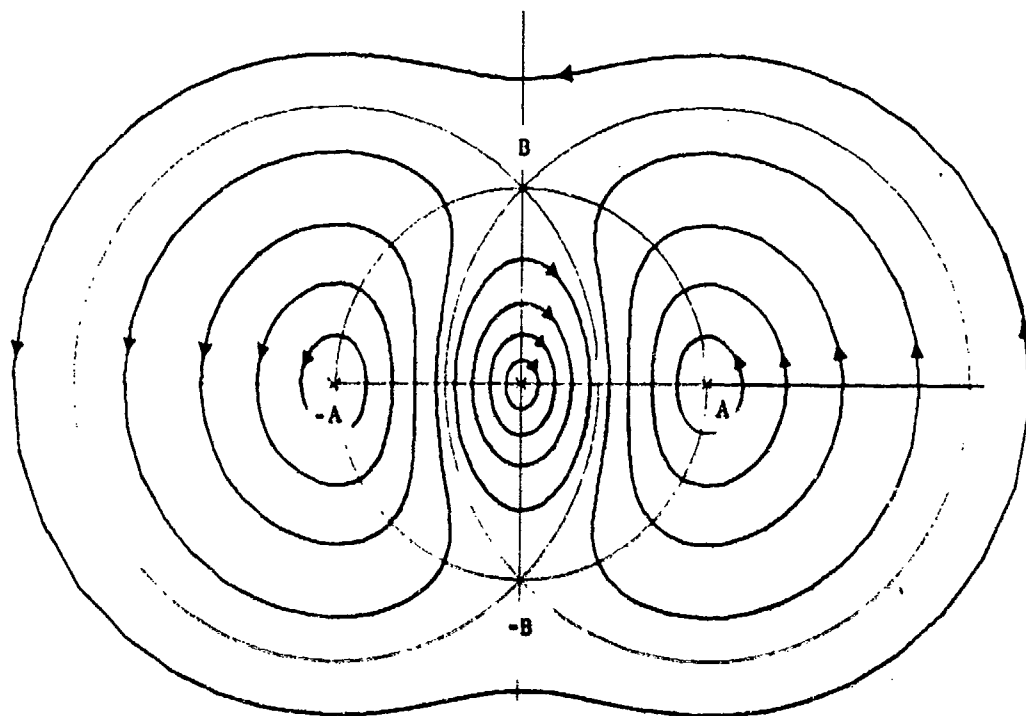


Figure 4. Polhode Trajectories at 10-Deg Intervals in -A, +C, and +A Families and 40-Deg Trajectory in -C Family ($\theta_s = 45$ Deg)

where P is the pendulosity vector and ω is the spin vector and the MUM vector is normalized for maximum length of unity.

For nonzero forcing the length of the MUM vector is changed and the phase of the signal is changed. The computer compensates the net phase shift of the MUM vector and the MUM vector is normalized to its maximum value. Therefore, the compensated MUM vector is defined by Eq (14) if forcing gain and phase are constant. If rotor speed changes, the forcing gain and phase will change and so MUM vector will change as defined by the equations in Appendix A.

The direction of the MUM vector as described by Eq (14) is shown in Figure 5 for one trajectory in each region.

The MUM vector modulates the capacitance as seen from the cavity electrodes. This information is demodulated and sent to the computer as two vectors, α_M and β_M which represent the cos and sin components of the demodulated MUM signal. Physically α_M and β_M represent the position of the MUM vector at 0 and 90 deg of one rotor revolution which is relative to the phase of the demodulation reference.

The amplitude of the MUM signal is modulated by the polhode motion as can be seen in Eq (14) since the ω vector follows the polhode trajectory. For the case in which the pendulosity vector is exactly along the -C axis, the MUM magnitude is minimum when ω is in the A-C plane and is maximum when ω is in the A-B plane for

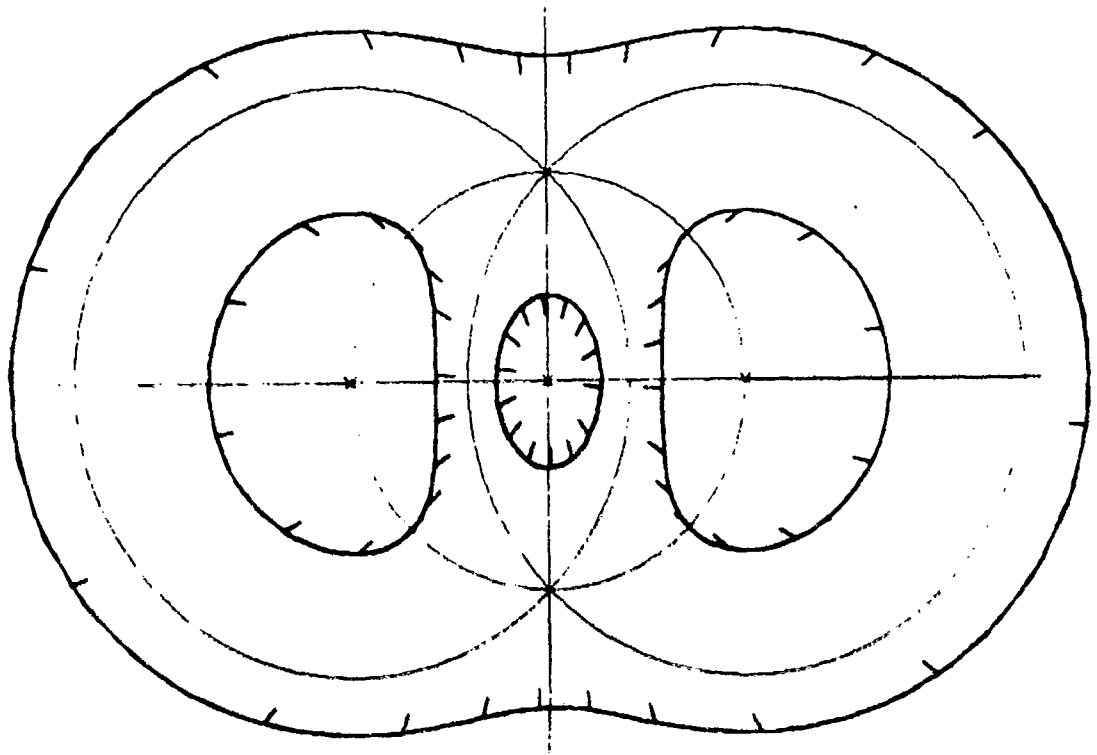


Figure 5. MUM Vector Directions in $\pm A$ and $\pm C$ Families
($\theta_s = 45$ deg, $T_A = 2.83$ sec)

A family polhodes and in the C-B plane for C family polhodes. Therefore, the dominant frequency in MUM magnitude is second harmonic of polhode frequency. The locus of unity MUM magnitude is on the A-B plane.

Due to unintentional imperfections in the rotor a component of the pendulosity will lie on the -A axis. In the past this component of mass unbalance has been the sole means of distinguishing the $\pm A$ axes by defining the mass unbalance to be on the -A axis. It is very important to always damp the rotor in on the same axis so $\pm A$ axes must always be identified. The pendulosity component on the -A axis has always fallen in the range of 6 percent to 0.2 percent of total pendulosity. Of course, there is always the danger of manufacturing a perfect rotor which has no pendulosity component on the -A axis and hence the sign convention fails. An alternate sign convention now implemented is to intentionally rotate the pendulosity vector approximately 4 deg toward the -B axis. Mass unbalance on the B axis causes no degradation in gyro performance while mass unbalance on the A axis causes g-sensitive drift rates.

Small mass unbalance on the A and B axes rotate the locus of unity MUM magnitude away from the A-B plane. The locus of unity MUM magnitude is defined by the plane orthogonal to the pendulosity vector so mass unbalance on -A axis rotates the plane about +B axis and mass unbalance on -B axis rotates the plane about -A axis. The dissymmetry of the pendulosity vector relative to the polhode pattern causes the two maxima and two minima of MUM magnitude per period to be unequal in general.

Figure 6 shows the great circle locus of unity MUM magnitude as a heavy line for pendulosity on -A and -B of 10 percent each and $\theta_S = 45$ deg. Several polhode trajectories are also shown to illustrate the major variations in MUM magnitude patterns. The approximate points of high and low maximum and high and low minimum are also shown. Notice trajectory 3 in the C family has a double maximum near -B axis. Also the trajectories 1 and 5 in the neighborhood of the C and A axes have only a single maximum and minimum. Figure 7 shows the MUM magnitude time histories for the same five trajectories of Figure 6. Each time history plot is started on the great circle segment between +C and +A axes and continues for slightly over one period.

The most prominent features of all polhode trajectories can be summarized with a plot of the maxima and minima MUM magnitude versus polhode latitude as shown in Figure 8. The difference between the high and low max or Δmax is shown in Figure 9. The peak to peak amplitude of MUM magnitude is shown in Figure 10. The angle from the trajectory normal to the MUM vector can be visualized from Figure 5. The angle is plotted versus latitude for the max and min points on the trajectory in Figure 11.

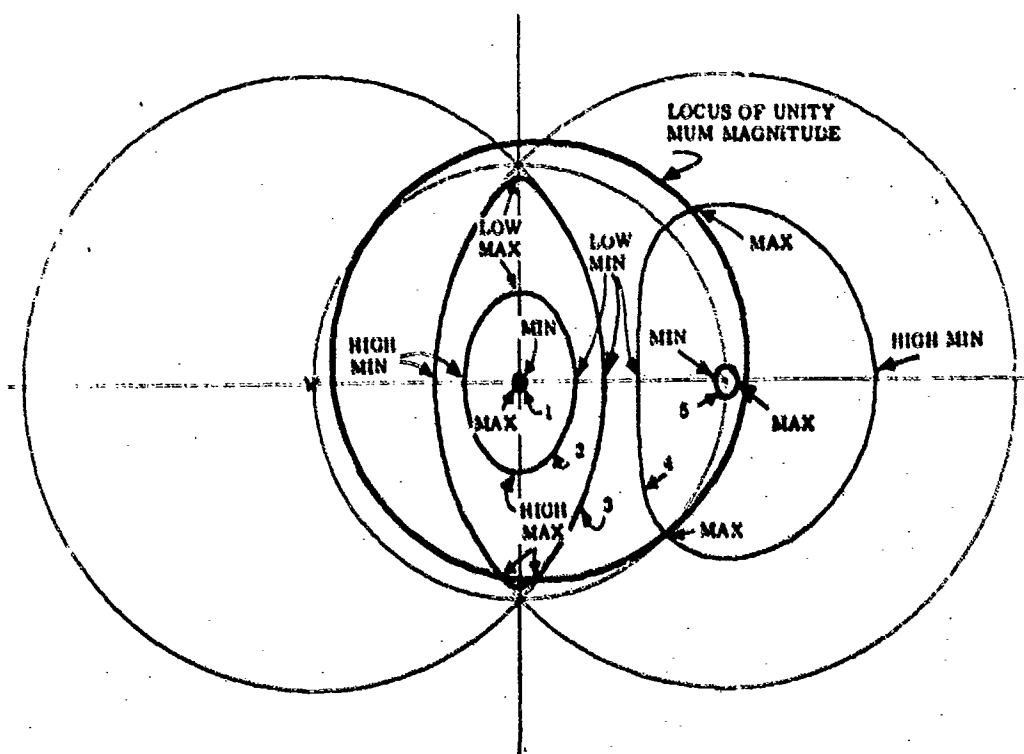


Figure 6. Five Representative Polhode Trajectories and Locus of Unity MUM Magnitude ($\theta_S = 45$ deg)

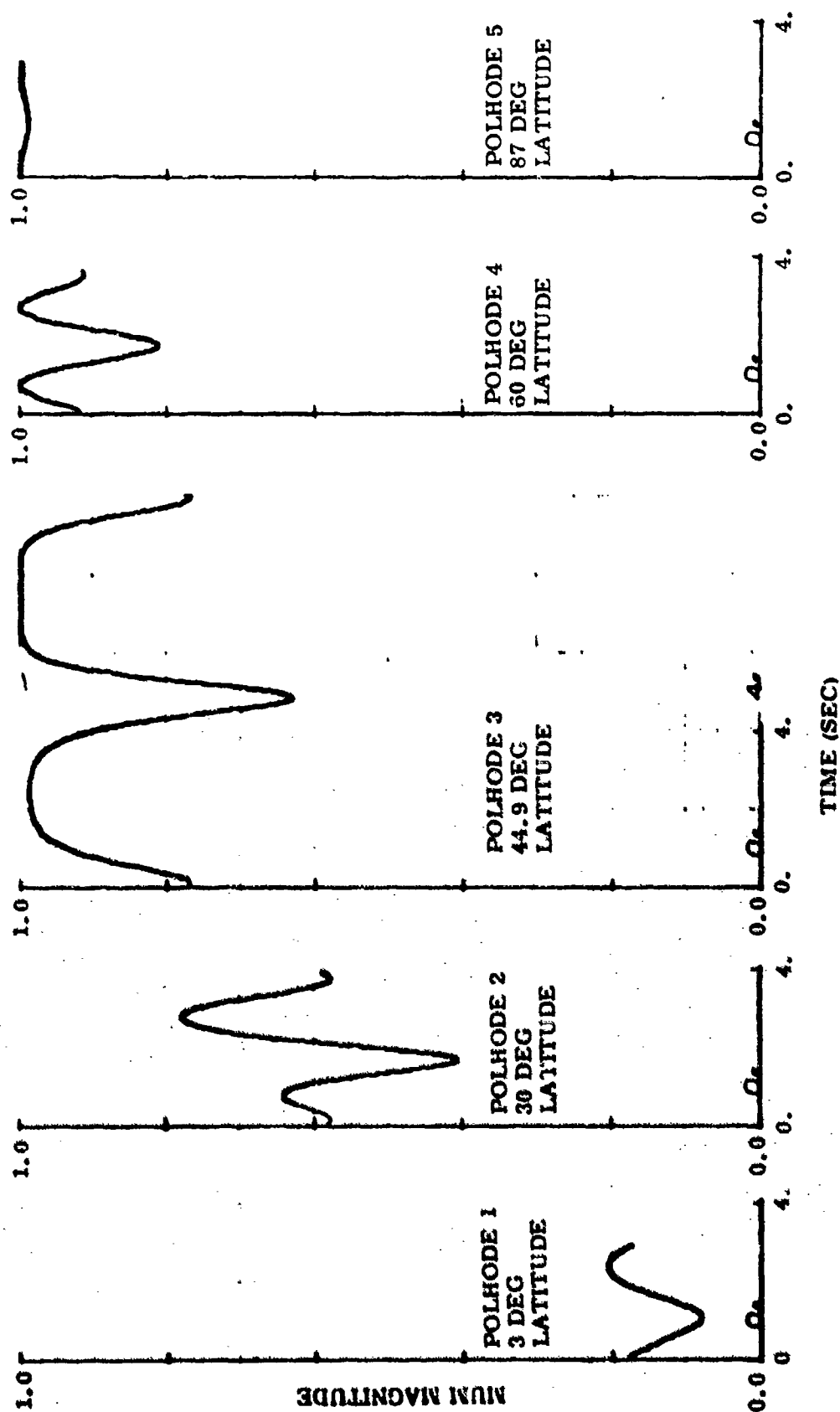


Figure 7. MUM Magnitude Time Histories Over One Polhode Period for Five Polhode Trajectories of Figure 6 ($\theta_5 = 45$ Deg, $T_A = 2.83$ Sec)

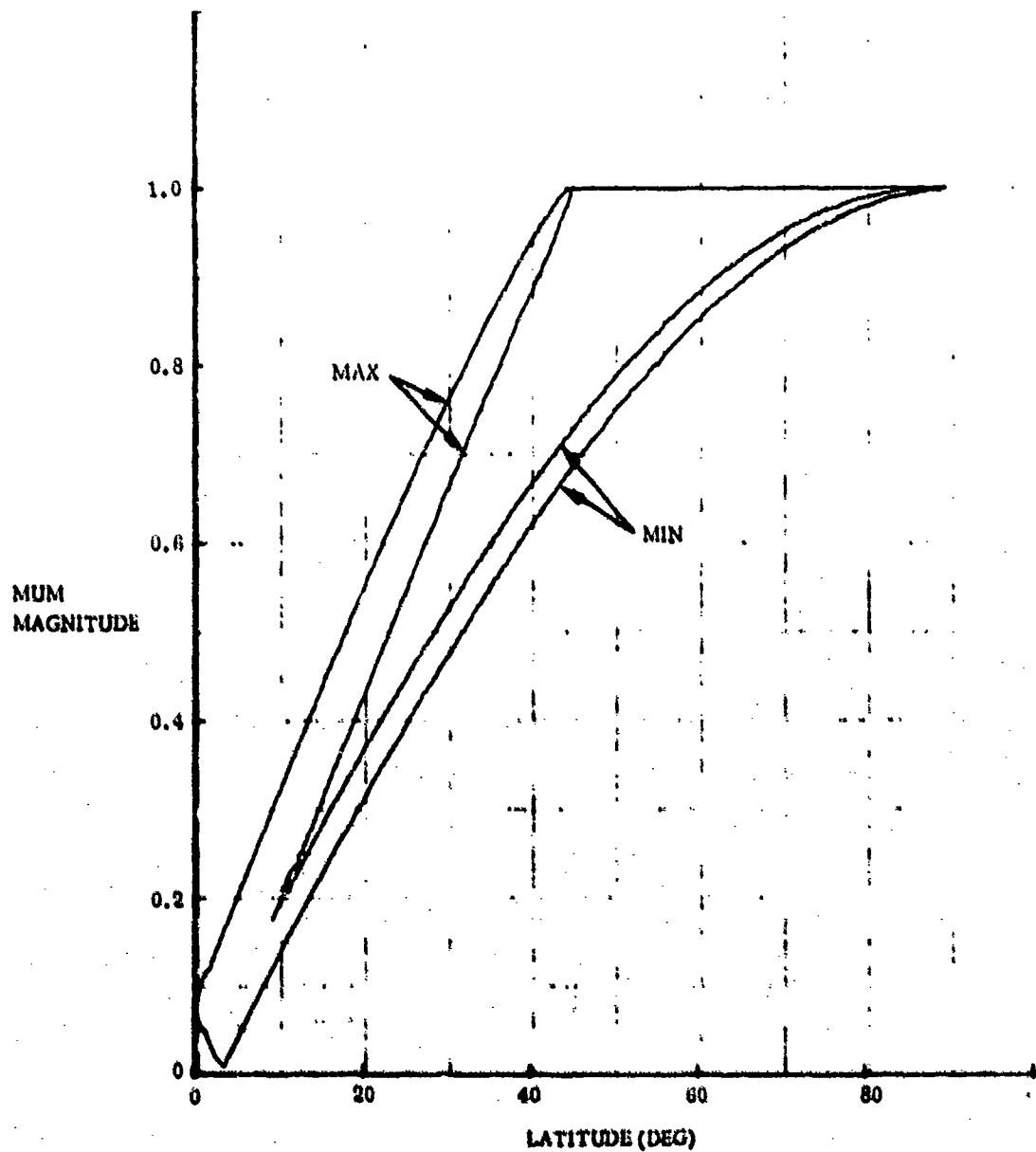


Figure 8. MAX and MIN MUM Magnitude (45 Deg Separating Polhode, 0.03, 0.07 Pendulosity on A and B Axes Respectively)

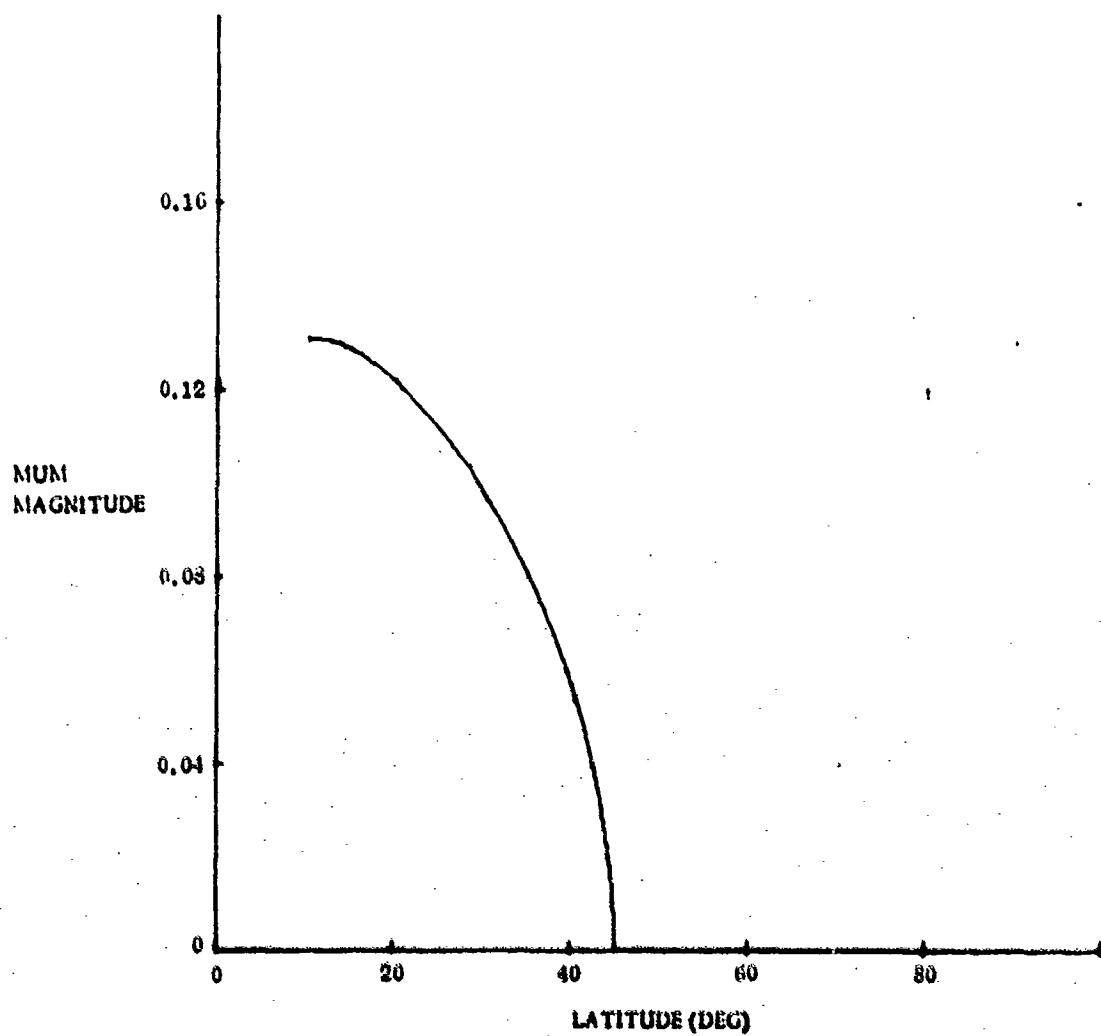


Figure 9. Difference Between High and Low Maxima, Δ Max (45 Deg Separating Polhode, 0.03, 0.07 Pendulosity on A and B Axes Respectively)

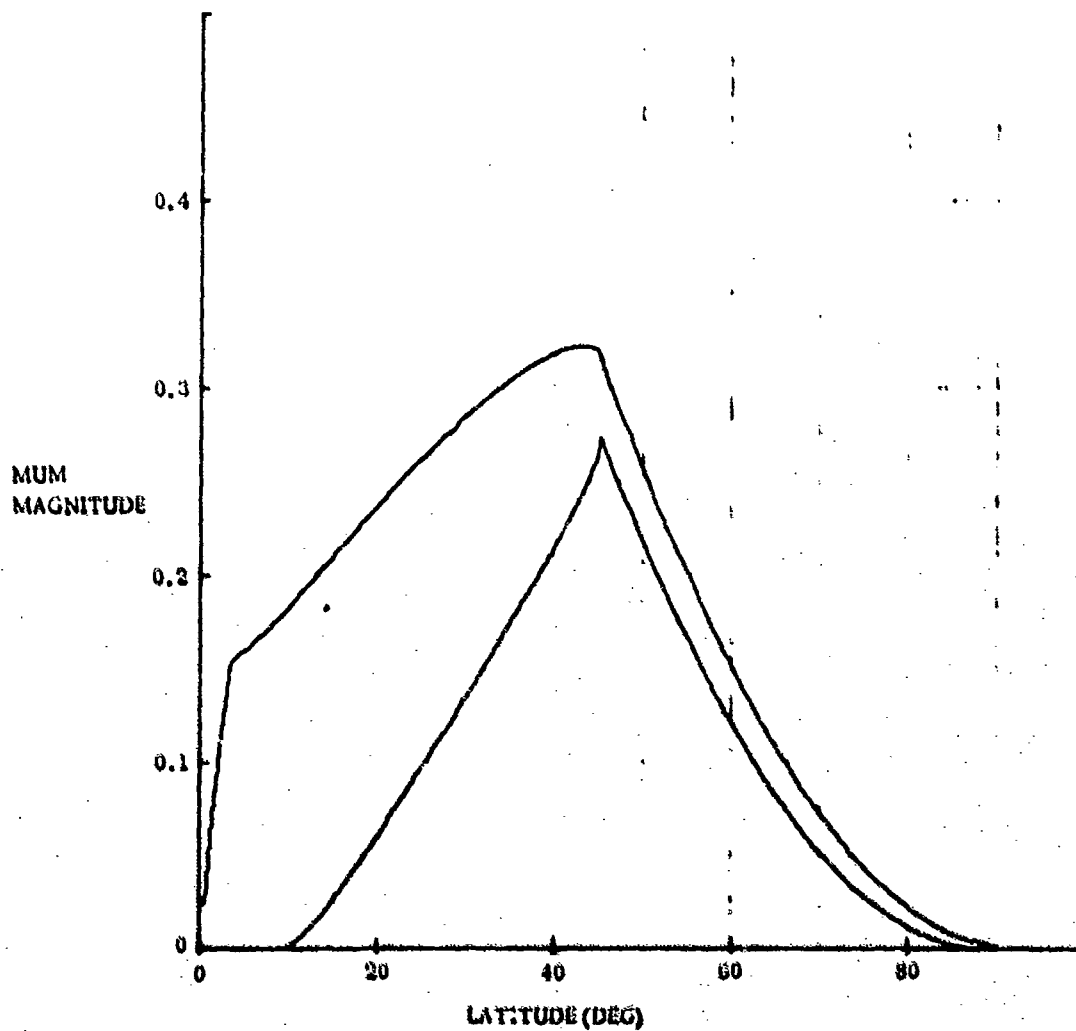


Figure 10. Peak to Peak MUM Magnitude (45 Deg Separating Polhode, 0.03, 0.07 Pendulosity on A and B Axes Respectively)

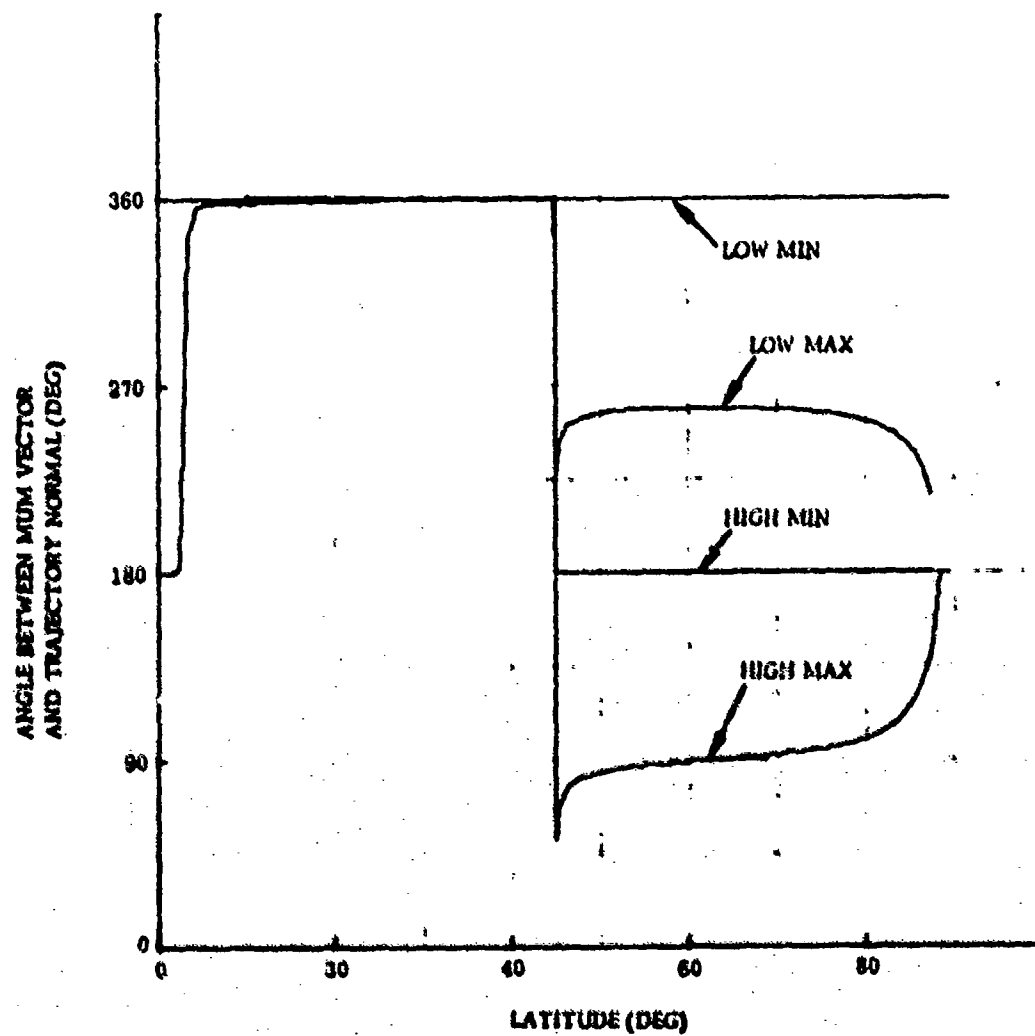


Figure 11. Angle Between MUM Vector and Trajectory Normal at Min and Max Points in +C and +A Families (45 Deg Separating Polhode, 0.03, 0.07 Penchulosity on A and B Axes Respectively)

SECTION III

TORQUING EQUATION

The MESG has three torquing coils centered on the x, y, and z gyro axes. The equation defining the necessary currents in the three coils to produce the desired torque is developed in Ref 1 and repeated here.

Equation (2) defines polhode motion and the effect produced by torquing. The equation is in rotor coordinates and so the torque vector must be fixed in the rotor and orthogonal to spin. In general, the torque vector can make any angle with respect to the MUM vector.

Define an orthonormal vector triad (α, β, γ) centered in the rotor but not rotating with the rotor. γ is along the rotor spin vector, α is rotated an angle θ about γ from the MUM vector at time zero, and β is $\gamma \times \alpha$. The torque unit vector is defined

$$Q = \alpha \cos \omega_D t + \beta \sin \omega_D t \quad (15)$$

where ω_D is the angular rate of the rotor with respect to the α, β, γ coordinate frame. At time zero the torque vector is along α and hence it is angle θ from the MUM vector.

Torque is generated by a flux vector rotating about the torque vector. A rotor fixed orthonormal vector triad is defined (γ, Q, Q_F) where

$$Q_F = -\alpha \sin \omega_D t + \beta \cos \omega_D t \quad (16)$$

The flux unit vector to generate Q is

$$\text{FLUX} = \gamma \cos (\omega_F t + \phi) + Q_F \sin (\omega_F t + \phi) \quad (17)$$

where ω_F is the frequency at which the flux vector rotates about the torque vector and ϕ is the initial phase angle. They are both completely arbitrary.

Eliminating Q_F in Eq (17) gives

$$\begin{aligned} \text{FLUX} = & \alpha \left(\sin \omega_F t \sin (\omega_F t + \phi) \right) + \beta \left(\cos \omega_F t \sin (\omega_F t + \phi) \right) \\ & + \gamma \left(\cos (\omega_F t + \phi) \right) \end{aligned} \quad (18)$$

which is a valid torque equation. The computer supplies vectors α, β, γ to the torquing electronics which then generate the three components of flux using Eq (18). The electronics mechanization can be simplified if

$$\begin{aligned} \omega_F &= \omega_D \\ \phi &= 0 \end{aligned} \quad (19)$$

which gives

$$\text{FLUX} = \alpha 1/2 (1 - \cos 2 \omega_D t) + \beta (1/2 \sin 2 \omega_D t) + \gamma \cos \omega_D t \quad (20)$$

Equation (20) is actually mechanized in the electronics.

Notice that α , β vectors supplied by the computer are the normalized MUM demodulator outputs rotated an angle θ .

$$\alpha = \alpha_M' \cos \theta + \beta_M' \sin \theta$$

$$\beta = -\alpha_M' \sin \theta + \beta_M' \cos \theta$$

$$\gamma = \alpha_M' \times \beta_M'$$

(21)

α_M' , β_M' - MUM demodulator output vectors normalized to unit length. MUM vector rotation caused by electrostatic suspension forcing at rotor frequency and by phase shifts in MUM pickoff electronics is compensated by adding a fixed bias to angle θ .

SECTION IV

CONTROL LAWS

The control law specifies the torque vector that is normal to the untorqued trajectory. It must specify torque to cross the separating polhode on the desired direction and it must provide terminal control to place the spin vector on the A axis. Separate control laws are used for each purpose. The control laws are described in terms of their location relative to a unit vector along MUM, 1_{MUM} , and a quadrature unit vector, $1_{MUM Q}$. The C and A family control laws can be readily deduced by referring to the plot of MUM direction in Figure 5.

The +C family control law is

$$\text{Torque direction} = -1_{MUM}$$

The -C family control law is

$$\text{Torque direction} = 1_{MUM}$$

The A family control law is

$$\text{Torque direction} = 1_{MUM} \cos \theta + 1_{MUM Q} \sin \theta$$

where θ is the polhode phase which is zero on the C to A and -C to -A great circle segments. Notice that this control law works for both +A and -A families. The torque vectors point outward in the +C and -A families and inward to the +A family.

A special control law is required to cross the separating polhode on the +A family side. The transition region is defined as a band on either side of the separating polhode that is wide enough so that the separating polhode cannot be crossed in half a polhode period starting from an edge of the transition region and applying either the A or C control laws.

The transition control law must work in both the C and A families since the exact crossing point is unknown and the A or C family can only be identified after a complete cycle in that family. Furthermore, the control law should make the transition from C to +A family and not enter the -A family. A simple solution is to apply the sum of the A and C family control laws. The C family control law produces no net change in polhode latitude in the A family and vice versa. The transition control law is

$$\text{Torque Direction} = 1_{MUM} \left(\frac{\cos \theta - (+1)}{2} \right) + 1_{MUM Q} \left(\frac{\sin \theta}{2} \right) \quad (22)$$

where the + sign is taken for the + transition and the - sign for the - transition. Equation (22) is not a unit vector and must be normalized. The torque magnitude is zero on the half polhode period for which the term in Eq (22) $(\cos \theta - (+1))$ is less than 1. Figure 12 shows the torque direction for the + transition control law about trajectories in the +A and +C families. The +transition control law can also be used to cross from the -A family into the -C family or with a 180 deg reversal of θ in Eq (22) it can be used to cross from the +A into the -C family.

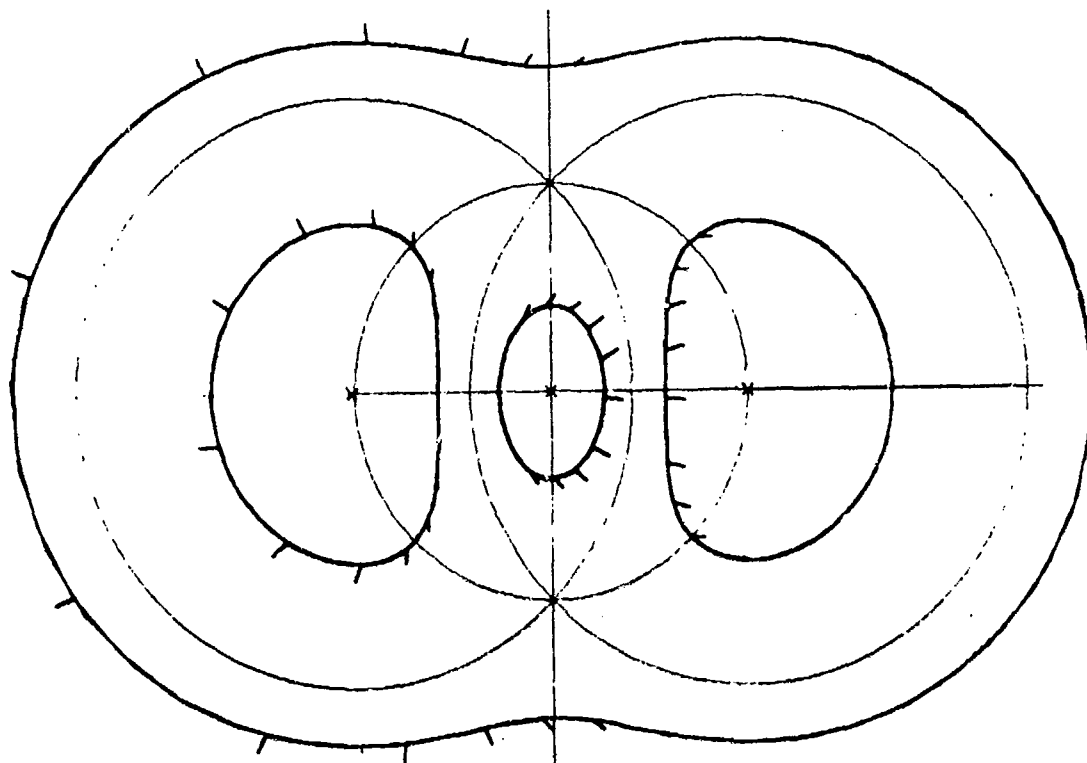


Figure 12. +Transition Control Law Torque Vectors ($\theta_s = 45$ deg.
 $T_A = 2.83$ sec)

The direction of the MUM vector changes radically in a small neighborhood about the $\pm C$ axes. Figure 13 shows the MUM vector on trajectories in a neighborhood of the $+C$ axis. The point at which an extension of the pendulosity vector would intersect the surface of the sphere is shown which is the point of zero MUM magnitude. In this neighborhood it is very difficult to tell whether or not the trajectory encloses the zero MUM magnitude point. A simple control law in this region is to only apply the C family control law over approximately half the polhode period centered on the high max MUM magnitude point.

The terminal control law in the neighborhood of the $+A$ axis is the same as the A family control law except proportional control is used by varying the time interval that torque is applied.

The rate of change of torque magnitude is limited in the current mechanization. This feature now appears unnecessary as step functions in the flux field cause no ill effects.

The A and C family control laws are attempting to approximate the normal control law. The torque direction for the normal control law is normal to the untorqued trajectory. The efficiency of the normal control law will be computed for small torques.

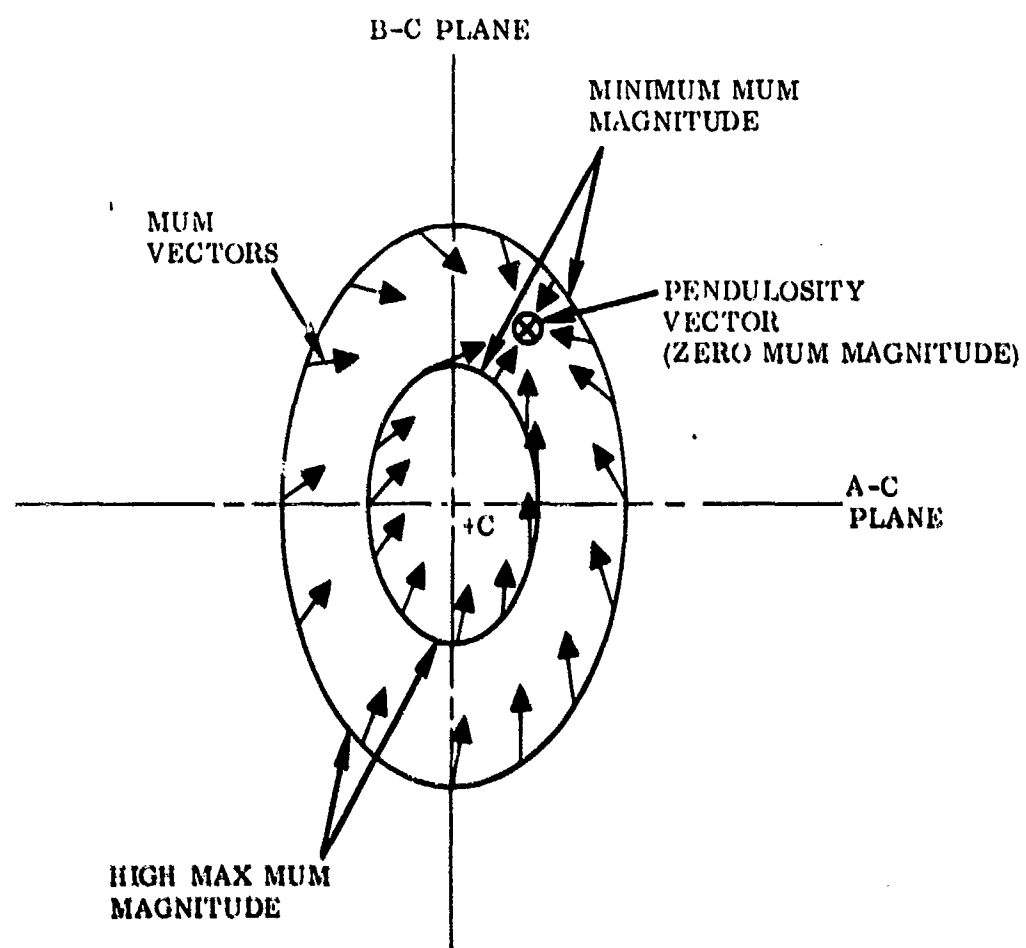


Figure 13. MUM Vectors in the Neighborhood of the +C Axis

The torque vector, T_Q , will be defined in units of precession rate as

$$T_Q = \frac{1}{\omega_0} \begin{bmatrix} Q_A/A \\ Q_B/B \\ Q_C/C \end{bmatrix} \quad (23)$$

where (Q_A, Q_B, Q_C) is the physical torque vector defined in Eq (2) and ω_0 is the magnitude of rotor angular rate when in the A-C plane. The change in polhode latitude introduced by a unit torque impulse at time t is

$$\text{Torque Efficiency} = \frac{\partial \theta}{\partial \omega} \omega \quad (24)$$

where θ is polhode latitude. This function is a measure of torquing efficiency vs polhode phase and latitude. The function is plotted in Figure 14 vs polhode phase for several polhode latitudes. The average torquing efficiency is computed by averaging

$\frac{\partial \theta}{\partial \omega} \omega$ over the polhode period which will be called $\overline{\frac{\partial \theta}{\partial \omega}} \omega$.

A similar computation can be made for the A and C control laws by recognizing that only the normal component of torque changes polhode latitude. The tangential component of torque averages to zero over one period. Figure 15 shows the efficiencies of the normal, A, and C control laws. The C control law is the least efficient because it is a radial control law. Its efficiency could be improved with a small second harmonic correction to the torque direction.

The net efficiency for damping from C to A axes cannot be computed without including a technique for crossing the separating polhode. An optimistic efficiency estimate can be obtained by simply computing the average efficiency for each control law which is

normal control law	79.3%
A control law	78.8%
C control law	75.8%

Therefore to damp from C to A axes with a 45 degree separating polhode requires torquing through an angle of 45 degree $\left(\frac{1}{.758} + \frac{1}{.788} \right) = 117$ deg. If torque is only applied near the A-C great circle torquing efficiency approaches 100 percent.

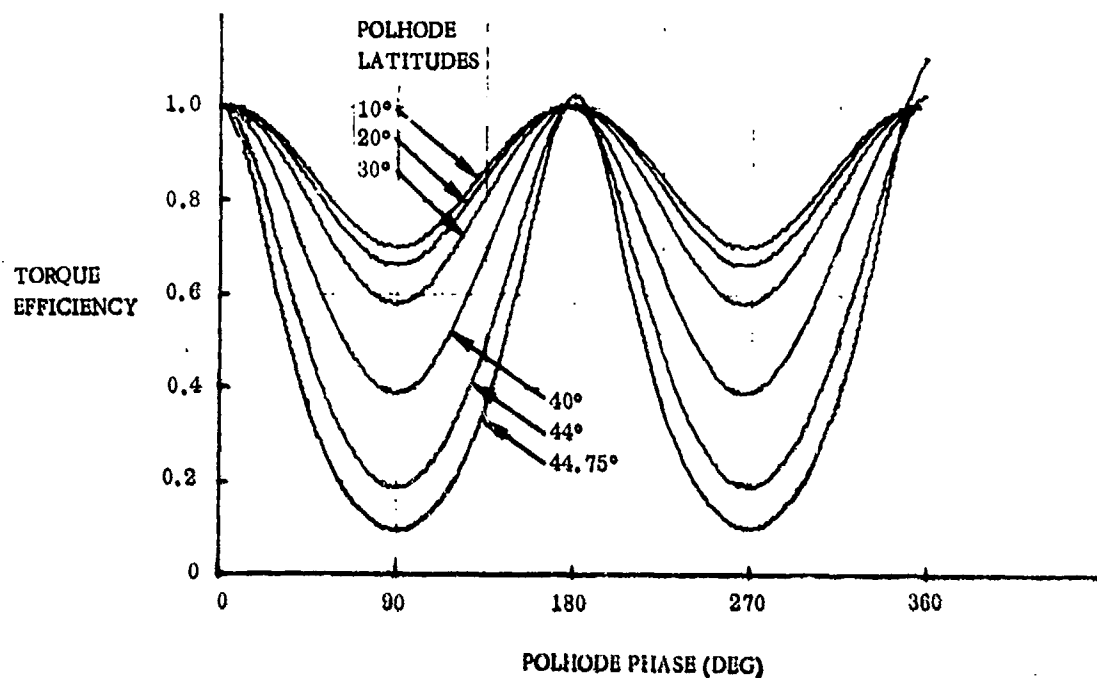


Figure 14. Normal Control Law Torque Efficiency vs Polhode Phase for Several Polhode Latitudes (45 Deg separating Polhode)

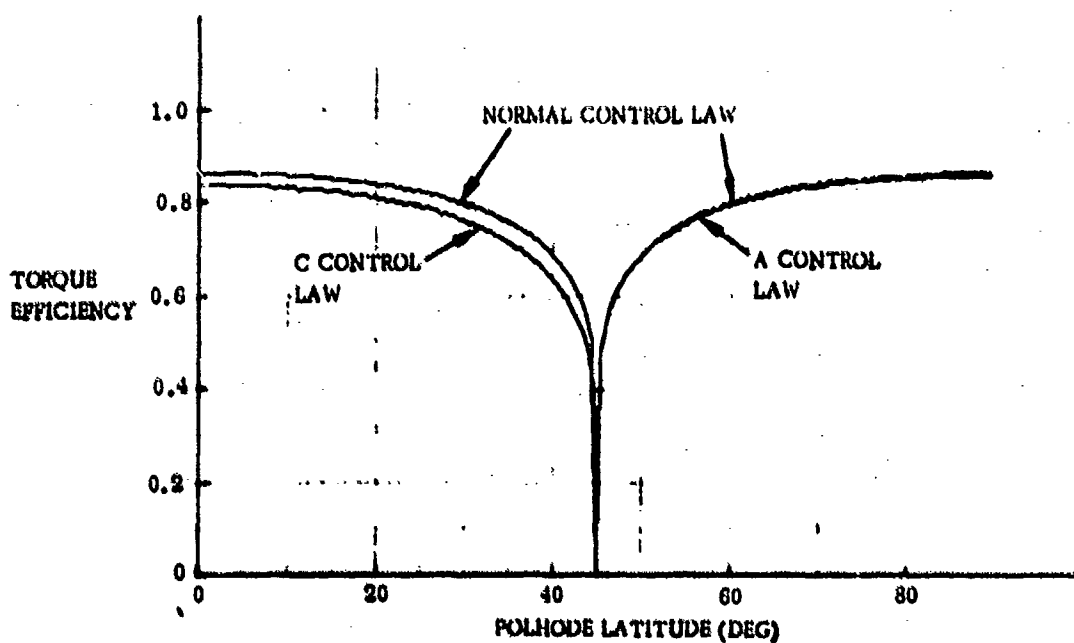


Figure 15. Average Torque Efficiency vs Polhode Latitude

SECTION V

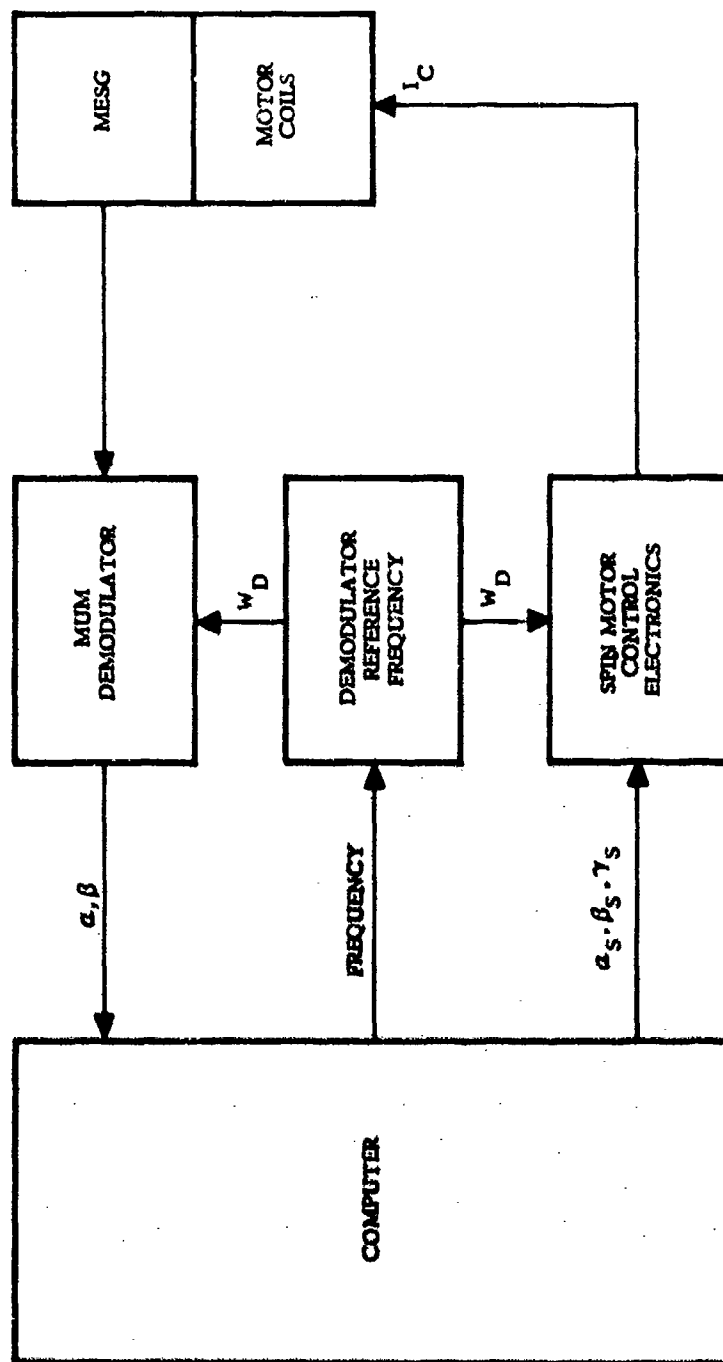
AUTOMATIC DAMPING

A block diagram of the hardware used for automatic damping in the N57A navigator is shown in Figure 16. The MUM demodulator supplies the MUM data α , β to the computer in the form of 6 digital words. In the N57A navigator frequency for the demodulator is supplied by the computer. In the tests reported here the frequency was supplied by a phase locked loop within the MUM demodulator. In either case the same frequency is supplied to the spin motor control electronics. Nine digital words in the form of three vectors α_S , β_S , γ_S command the torque from the computer. The current in the motor coils, vector I_C , is given by the equation at the bottom of the figure which is the one derived in Section III.

The general description of the automatic damping program is presented here. An indepth description of the automatic damping program is presented in Appendices C and D. The logic is laid out as much as possible to allow very large tolerances on the automatic damping parameters. The nominal gyro and system parameters will be used to determine the automatic damping parameters. Variations from nominal of ± 10 percent or greater can be tolerated without changing the damping parameters. The method of determining the automatic damping parameters is described in Paragraph 2 of Section VIII.

The computer cycle time for the automatic damping program was planned for 1/16 sec since that is a basic rate in the N57A navigation computer. The polhode period of the N57A gyros near the A axis is 4 sec. The polhode period of the gyros used here is about 7 to 9 sec depending on the temperature. The computer cycle time was increased to 0.1 sec so that the same program could be used here and on the N57A gyros by maintaining a relatively constant number of computer cycles per A axis polhode period.

Automatic damping problem will be divided into two subproblems, estimation and control. The estimation problem must identify and track the polhode parameters needed for the control laws. The control laws must specify the direction and magnitude of torque to efficiently damp the rotor. Minimum polhode information required for control is polhode phase, family identification, and special regions within the families. Polhode phase relative to one polhode period must be tracked continuously. Polhode phase is the basic information used by the control law to rotate the torque vector to the desired direction. Polhode phase implicitly identifies the +A and -A axes. If phase lock is lost (phase error greater than 90 deg) the control will actually undamp the rotor. Therefore, polhode phase tracking appears to be one of the most critical aspects of the problem. The control strategies in the A and C families are completely different. A special control strategy is required in crossing the separating polhode to be assured of always entering the +A family. Finally, a terminal strategy is



$$I_C = \alpha_S \left[\frac{1}{2} (1 - \cos 2\omega_D t) \right] + \beta_S \left[-\frac{1}{2} \sin 2\omega_D t \right] + \gamma_S \left[\cos \omega_D t \right]$$

Figure 16. System Block Diagram

required to complete the damping on the +A axis. The overall organization of the computer program is shown in Figure 17.

1. ESTIMATION

Estimation can be reduced to two subproblems, phase tracking and family identification.

a. Phase Tracking

The polhode phase parameter as used here is loosely defined with the following properties:

1. Phase has 360-deg monotonic increasing variation within one polhode period.
2. Phase is equal to multiples of 90 deg at quadrature points in polhode trajectory (intersections with A-B, B-C, or C-A planes).
3. Zero phase is at the intersection of either great circle segment -A to +C or +A to -C.

The phase variable defined here is solely related to the polhode pattern. Phase tracking must be based on MUM magnitude information. In most cases MUM magnitude has a strong component of second harmonic cosine of the phase variable. However, due to pendulosity components along A and B axes the phase of the MUM magnitude signal is shifted a small amount relative to the polhode pattern.

The ultimate use of the phase variable is to direct the torque vector as described in Section III and Eq (21). The ideal phase variable in the A family is the angle between the MUM vector and the unit vector normal to the unforced polhode trajectory assuming the normal control law is desired.

The second harmonic component of MUM magnitude leaves a 180-deg uncertainty in the phase variables. This can only be resolved by recognizing the pendulosity components on either the A or B axes. The pendulosity component on the A axis produces high and low minima or a fundamental cosine component of MUM magnitude in both the A and C families. The pendulosity component on the B axis produces high and low maxima or a fundamental sine component of MUM magnitude only in the C family. The A family maxima are always unity except in a small neighborhood about the +A axis. A pendulosity component on the B axis does produce relatively subtle changes in MUM magnitude waveform between the +A and -A families.

The 180 deg uncertainty in the phase variable is directly related to identification of the +A axis. Since the mass center is located along -C and tipped 4 deg towards -B, the +A axis is implicitly defined in a right hand coordinate frame. Table 1 relates the MUM magnitude maxima to the B axis and the value of the phase variable.

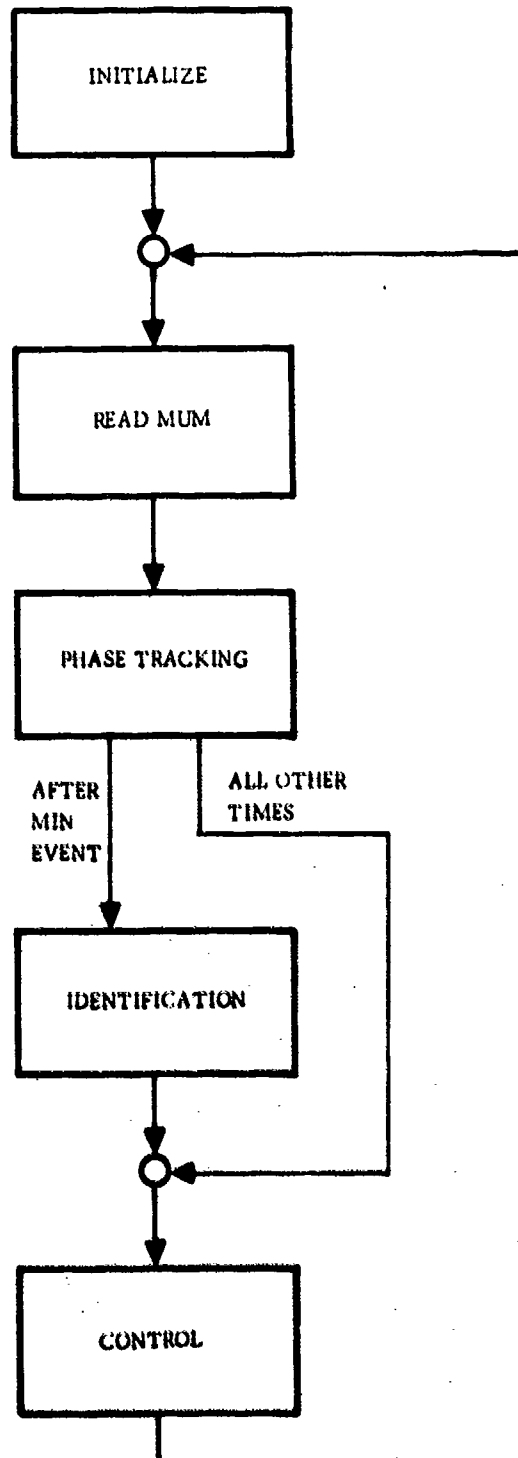


Figure 17. Automatic Polhode Damping Block Diagram

Table 1. Sign Convention

	+C Family	-C Family	A Family
Closest Approach to +B Axis	Low Max Phase Variable = 90°	High Max Phase Variable = 90°	Max Phase Variable = 90°
Closest Approach to -B Axis	High Max Phase Variable = 270°	Low Max Phase Variable = 270°	Max Phase Variable = 270°

Three approaches for maintaining phase lock will be described. The techniques will be called simulation, Fourier analysis, and max/min tracking.

(1) Simulation Mechanization

The simulation technique involves integration of the differential equations of polhode motion defined by Eq (2). This approach would clearly yield the most precise tracking of the polhode motion if all parameters were well defined. There are many difficulties that make this approach appear to be the most impractical of the three.

The initial conditions of the differential equation must be specified which requires initial phase and polhode latitude while the initial statement of the estimation problem only requires phase. The approach requires all polhode parameters including torquing parameters to be precisely known for use in the differential equation. Finally, a closed loop control based on MUM magnitude must be generated to keep the differential equation solution synchronized with the real world polhode motion both in phase and latitude. This approach was dismissed on the basis that simpler solutions exist.

(2) Fourier Analysis Mechanization

The polhode phase variable is based on a constant frequency per polhode period. Sine and cosine of polhode phase are generated and the first and second harmonic Fourier coefficients of MUM magnitude are computed from the sinusoids. A sampled data phase locked loop is constructed to maintain polhode phase lock by nulling second harmonic sine Fourier coefficient. The 180-deg phase uncertainty is resolved by requiring the first harmonic cosine Fourier coefficient to be positive.

This approach has been simulated as reported in Appendix B. The primary difficulty was caused by the frequency uncertainty and the large changes in frequency from one polhode period to the next when torquing. Polhode frequency is zero on the separating polhode due to the singularity on the B axis. Phase lock could not be reliably maintained while crossing the separating polhode and therefore the technique was discarded.

(3) Max/Min Mechanization

The singularity on the B axis can best be understood by looking at the time history of MUM magnitude as shown in Figure 18 for polhode latitudes 46 deg, 45.1 deg, and 45 deg with pendulosity components of 1 percent on -A and -B axes. The singularity problem is simply that MUM magnitude can hang up near its maximum value for an arbitrarily long period of time. A mechanization working in the time domain can easily recognize this. The obvious characteristics of MUM magnitude in the time domain are its local maxima and minima points. The maxima and minima occur at polhode quadrature points when pendulosity is along -C.

The basic operation consists of continuously tracking maxima and minima. When a maxima or minima occurs the phase variable is reset to the next quadrature point (0 or 180 deg at min events and 90 or 270 deg at max events). The phase variable is not allowed to cross a quadrature point until a maxima or minima occurs. Between max/min events the phase variable is extrapolated at constant frequency based on time between three minima except special conditions apply after a max event. After a max event the phase variable is frozen at the quadrature value until the MUM magnitude drops a prescribed amount such as 5 percent of its previous peak-to-peak value. It is then extrapolated.

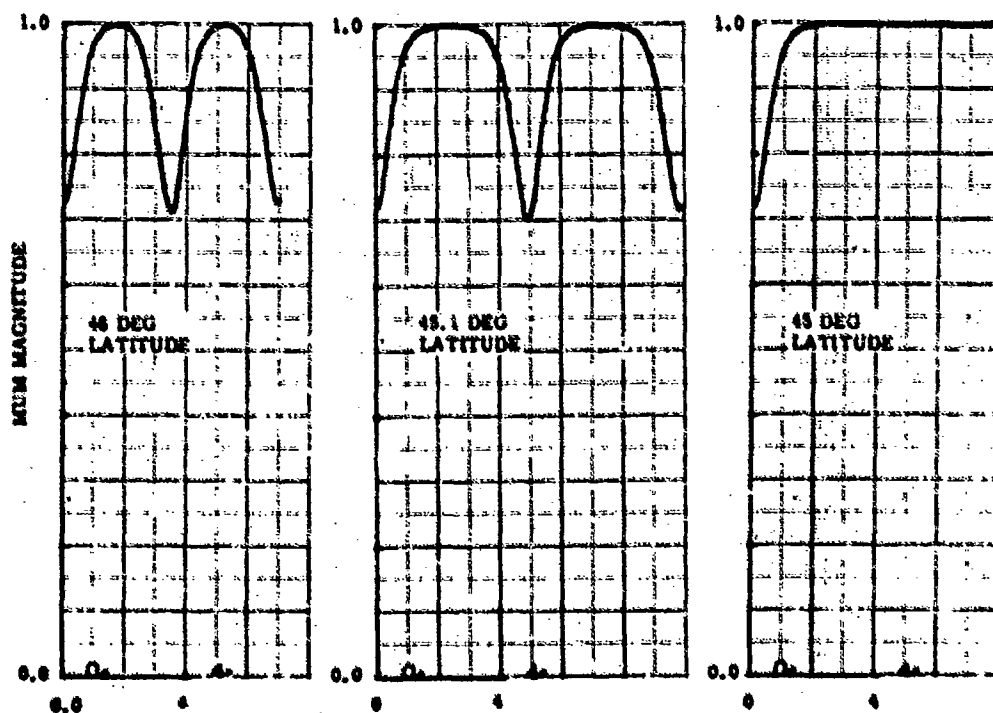


Figure 18. MUM Magnitude Time Histories Over One Polhode Period ($\theta_g = 45$ deg, $T_A = 2.83$ sec)

The 180-deg phase uncertainty is resolved by observing the values of three successive maxima. If the slope of a straight line between maxima 1 and 2 is S_1 and the slope of a straight line between maxima 2 and 3 is S_2 then maxima 3 is:

1. High max if $S_2 > S_1$ and
2. Low max if $S_1 > S_2$.

The phase variable is related to the high and low max as indicated in Table 1.

The mechanization is inherently stable even if the phase variable extrapolation has large errors unless a false min and max are obtained which produces a 180-deg phase error. The high/low min or max is tracked even during torquing so the phase error will be recognized and the problem restarted if it occurs. Noise on the MUM signal is the most likely cause of problem. The max/min recognition algorithm must employ smoothing. Also reasonableness tests can be applied to the max/min events. The time of the event and MUM amplitude of the event can be predicted from past history to verify reasonableness.

The max/min phase tracking mechanization is used in the automatic damping mechanization.

b. Family Identification

It is necessary to identify which of several regions of the sphere contain the polhode trajectory. The region identified determines mode switching in the phase tracking and control routines. Complete information is contained in polhode latitude for longitude of 0 or 180 deg. However, less detailed information is sufficient. First, three families must be distinguished: A families, +C family, and -C family. The $\pm A$ families are not explicitly distinguished. Two additional regions called \pm transition regions are small bands about the separating polhode. The band in the C families must be at least as wide as the area swept out by torquing for one polhode period. Small regions about the A and C axes must be identified for estimation since the MUM magnitude may have only one min and max per polhode period. The MUM magnitude signal may shift as much as 90 deg relative to the polhode period near the C axis for B pendulosity much greater than A pendulosity. A small region about the $\pm A$ family must be identified for terminal control law.

The nature of MUM magnitude in each of these regions can be seen in the curves of Figures 2, 8, 9, and 10. Phase tracking extracts the max and min values from MUM magnitude plus the peak-to-peak value, the difference between high and low max, Δmax , and the slopes of the max and min for use in identification.

In the C family the max is less than its largest possible value, the max has a slope with respect to latitude, and the two max are not equal. In the A family the max has its largest possible value, the max is constant with respect to latitude, and the two max are equal. In the transition zone the polhode period is long, the peak-to-peak value is large and the max is near its largest value. In the ANbhd the conditions of the A family are satisfied and the peak-to-peak value is small. In the CNbhd the conditions for the C family are satisfied and the min is small. Also in the CNbhd the max and min slope with latitude are of opposite sign as shown in Figure 8.

Several special cases must be checked to complete identification.

Near the A and C axes only one min occurs per polhode period while elsewhere there are always two min. The transition between one and two min must be recognized to avoid a 180 deg phase tracking error.

The sign of the $\pm C$ and \pm transition regions cannot be distinguished by static observations of MUM magnitude unless each gyro's axial mass unbalance is individually calibrated. The simplest strategy is to apply the control law with an assumed sign. If the assumption is wrong the MUM magnitude will decrease.

The 180 deg uncertainty of the phase variable must be resolved in the C family as indicated in Table 1.

If the 180 deg phase variable uncertainty is not resolved and polhode motion is in the A family, the spin vector must be torqued out of the A family by reversing the phase variable to make the min values have a negative slope.

When torquing out of the A family the torquing must be stopped after the C family is entered. The 180 deg phase variable uncertainty is resolved and then the spin vector is torqued back into the A family.

Terminal control in the ANbhd requires a number of special identification functions. The control angle or estimated colatitude must be computed as a function of the peak-to-peak MUM. The damping complete decision must be made. The MUM magnitude signal is heavily filtered in the ANbhd because of the very small peak-to-peak amplitude signal in this region. Filtering is changed to match the number of minima per polhode period. MUM magnitude average slope due to rotor speed changes can overwhelm the peak-to-peak variations. The peak-to-peak amplitude must be corrected for the average slope and the max/min filter must remove the average slope when recognizing max and min.

As a safety precaution special logic prevents the spin vector from leaving the ANbhd after the 180 deg phase variable uncertainty is resolved. If through some malfunction phase lock is lost and the spin vector is being torqued away from the A axis the min slope will be large negative. The phase variable is changed by 180 deg to bring the spin vector back towards A axis.

SECTION VI

AUTOMATIC DAMPING SIMULATION

The automatic damping program was developed and checked out with a polhode motion simulator also programed on the IBM 1130 computer. The simulator was relied on almost completely since the hardware was only available for a few weeks at the end of the project.

Two simulation results are presented here representing two of the extreme conditions. The simulated gyro has 45 deg separating polhode, 2.83 sec polhode period near the A and C axis, and one percent pendulosity components along -B and -A axis. The maximum torquing rate is 0.123 rad/sec.

The first simulation is shown in Figure 19 for the initial spin vector 1.0 deg from the +C axis. An enlarged projection of a 5 deg region about the +C axis is presented in Figure 20 to more clearly show the initial trajectory. An enlarged projection of a 5 deg region about the +A axis is presented in Figure 21 to more clearly show the final trajectory. The initial C family sign is wrong and is reversed on the second identification. Torquing is continuously applied thereafter until the transition zone is entered. Since the MUM magnitude slope was so large some minima were missed and the +A axis was not yet identified. Torquing stops for one polhode period after entering the transition zone while the +A axis is identified. This feature is no longer required and not now programed. Torquing resumes through the transition zone. After 3 maxima on the A family side of the transition zone, SMAX is zero and A family control is now used. When the ANbhd is entered control is applied until the desired control angle, NANG, is achieved. The sudden changes in trajectory direction shown in Figure 21 make it easy to see the times at which torque is applied. Table 2 lists the major events during simulation and their time of occurrence. The damping was completed in 67.8 sec with the spin vector 0.02 mrad from the +A axis.

The second simulation is shown in Figure 22 for the initial spin vector 3 deg from the -A axis. An enlarged projection of a 5 deg region about the -A axis is presented in Figure 23 to more clearly show the initial trajectory. An enlarged projection of a 0.5 deg region about the +A axis is presented in Figure 24 to more clearly show the final trajectory. The initial polhode phase was wrong by 180 deg causing the initial torque to move the spin vector towards the -A axis. The phase is automatically corrected by the "pig tail" motion shown in Figure 23 and torquing moves the spin vector into the +C family. After 3 maxima on the C family side of the transition zone, torquing is stopped for one polhode period while the +A axis is identified. Torquing is resumed moving the spin vector into the +A family. From this point all events are similar to the first simulation. Table 3 lists the major events during simulation and their time of occurrence. The damping was completed in 71.7 sec with the spin vector 0.012 mrad from the +A axis.

The torquing rate used here is near the maximum allowable rate since it introduces such a steep slope in MUM magnitude near the C axis that the min and max cannot be recognized. The maximum allowable torquing rate appears to be near 20 deg/polhode period. As shown in Tables 2 and 3 major portion of the time is spent in ANbhd control. The time spent in ANbhd is not torque limited since control is not

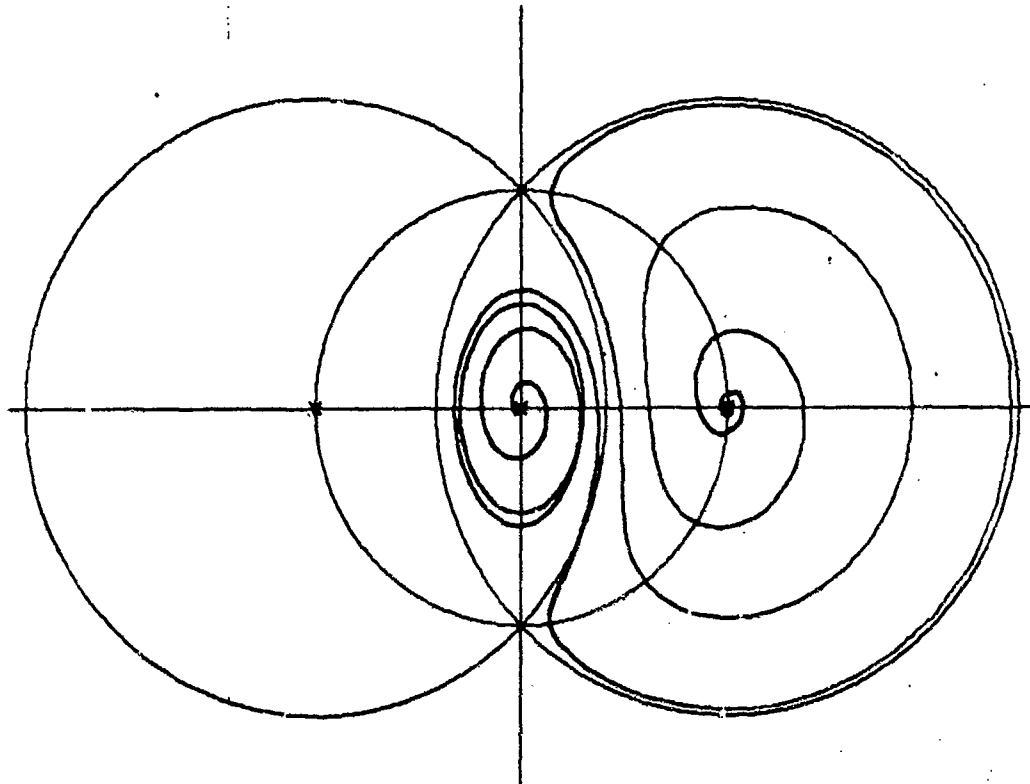


Figure 19. Automatic Polhode Damping Starting 1 Deg Away From +C Axis
(45 Deg separating polhode, 1 percent pendulosity on A and B,
2.83 sec ANbhd polhode period, 0.123 rad/sec max torque)

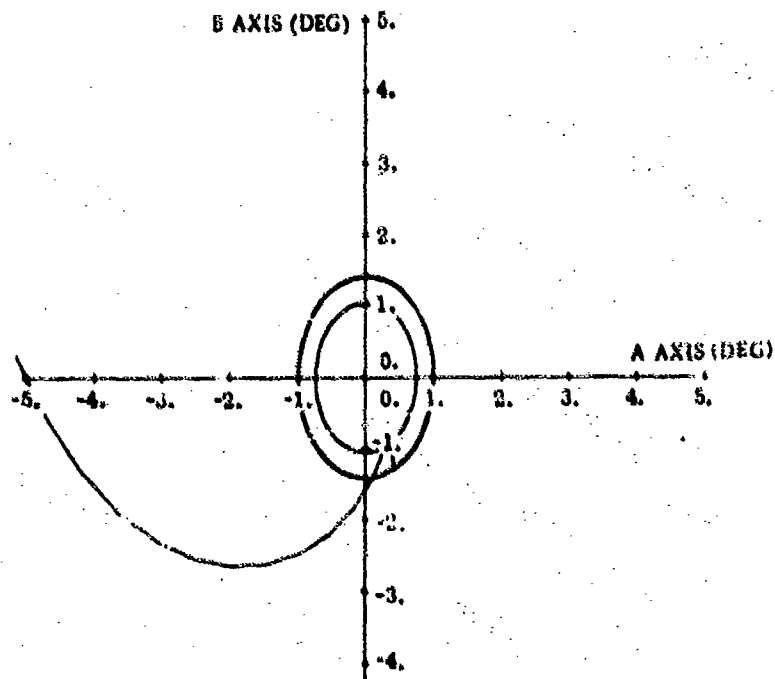


Figure 20. Initial Trajectory of Automatic Polhode Damping
Starting 1 Deg Away From +C Axis

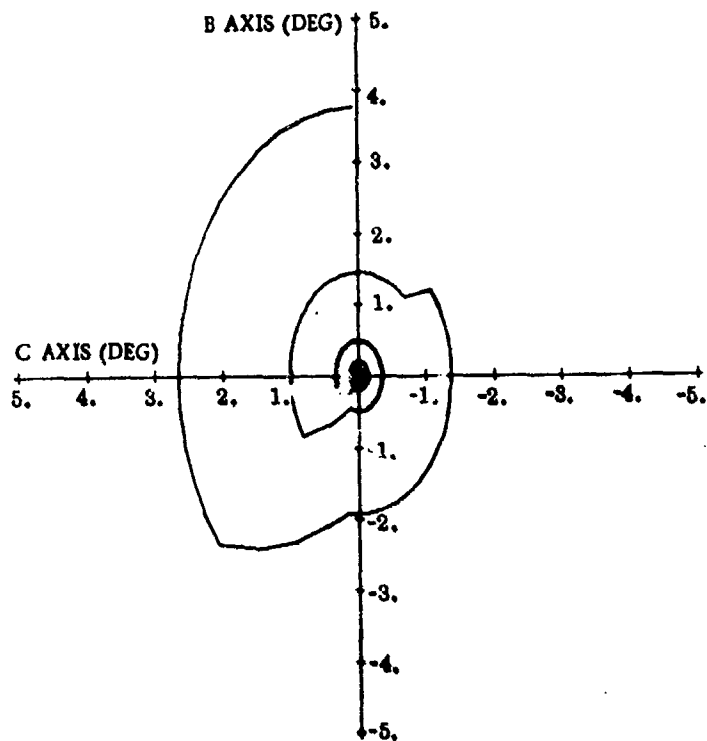


Figure 21. Final Trajectory of Automatic Polhode Damping Starting 1 Deg Away From +C Axis

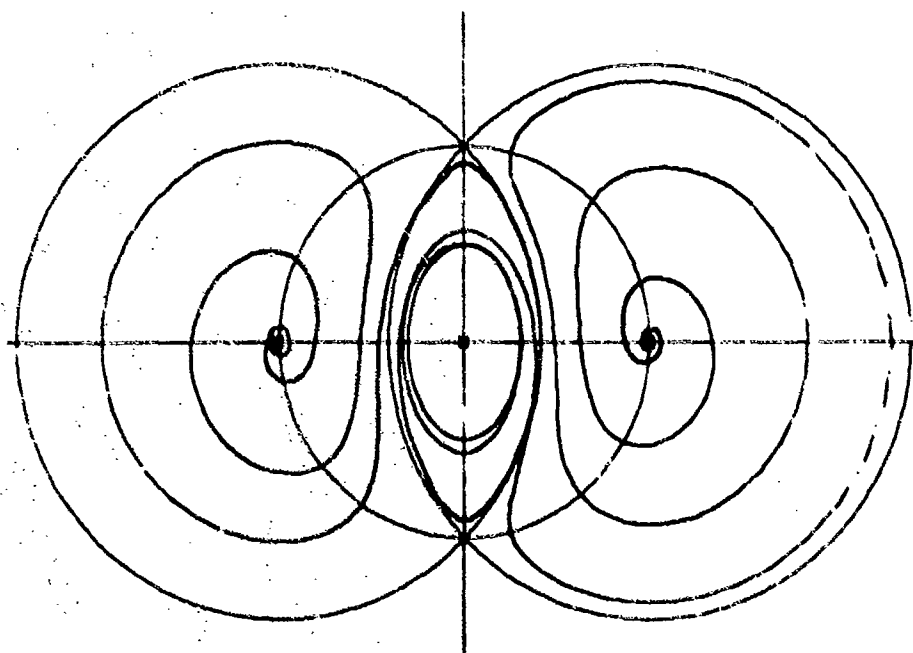


Figure 22. Automatic Polhode Damping Starting 3 Deg Away From -A Axis (45 deg separating polhode, 1 percent pendulosity on A and E, 2.83 sec ANbhd polhode period, 0.123 rad/sec max torque)

Table 2. Table of Events During Automatic Polhode Damping Starting 1 Deg Away From +C Axis

Time (sec)	Number of Polhode Periods	Region		Event
		IFAM	Name	
0	0	6	Undefined	Start program
8.5	3	1	CNbh	First identification - start torquing
11.4	4	1	CNbh	Reverse sign of C Family
15.8	5.5	1	CNbh	NMIN changes from 1 to 2
17.6	6	6	No Torque	Stop torque to identify +A axis
21.6	7	3	Transition	Start torquing again
35.5	9.5	4	A Family	Separating polhode has been crossed
40.2	11	5	ANbh	Enter ANbh
48.7	14	5	ANbh	NMIN changes from 2 to 1
67.8	21	5	ANbh	Damping is complete

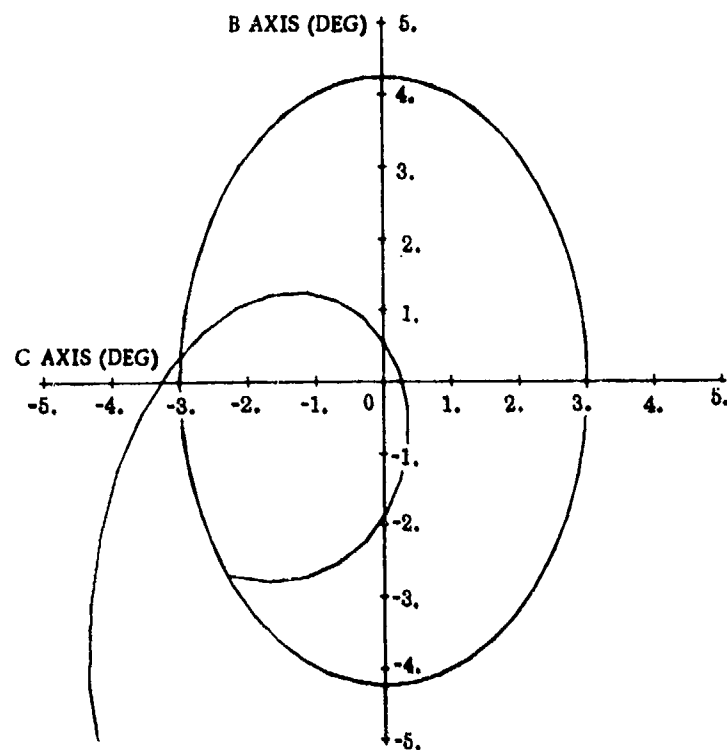


Figure 23. Initial Trajectory of Automatic Polhode Damping Starting 3 Deg Away From -A Axis

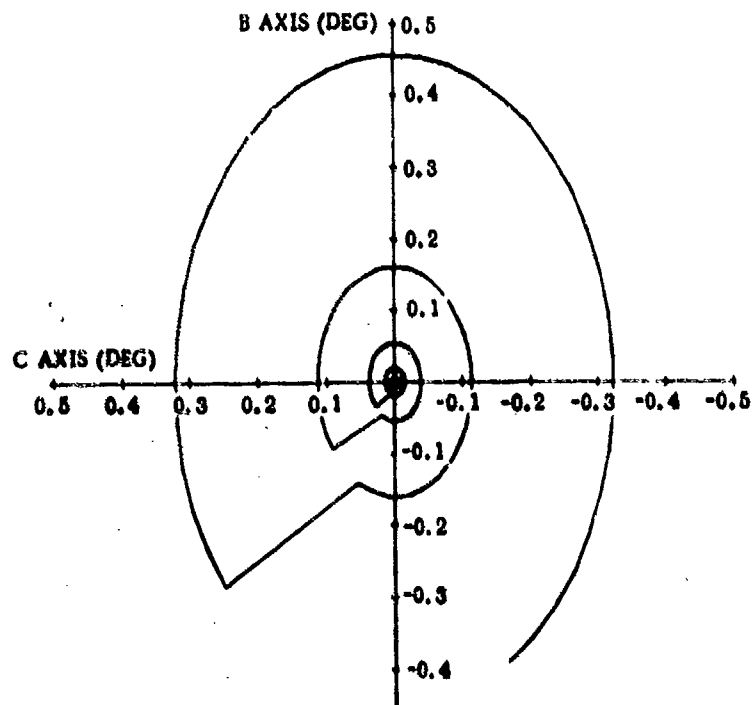


Figure 24. Final Trajectory of Automatic Polhode Damping Starting 3 Deg Away From -A Axis

Table 3. Table of Events During Automatic Polhode Damping Starting 3 Deg Away From -A Axis.

TIME (SEC)	NUMBER OF POLHODE PERIODS	REGION		EVENT
		IFAM	NAME	
0	0	6	Undefined	Start program
4.5	1.5	5	ANbhd	First identification - start torquing
7.7	2.5	4	A Family	Enter A Family
10.9	3.5	3	Transition	Enter Transition zone
25.8	6	6	No Torque	Separating polhode has been crossed - Stop torque to identify +A axis.
29.8	7	3	Transition	Start torquing again
42.3	9	4	A Family	Separating polhode has been re-crossed
47.0	10.5	5	ANbhd	Enter ANbhd
55.5	13.5	5	ANbhd	NMIN changes from 2 to 1
71.7	19.5	5	ANbhd	Damping is complete

applied all of the time. The proportional control gains could be increased to reduce the time required but this would increase the danger of instability and phase loss. If the pendulosity component on the A axis, θ_0 , was calibrated for each rotor, a more efficient ANbhd control law could be devised.

SECTION VII

SPIN MOTOR CONTROL ELECTRONICS

The function of the Spin Motor Control Electronics is to control the inputs to the motor coil windings of the MESG as directed by the computer. A block diagram of these electronics is shown in Figure 25. The Spin Motor Control Electronics can perform the following functions:

1. Rotor Heating
2. Rotor Spin-Up
3. Polhode Motion Damping of the Rotor
4. Rotor Spin Axis Positioning
5. Rotor Braking

The electronics have the capability of performing any control law which may be derived for polhode motion damping. These electronics have been designed so that two MESG's may be controlled by a single power amplifier.

The Spin Motor Control Electronics consist of three different modules:

1. Spin Motor Controller
2. Spin Motor Timing
3. Spin Motor Power Amplifier

A description of the operation of each of these modules is given in the following sections.

1. SPIN MOTOR CONTROLLER MODULE

The Spin Motor Controller Module is a plastic laminated module with overall dimensions of 4.3 by 6.18 in. The functional block diagram of this module is shown in Figure 26. The Spin Motor Controller accepts nine data words from the computer ($A_x, A_y, A_z, B_x, B_y, B_z, S_x, S_y, S_z$) and then performs the operations described in the following equation:

$$\bar{F} = \bar{A} (1/2 \{1 - \cos 2 \omega_s t\}) - \bar{B} (1/2 \sin 2 \omega_s t) + \bar{S} \cos \omega_s t$$

where

\bar{F} is a 3 x 1 vector representing the X, Y and Z components of the motor flux

\bar{A} is a 3 x 1 vector representing the X, Y and Z components of the in-phase component of the MUM vector.

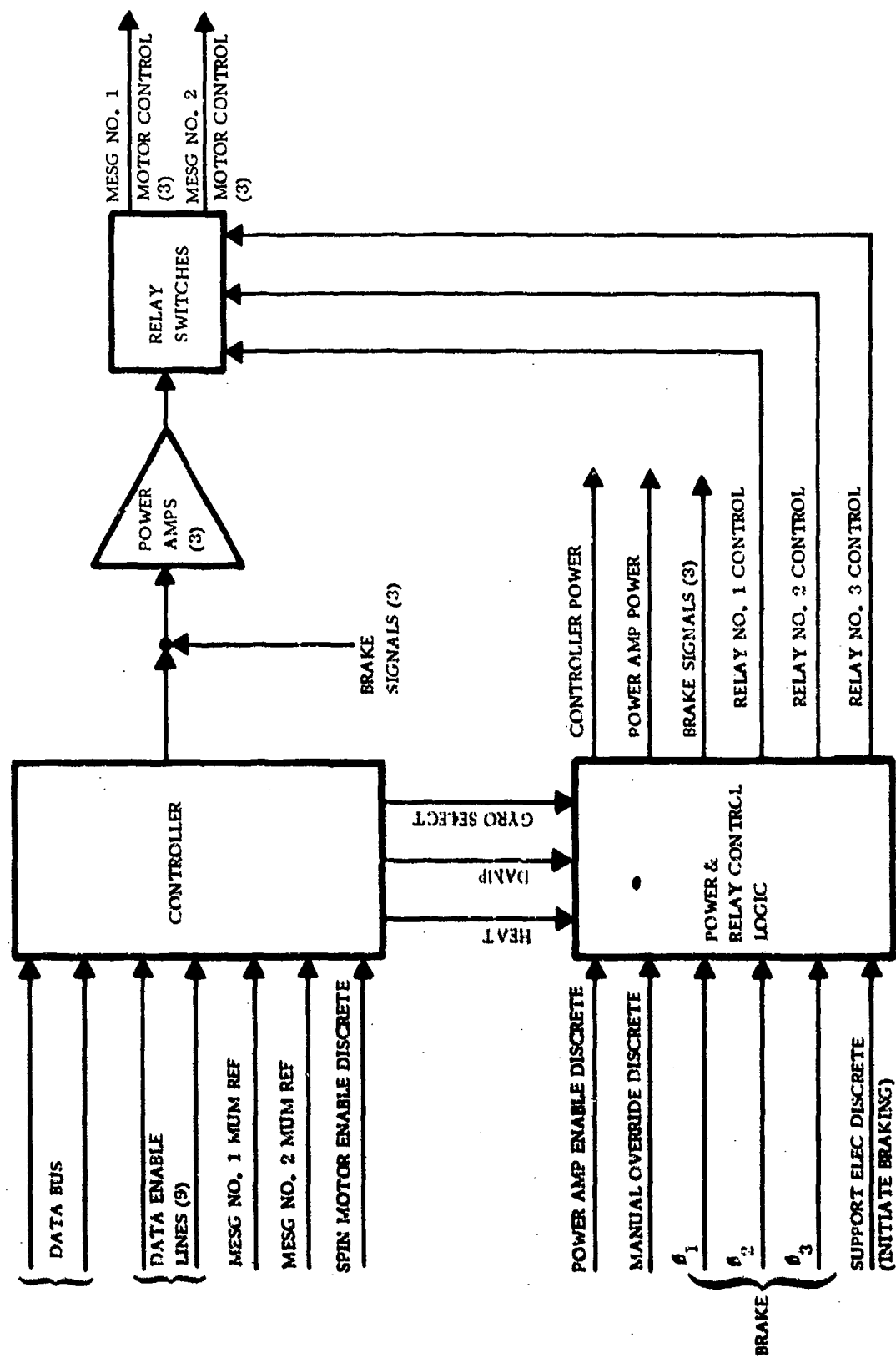


Figure 25. Functional Block Diagram of Spin Motor Control Electronics

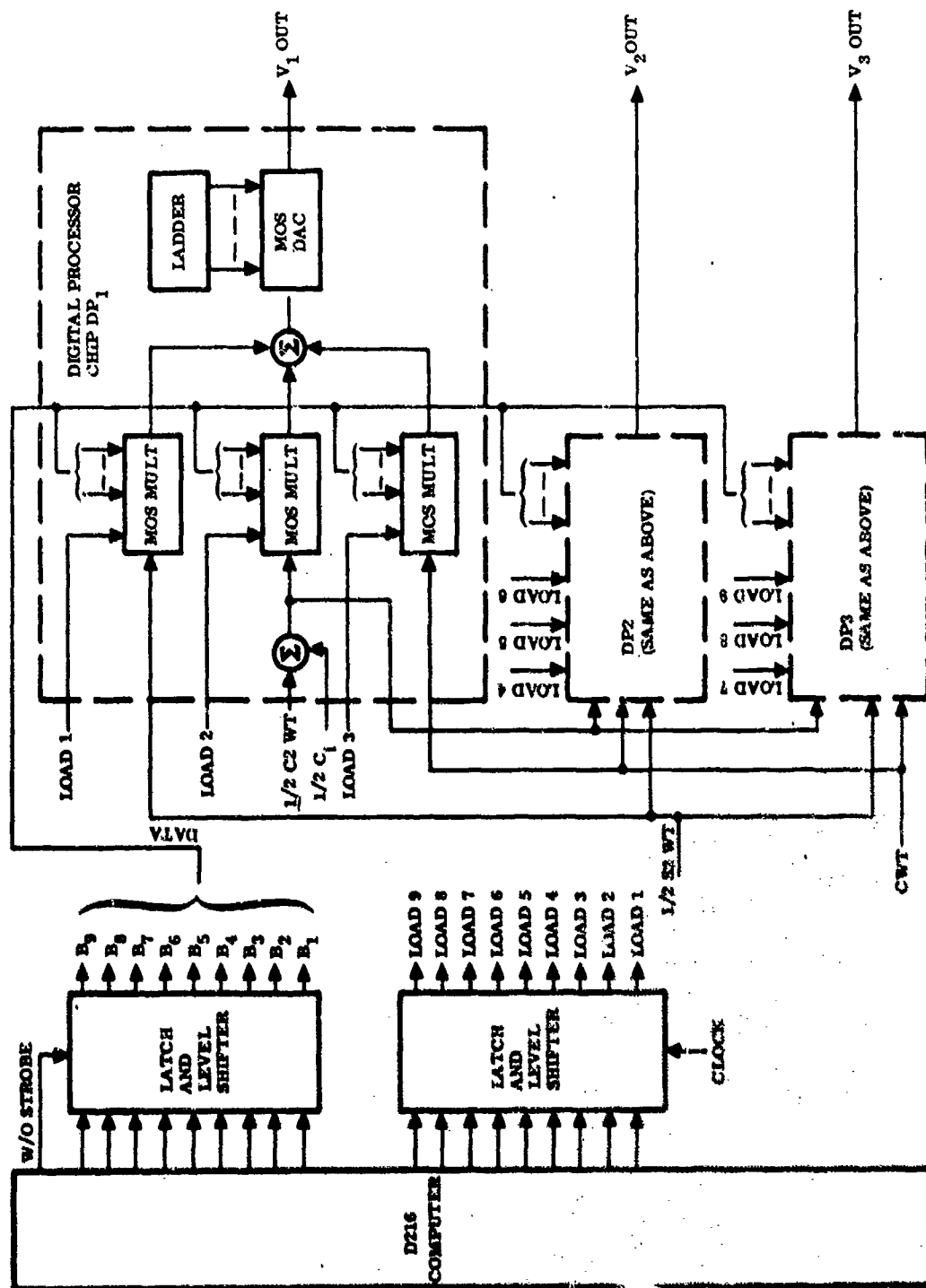


Figure 26. Spin Motor Controller Module Block Diagram

\bar{B} is a 3 x 1 vector representing the X, Y and Z components of the quadrature component of the MUM vector

\bar{S} is a 3 x 1 vector representing the X, Y and Z direction cosines of the MESG spin axis in case coordinates

ω_s is the MESG spin rate

The following damping function is satisfied by the above equation. The Heat and Spin-Up functions are accomplished by controlling the values of the \bar{A} , \bar{B} and \bar{S} vectors. The heat function requires only the \bar{B} terms to be set, with \bar{A} and \bar{S} being set equal to zero. The Spin-Up function requires the \bar{A} and \bar{B} terms to be set with the \bar{S} terms set equal to zero and the dc component of the $(1 - \cos 2\omega_s t)$ term removed.

The digital data words are transmitted from the computer to the Spin Motor Controller sequentially in nine words. The order of the digital data words is as follows:

Word 1	Ax + 3 Control Bits
2	Bx
3	Sx
4	Ay
5	By
6	Sy
7	Az
8	Bz
9	Sz

The Control Bits in Word 1 are as follows:

	T_3	T_2	T_1
Heat	0	0	1
Damp	0	1	0
Gyro Select 1	0	0	0

2. SPIN MOTOR TIMING MODULE

The Spin Motor Timing Module, Figure 27, is packaged on a fiberglass printed circuit board with dimensions of 6.18 by 4.3 in. This module phase locks to the gyro rotor frequency and generates all the necessary timing and clock signals for the Spin Motor Controller module.

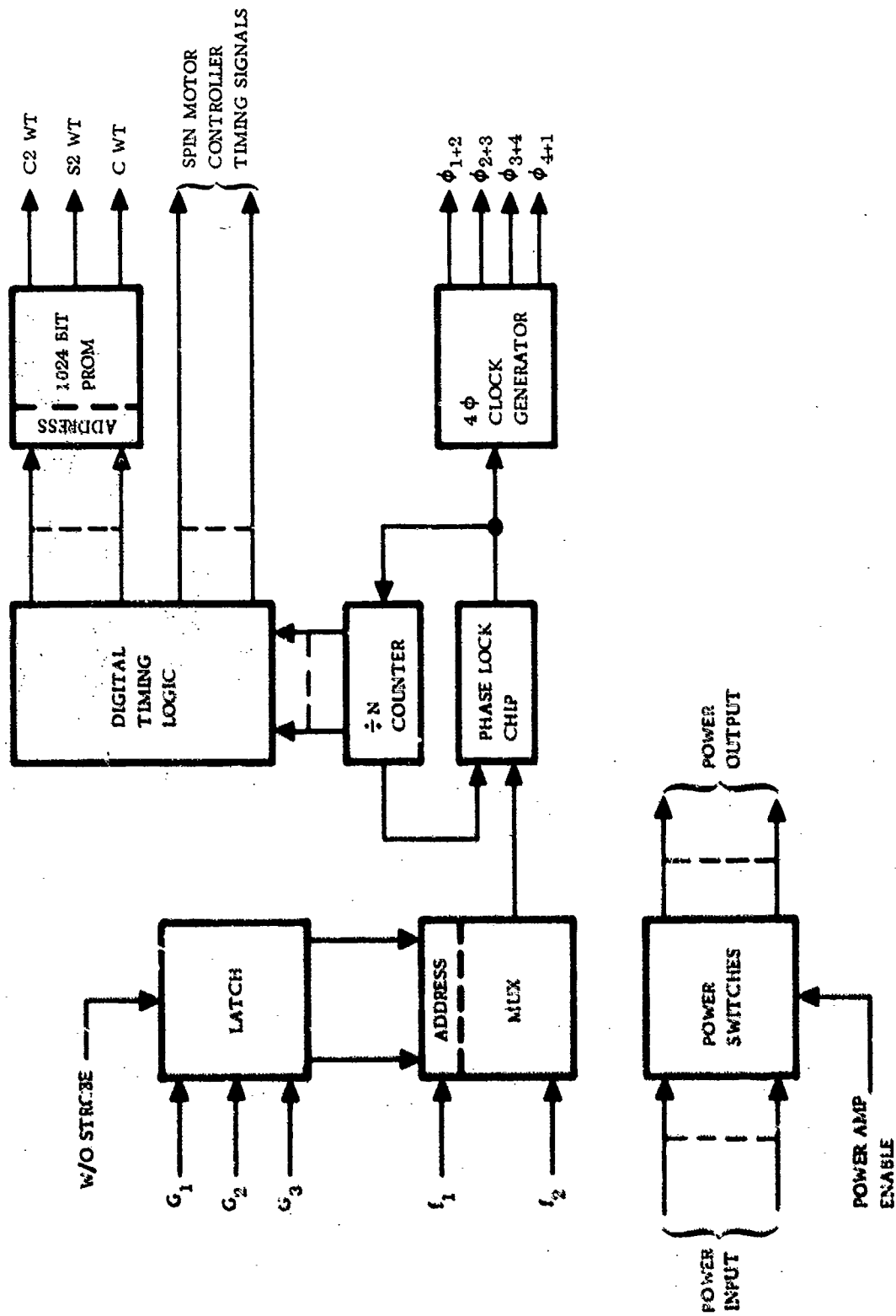


Figure 27. Spin Motor Timing Module Block Diagram

3. SPIN MOTOR POWER AMPLIFIER

A block diagram of the Spin Motor Power Amplifier is shown in Figure 28. Relays and logic have been incorporated into this design so that the power amplifier can be used for either of the two MESH's as determined by the state of the Gyro Select Discrete. The application of one of the Braking Discretes (ϕ_1 , ϕ_2 , or ϕ_3) results in a dc current applied simultaneously to one MESH motor coil on each gyro. Braking is accomplished by sequentially applying a dc current to each of the coils for 6.5 sec.

The amplifier is presently limited to 1 ampere maximum output current and a peak voltage swing of 24 volts. Transistors are available, however, which could be used to replace those presently being used so that the peak output voltage would be about 60 volts. The dimensions of the Spin Motor Power Amplifier are 5.27 by 2.06 by 6.00 in.

4. HARDWARE PROBLEMS

The MOS/LSI Serial/Parallel Multipliers and Shift Register/Address used for the digital multiplication function have presented problems due to limitation in operating speed. The clock for these devices must be phase locked to the rotor speed, and is therefore proportional to the rotor speed. If the rotor is damped at 2500 Hz, a clock frequency of approximately 1 MHz is required. However, process changes when manufacturing these MOS devices has resulted in an extremely low yield in the number of devices which will operate at this frequency. The majority of these devices will operate at a clock frequency less than 820 kHz, which required a proportionate reduction in speed at which the rotor is damped.

Better filtering was found to be required on the -5 volt reference to the MOS devices. A capacitor was added to provide this filtering.

In order to assure that the words from the computer were loaded into the proper multiplier, the word strobe was synched with the word load command.

5. PROPOSED ELECTRONICS DESIGN IMPROVEMENTS

As a result of the studies and tests conducted on this program, a number of hardware design improvements have been identified.

An improved mechanization for the Spin Motor Controller and Spin Motor Timing Modules is shown in Figure 29. The new electronics reduce the component count from 159 for the existing system to 76 for the new design. This very significant reduction is accomplished by performing the nine multiply operations with switches which are driven by quasi-square wave reference signals. The analog inputs to these switches are the nine coefficients from the computer which are required for spin motor control. The output from the switches are then summed and filtered with two first order low pass filters. The resulting waveform contains 9.5 percent distortion on the fundamental harmonic and 3.8 percent distortion on the second harmonic, which is satisfactory for polhode damping. The quasi square wave electronics will be capable of operating at full rotor speed of 2430 Hz.

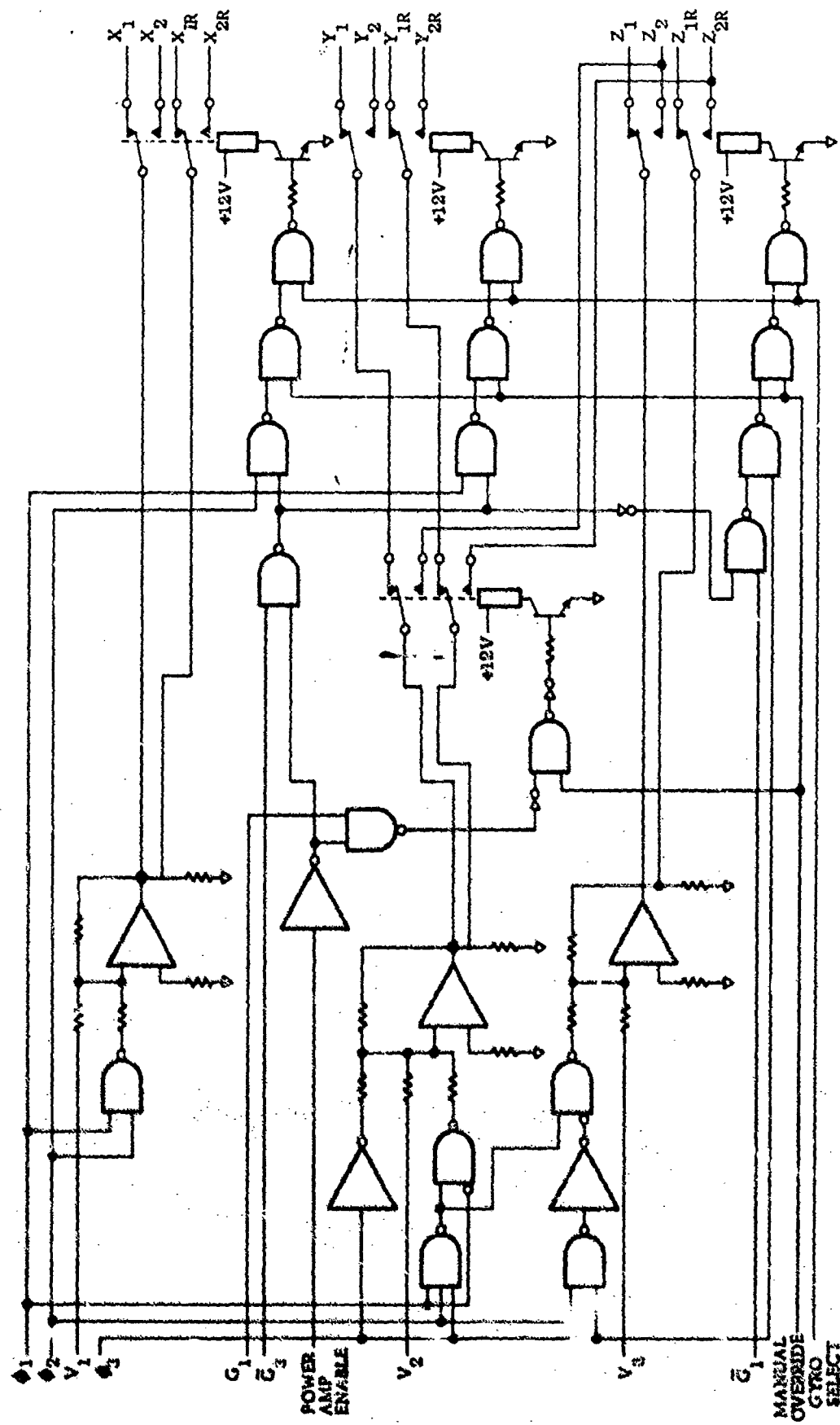


Figure 28. Spin Motor Power Amplifier Functional Block Diagram

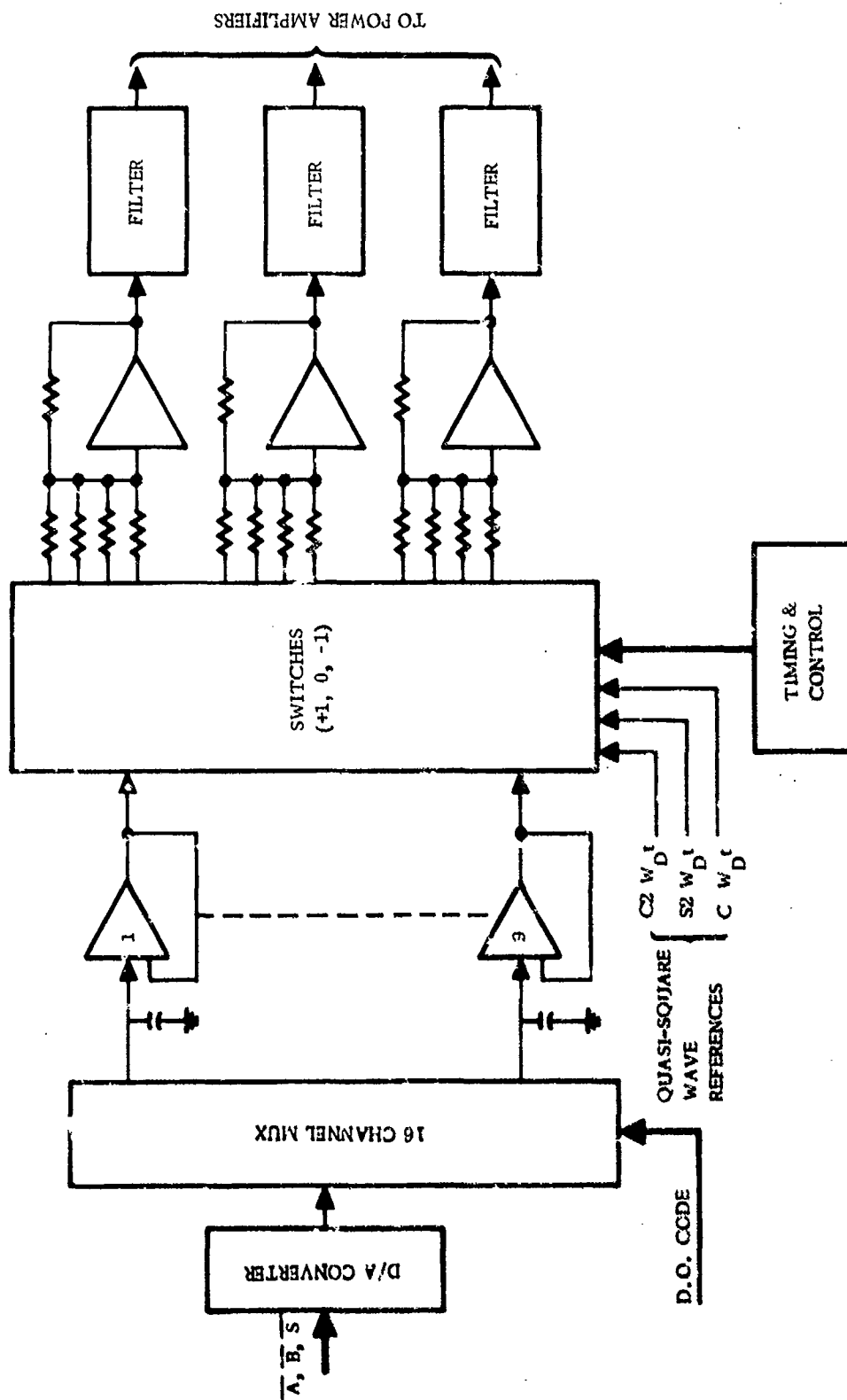


Figure 25. Simplified Spin Motor Control Electronics

SECTION VIII

TEST RESULTS

1. MUM MAGNITUDE SIGNAL

The observed MUM magnitude signal behaves like the simulated MUM magnitude signal except for very small signals near the A axis. Here the A/D converter quantization and noise become very significant. Also the rotor speed variation due to torquing and electrostatic forcing cause very significant MUM magnitude variations near the A axis as described in Appendix A.

The effects of A/D converter quantization and noise are controlled by sampling MUM data many times and digitally filtering MUM magnitude with a first order filter. The time constant of the filter depends on the expected frequency content and amplitude of the MUM magnitude signal. For one min per period in the ANbhd the time constant is 0.8 sec, for two min per period in the ANbhd the time constant is 0.4 sec, and otherwise it is .05 sec. The data window size of the max/min filter should be approximately half the time between minima for maximum noise rejection. The normal window size is 1.7 sec which is adequate for two min per period. However it is inadequate for one min per polhode period in the ANbhd. Therefore the max/min filter is only entered every other computational cycle when number of minima is one in the ANbhd to give an effective window size of 3.4 sec. Figures 30 and 31 show MUM magnitude data filtered with a 0.8 and 0.05 sec time constant respectively. The rotor is very close to the A axis but is not completely damped. Both figures show the same polhode trajectory. The triangles plotted in Figure 30 represent the computer estimates of the max and min points. The value of the least significant bit of the A/D converter is also shown on Figure 30.

The MUM magnitude variation with rotor speed due to electrostatic forcing can be seen in Figure 30. The max/min filter must know the average slope in order to find the max and min with small amplitudes. The slope may change significantly when torque is applied so only the untorqued slope should be used with the max/min filter. Figure 32 shows the MUM magnitude with torque pulses occurring every other polhode cycle. Both the torque and forcing effects on MUM magnitude can be seen.

The peak-to-peak amplitude is used for proportional control in the ANbhd. The peak-to-peak amplitude must be corrected for slope. For the larger signals in the ANbhd a smoothed slope of the maxima is used. This slope is not adequate for small amplitude signals since it is a combination of torquing and forcing effects. For small amplitude signals the peak-to-peak amplitude and untorqued slope are measured by observing untorqued polhode motion for one complete cycle between each period of torquing. This increases the terminal control damping time by a factor of two but it is absolutely necessary.

MUM magnitude slope also causes difficulty in undamping from the A axis. The signal can become "lost" due to the large slope caused by torquing and min cannot be found. The solution is to torque for a maximum of one half a polhode period between minima in ANbhd.

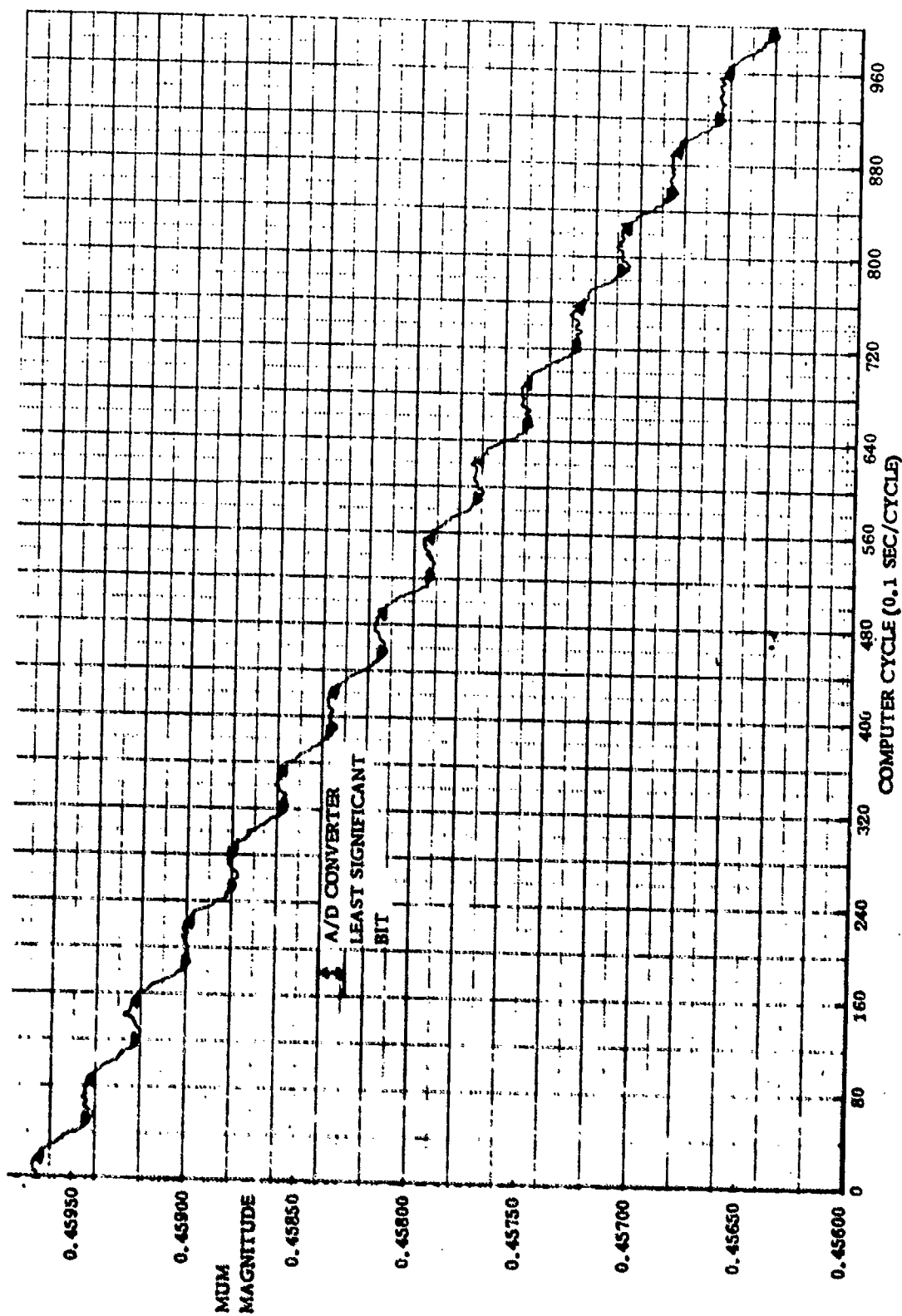


Figure 30. Polhode Motion Residual of Run 2, Gyro 59
(Filter Time Constant = 0.8 sec, PPF = 0.0002)

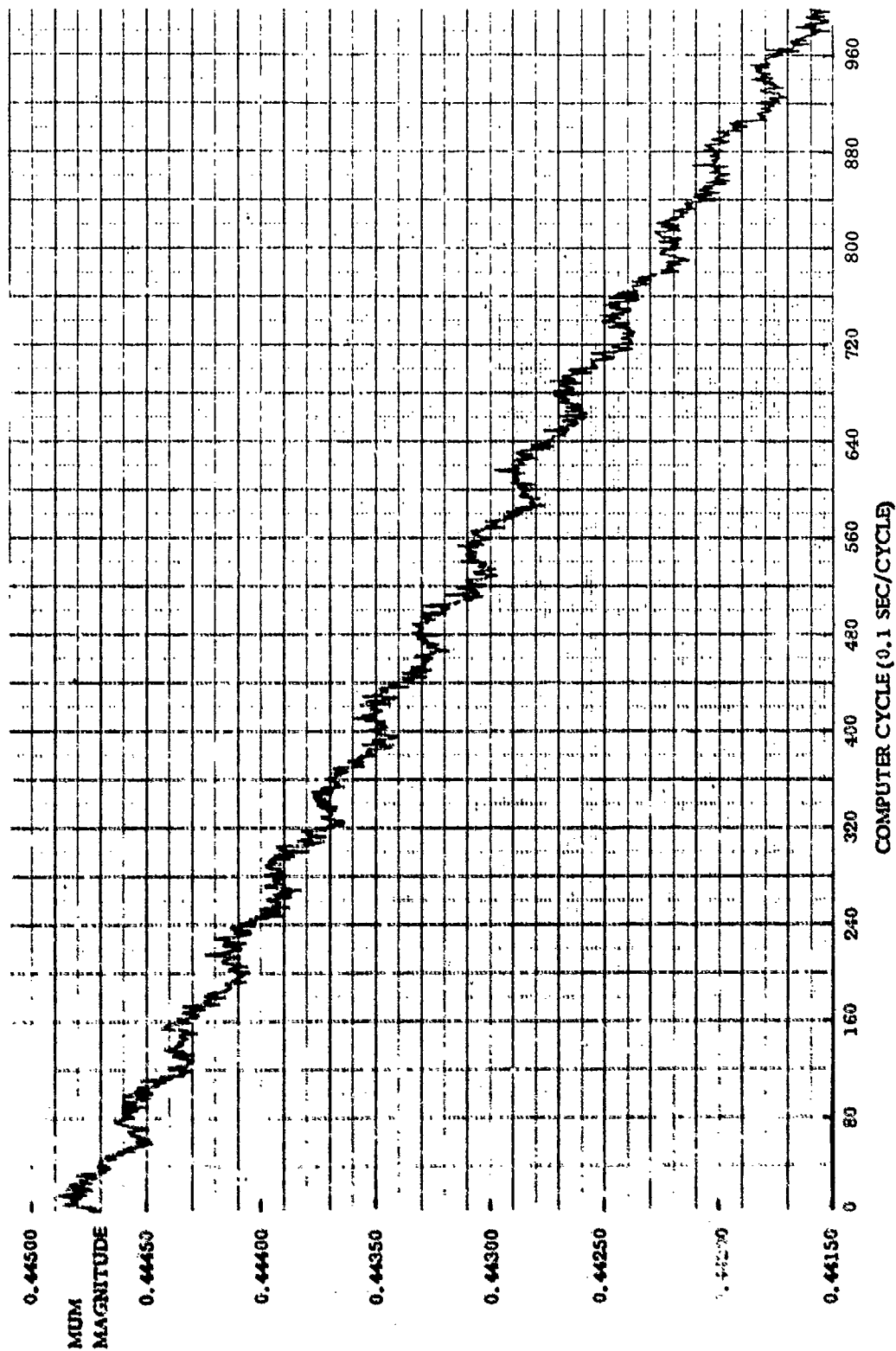


Figure 31. Polhode Motion Residual of Run 2, Gyro 59
(Filter Time Constant = 0.05 sec, PPF = 0.0002)

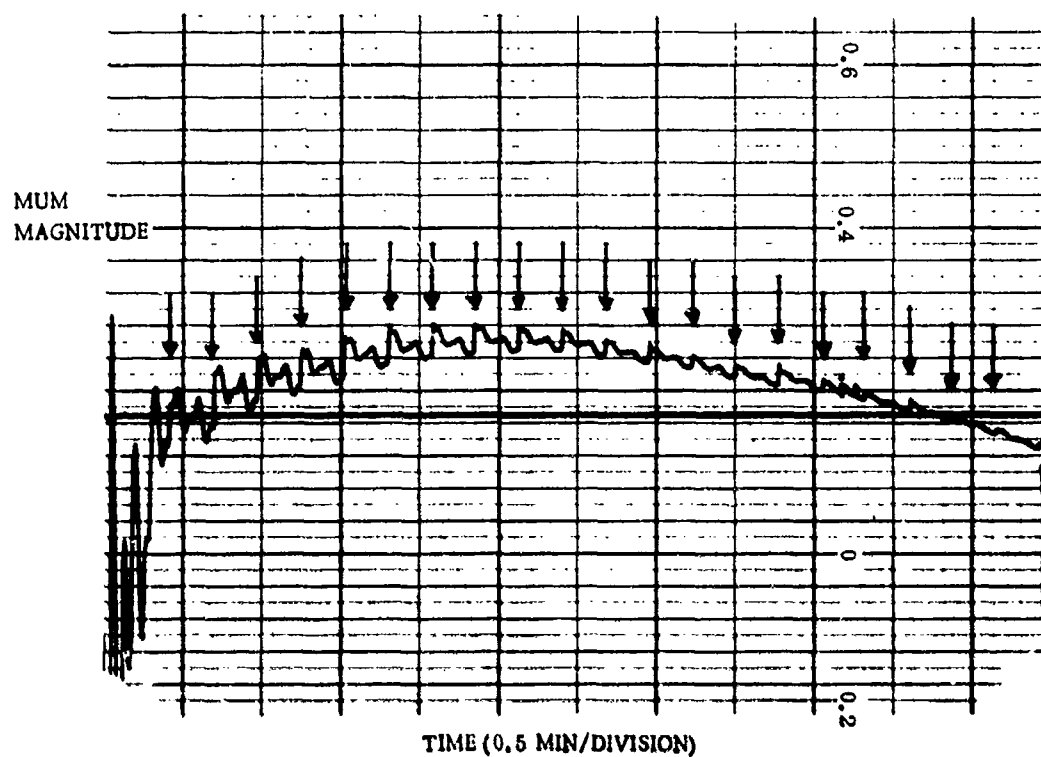


Figure 32. Small Angle Recorder MUM Magnitude Plot with Torque Pulses Applied at the Arrows

2. POLHODE DAMPING PARAMETER DETERMINATION

Automatic polhode damping primarily depends on 16 parameters that are related to hardware parameters. The nominal value of the hardware parameters and their maximum and minimum values are required. No calibration of individual gyros or electronics are required. A range of ± 10 percent of parameter values can be tolerated. A larger range can be tolerated on at least some parameters.

Only six basic hardware parameters are required. They are:

1. maximum torquing rate
2. maximum MUM magnitude
3. polhode period near A axis
4. polhode period near C axis
5. net phase shift on MUM signal
6. noise level on MUM magnitude as effects slope and Δ max computations.

Polhode parameters from Gyro 59 have been measured. They are given in Table 4. Pendulosity on A and B axes is also given so that the gyro can be simulated.

Net phase shift is measured by a special mechanization that adjusts the torque direction in the C family to lie tangent to the trajectory on the average. This is done by closed loop control that adjusts torque direction to force slope of minima to zero.

TABLE 4.

Polhode Parameters - Gyro 59, V Series Rotor

Parameter	Value
Maximum torquing rate	1.25 deg/sec
Maximum MUM magnitude	0.48
Polhode period near A axis	85 computational cycles
Polhode period near C axis	79 computational cycles
Net phase shift of MUM signal	36.6 deg
Noise on slope and Δ max computations	See: EPDS, EPDMA, EPSCN, EPSAN of Table 5
Pendulosity on A axis	4 percent
Pendulosity on B axis	14 percent

The net phase shift of the MUM signal is the angle of the final torque direction less 90 deg.

Maximum torquing rate is determined by applying C family control law to the gyro in the C family and recording max, min and the slopes of max and min. A simulation is performed to duplicate the results. The torquing rate used in the duplicating simulation is the same as the torquing rate in the hardware.

The noise level on slope and Δ max computations are bounds based on observing actual automatic damping results and computations without torquing.

The 16 automatic damping parameters are listed in Table 5. AMAP defines the ANbhd size and is arrived at through simulation using the appropriate torquing rate. PPF is determined by the noise level and A/D quantization level in the MUM magnitude. TMAX is directly measured on the gyro by applying C control law through the separating polhode. By looking at the data one can determine which polhode period the transition control law should have been invoked to correctly cross the separating polhode. GPAN2, which is the terminal control gain, is defined by

$$GPAN2 = \text{gain} / \sqrt{2} \text{ (minimum torque angle)}$$

where minimum torque angle = $1/8$ (.0022 rad/sec) (.1 sec).

For gain = $1/.85$, GPAN2 is 3056.

The average torque efficiency near A axis is 85 percent. GPAN2 calculated for automatic damping tests was too small by $\sqrt{2}$ through a computational error. The gain

TABLE 5.

Automatic Damping Parameters Gyro 59 - V Series Rotor

Parameter	Description	Value
AMAX	60 - 70 percent of max MUM	0.34
AMAP	Amplitude of peak to peak normalized MUM in ANbhd	0.015
PPF	Amplitude of peak to peak normalized MUM to terminate damping	0.0001
PHASE	MUM signal phase angle	36.6 deg
EPDS	Threshold for determining that $\max \neq 0$ or that max slope $\neq 0$.02
EPDMA	Threshold for determining that max slope = 0	.008
EPSCN	Threshold for determining that min slope in C family is negative	.004
EPSCN	Threshold for determining that min slope in A family is of wrong sign	.002
TA1	0.75 times polhode period near A axis (computational cycles)	64.
TA2	1.25 times polhode period near A axis (computational cycles)	106.
TC1	0.75 times polhode period near C axis (computational cycles)	59.
TC2	1.25 times polhode period near C axis (computational cycles)	99
TMAX	Minimum polhode period in transition zone (computational cycles)	96.
PTMAX	Maximum time without a min event (computational cycles)	200.
GPAN2	Terminal control gain with 2 min per polhode period	3056
MANG	Maximum control angle (NANG) for terminal control on alternate polhode periods.	80.

was then adjusted empirically as reported in paragraph 3, Section XIII. Only run No. 10 has the calculated value for GPAN2.

NANG is determined by the effect torquing has on MUM magnitude through rotor speed changes. The value is empirically determined.

3. AUTOMATIC DAMPING RESULTS

The final program modification was made on May 10, 1973 and test data was taken on May 11 and 14, 1973. Two gyros were used in the tests, gyros 59 and 68. Both gyros have V series rotors which implies that the rotors were taken from the same extrusion stock and therefore should have similar polhode characteristics. It seems reasonable that the variation in polhode characteristics of these two gyros should correspond to the variation in polhode characteristics between any two gyros taken off the same production line. Calibration data was taken from gyro 59 before the polhode damping tests began and the hardware parameters were estimated as discussed in the previous section. Calibration data has never been taken on gyro 68. The polhode damping parameters arrived at for gyro 59 were used on both gyros 59 and 68.

Two automatic damping parameters were changed during the tests and are not the same on all runs. The damping complete threshold, PPF, was set at .0002 for the first two runs which was too high and left too much residual polhode motion. It was changed to .0001 for the last 8 runs. An error of $\sqrt{2}$ was originally made in computing terminal control gain GPAN2. The gain was obviously too small and so it was empirically adjusted upwards. Before the tenth run the error in computation was discovered and the correct value was used. The history of GPAN2 adjustments is:

RUN	GPAN2
1, 2	2800
3	3500
4, 5, 6	4200
7, 8, 9	3800
10	3056

Even though the gain was grossly misadjusted on some runs the damping was always successfully completed.

Table 6 summarizes the test results. Approximate MUM magnitude plots are shown in Figures 33 through 42 as referenced in Table 6. The plots were recorded by the small angle analog recorder normally used for manual polhode damping and is not the same data processed by the computer. The MUM vector dotted onto a gyro fixed axis is plotted by the small angle recorder so Earth rate is also seen on the plots. Two pens are used to simultaneously record MUM magnitude. The difference in gain between the two pens is approximately 200. Recording speed was 2 divisions/min.

Difficulties were encountered on three of the runs. In each case the difficulty was overcome and damping was successfully completed. Run 3 encountered difficulty getting out of the -CNbhd and damped into the C axis before turning around. It was caused by a program logic error in deciding if the trajectory encloses the pendulosity vector. The initial trajectory of run 3 did not enclose the pendulosity vector however a decision was made that it did. The program found it made an error, automatically restarted, and came out correctly. The logic error is now corrected in the listing given in Appendix D.

Run 6 had a very large terminal control gain as explained earlier. As a result the polhode motion was over controlled and phase loss resulted. The rotor began to

TABLE 6
Test Summary

Run Number	Gyro Number	Total Damping Time (sec)	Time up to Terminal Control (sec)	Time in Terminal Control (sec)	Initial Gap (μin.)	Change in Gap (μin.)	Initial Rotor Speed (hz)	Change in Rotor Speed (hz)	Polhode Period Near A Axis (sec)	Figure Number	Spin Vector orientation with respect to:			Initial Polhode Trajectory
											Earth	Gyro Envelope		
1	59	266	108	158	301	2.5	2066	+9	6.3	33	Vertical	+1 plate		
2	59	401	216	185	299	4.8	2074	-33	7.2	34	Vertical	+1 plate		
3	59	378	200	178	285	5.3	2064	+49	8.4	35	Vertical	+1 plate		
4	59	337	181	156	277	3.3	2056	-11	9.4	36	Vertical	+1 plate		
5	68	282	118	164	310	4.4	2051	+20	7.7	37	North	-3 plate		
6	68	865	164	701	303	5.1	2086	+64	8.5	38	North	-3 plate		
7	68	459	222	237	298	4.2	2059	-114	9.4	39	North	-2, +4 plate		
8	68	409	194	215	295	6.1	2070	+14	10.5	40	North	+3, -2 plate		
9	68	560	259	301	289	6.1	2071	+42	11.3	41	North	+3, -2 plate		
10	68	271	128	143	296	2.4	2064	-25	7.5	42	Vertical	+1 plate		
														A near separating polhode

undamp. This was recognized and phase lock was re-established. The terminal control gain was reduced by one half and it slowly damped in. Because of the phase loss and reduction of terminal control gain the damping time is very long.

Run 7 encountered a very noisy segment of data during terminal control as can be seen in Figure 39. The suspension electronics has a sampling rate of 10 KHz. When the rotor frequency passes through 2000 hz aliasing causes noise that would otherwise be filtered to appear on the MUM magnitude data. Damping was completed with no difficulty.

It can be seen that a majority of the total damping time is spent in terminal control getting the last few deg. Without the problems of noise and rotor speed - MUM magnitude coupling terminal control can operate at least twice as fast. Terminal control time is also directly related to polhode period near the A axis. Notice as the polhode period increases on successive runs due to increased rotor temperature the terminal control time generally increases. Runs 1 and 9 represent almost a 2:1 increase in polhode period and terminal control time.

Plots of MUM magnitude vs time after damping was completed were taken by the computer for runs 2, 3, 8, 9, 10 and shown in Figures 30, 43, 44, 45, and 46. Runs 1 and 2 had a larger termination threshold and so there is some obvious residual polhode motion in Figure 30. The other 4 plots show almost no polhode residual. However the small angle recording of runs 8 and 9, Figures 40 and 41, show obvious polhode motion residual. This must either be due to greater resolution in the small angle recorder than in the computer interface or polhode modulation of angle readout. Since the small angle recorder indicates only one component of MUM it also responds to apparent attitude change of the spin vector with respect to gyro case. There was insufficient time to resolve this question.

The colatitude of the residual polhode trajectory can be estimated from the MUM magnitude plots if the pendulosity on the A axis is known. The relationship developed for terminal control in Appendix C is:

$$\Delta \theta = PP_N / 2 \theta_0$$

where $\Delta \theta$ is polhode colatitude, θ_0 is A pendulosity, and PP_N is normalized peak-to-peak MUM magnitude. θ_0 was measured for gyro 59 and is $\theta_0 = .04$. Based on data from automatic damping gyro 68 has approximately the same value for θ_0 as 59 has. The following residual polhode colatitudes are estimated from Figures 30, 43, 44, 45, and 46.

Run	Colatitude	PP_N
2	3.3 mrad	0.26×10^{-3}
3	1.6 mrad	0.13×10^{-3}
8	1.4 mrad	0.11×10^{-3}
9	2.3 mrad	0.18×10^{-3}
10	0.4 mrad	0.03×10^{-3}

The efficiency of the torquing can be estimated and compared with the theoretical values computed in Section IV. Run 2 has a known starting point of the A axis. It was undamped through the A family and into the C family possibly by 15 deg. It is then damped out of C and up to the terminal control region that starts at about 10 deg from A axis. With these assumptions the net polhode latitude change up to terminal control is 110 deg. The time spent torquing was 143.5 sec. At a torquing rate of 1.25 deg/sec the efficiency is 61 percent. This compares to the theoretical value of 79 percent.

Before and after each run the gap between rotor and envelope was measured. The change in gap is an indication of rotor and envelope heating. The thermal coefficients of expansion of the rotor and envelope are $0.39^{\circ}\text{F}/\text{min}$ and $0.76^{\circ}\text{F}/\text{min}$ respectively. Additional temperature measurements were made on run 10. Both gap and motor coil temperature measurements were made before damping and periodically for an hour after damping. The motor coil immediately after damping was 4.04°F hotter than before damping. However since no significant power was applied to the coils during the last 2.5 min the peak coil temperature is possible 20°F hotter than before damping. After damping the envelope cools down with a 20 min time constant, while the rotor has an 8 hr time constant. An hour after damping the gap reduced another 0.9μ in which is due to electrode cooling. The temperature changes of the rotor and cavity can be deduced:

$$\text{Rotor heating} = 3.3 \mu\text{in} = 1.3^{\circ}\text{F}$$

$$\text{Electrode heating} = 0.9 \mu\text{in} = 0.7^{\circ}\text{F}$$

for run 10. Heating on other runs should approximately scale as the ratio of the gap changes listed in Table 6.

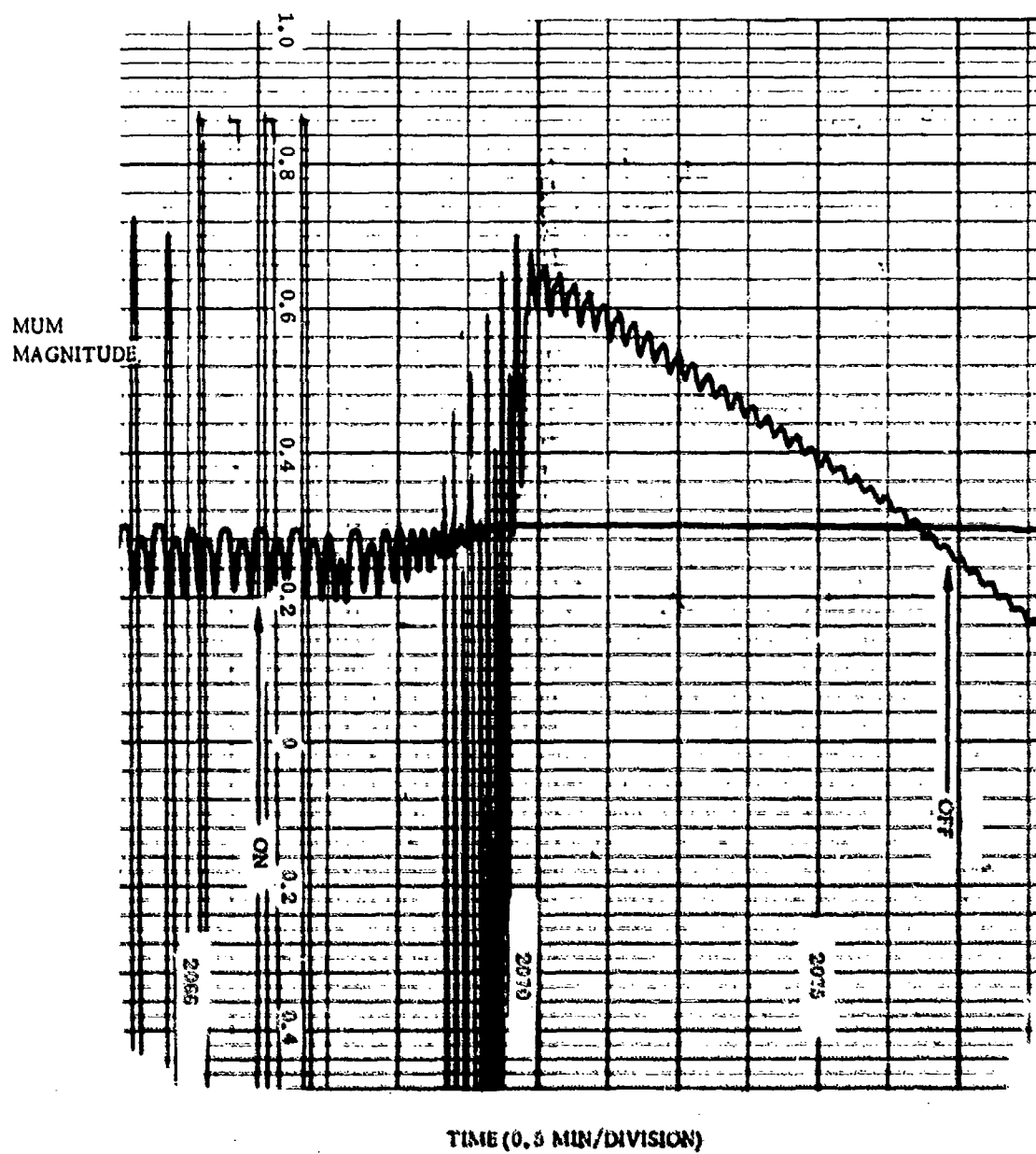


Figure 33. Small Angle Recorder Plot of Run 1, Gyro 54

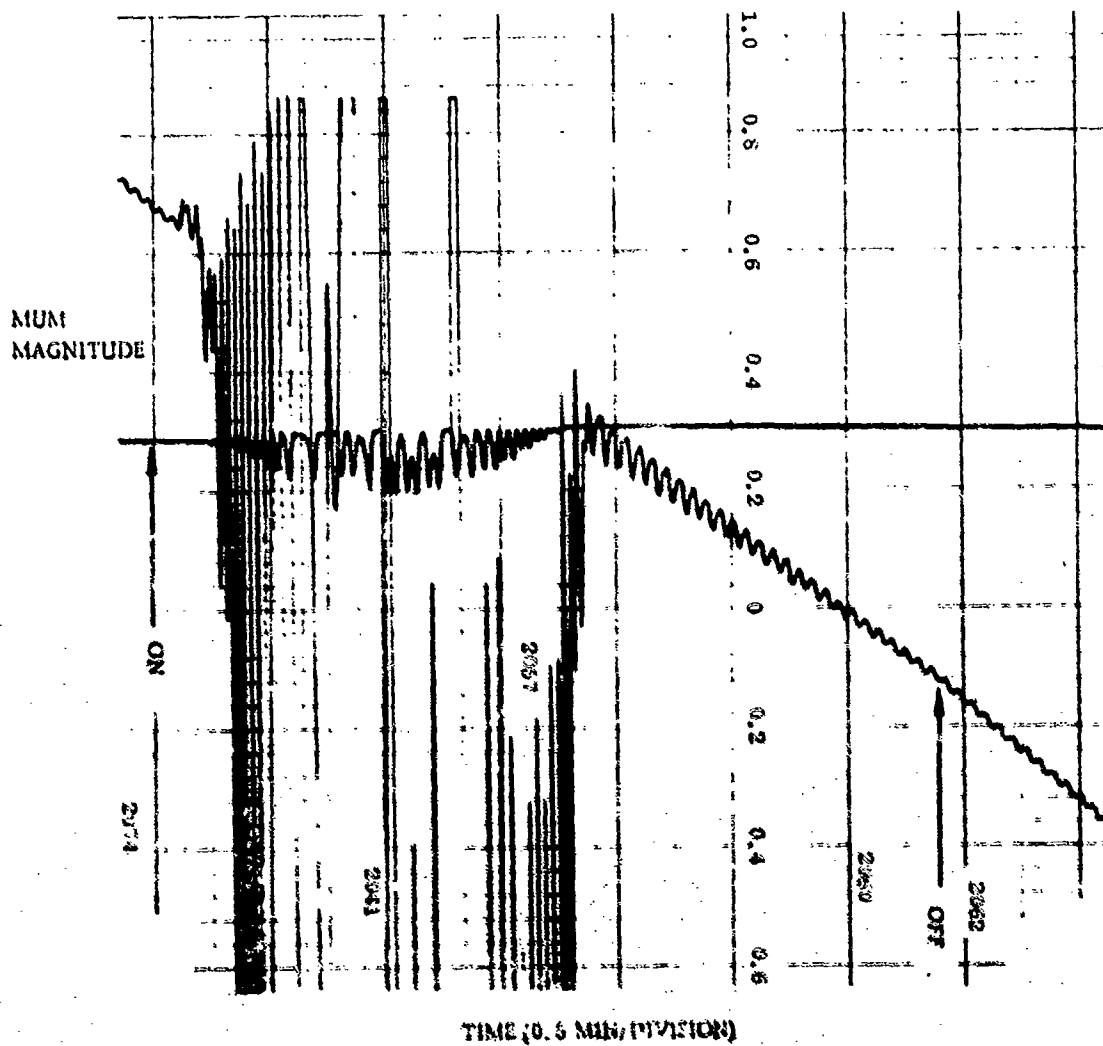


Figure 34. Small Angle Recorder Plot of Run 2, Gyro 08

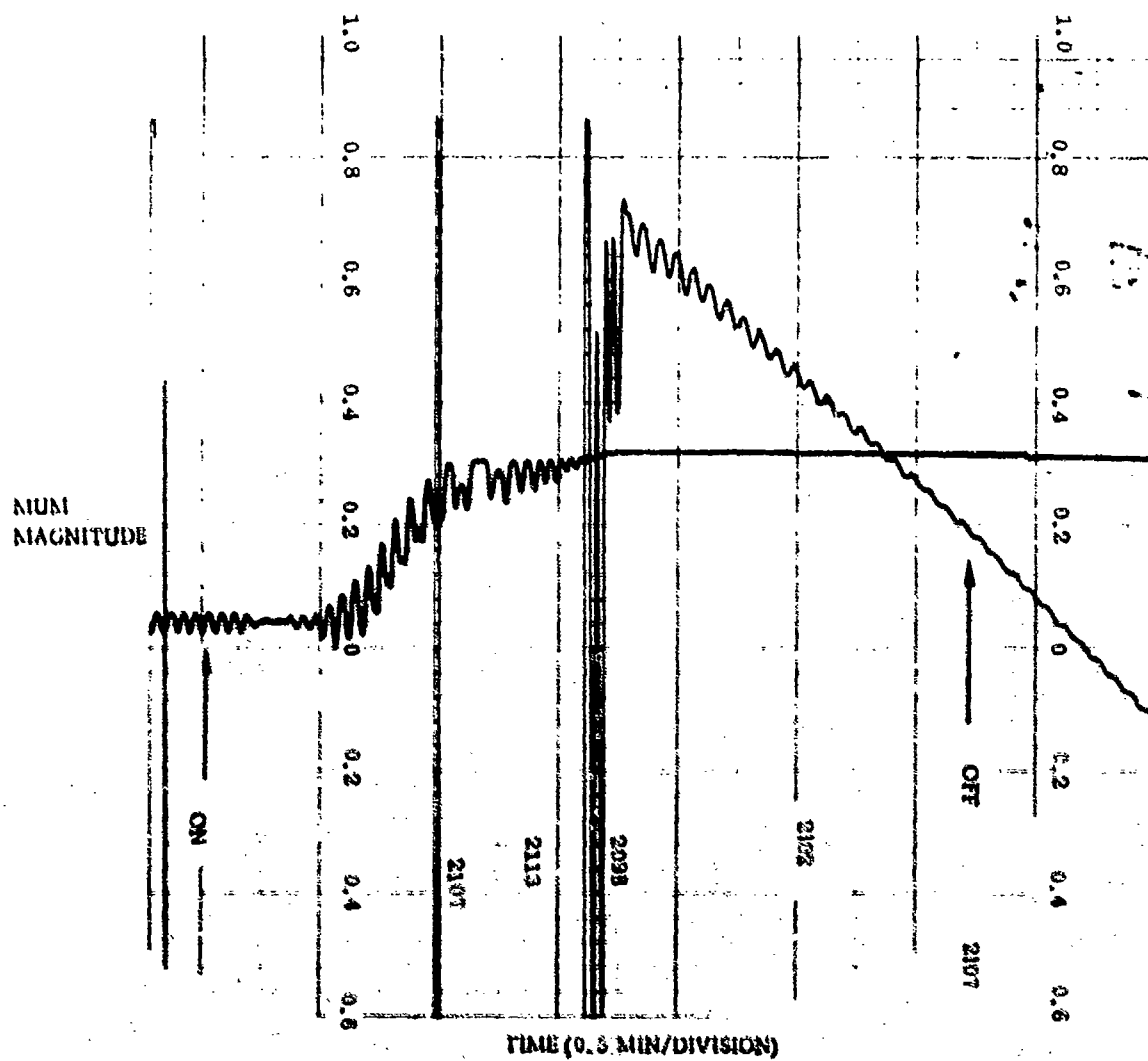
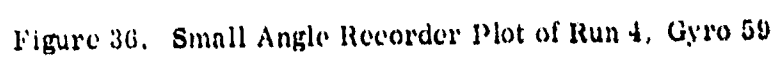


Figure 35. Small Angle Recorder Plot of Run 3, Gyro 59



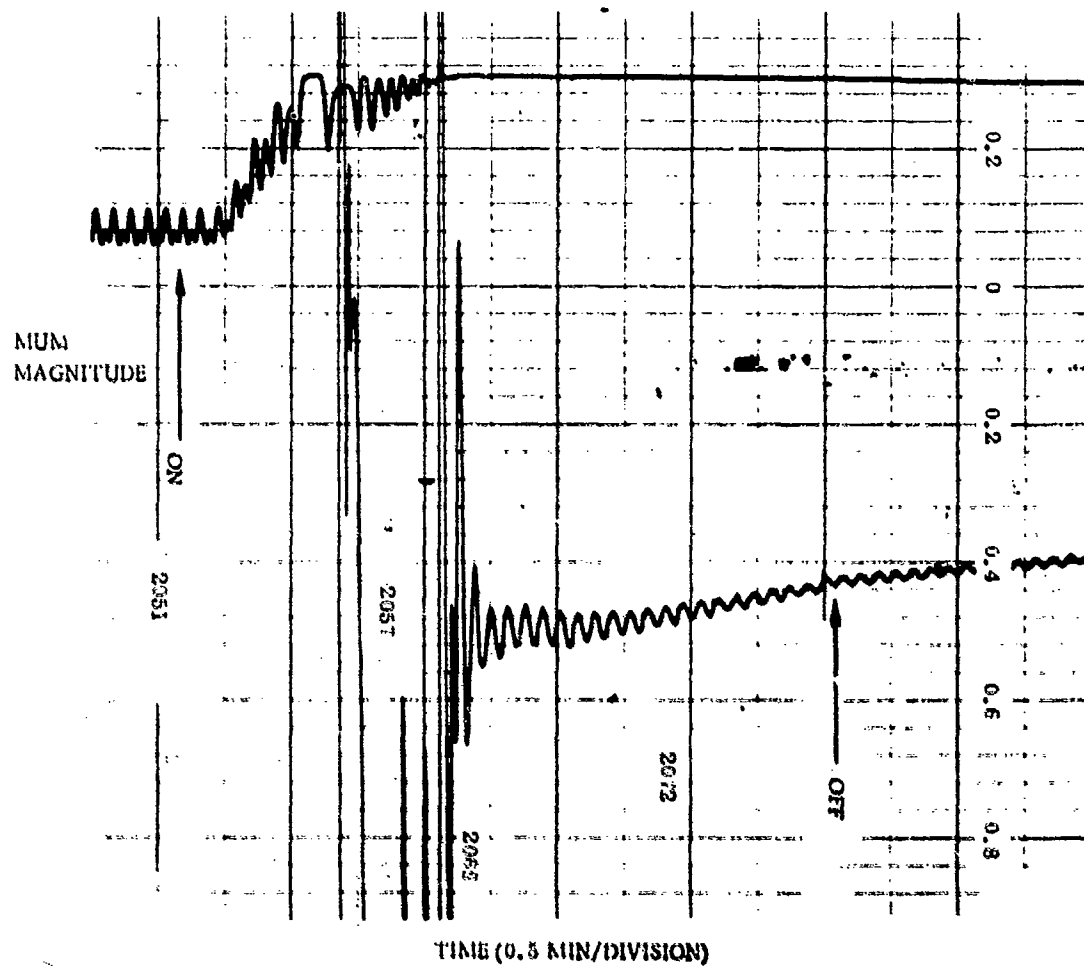


Figure 37. Small Angle Recorder Plot of Run 5, Gyro 68

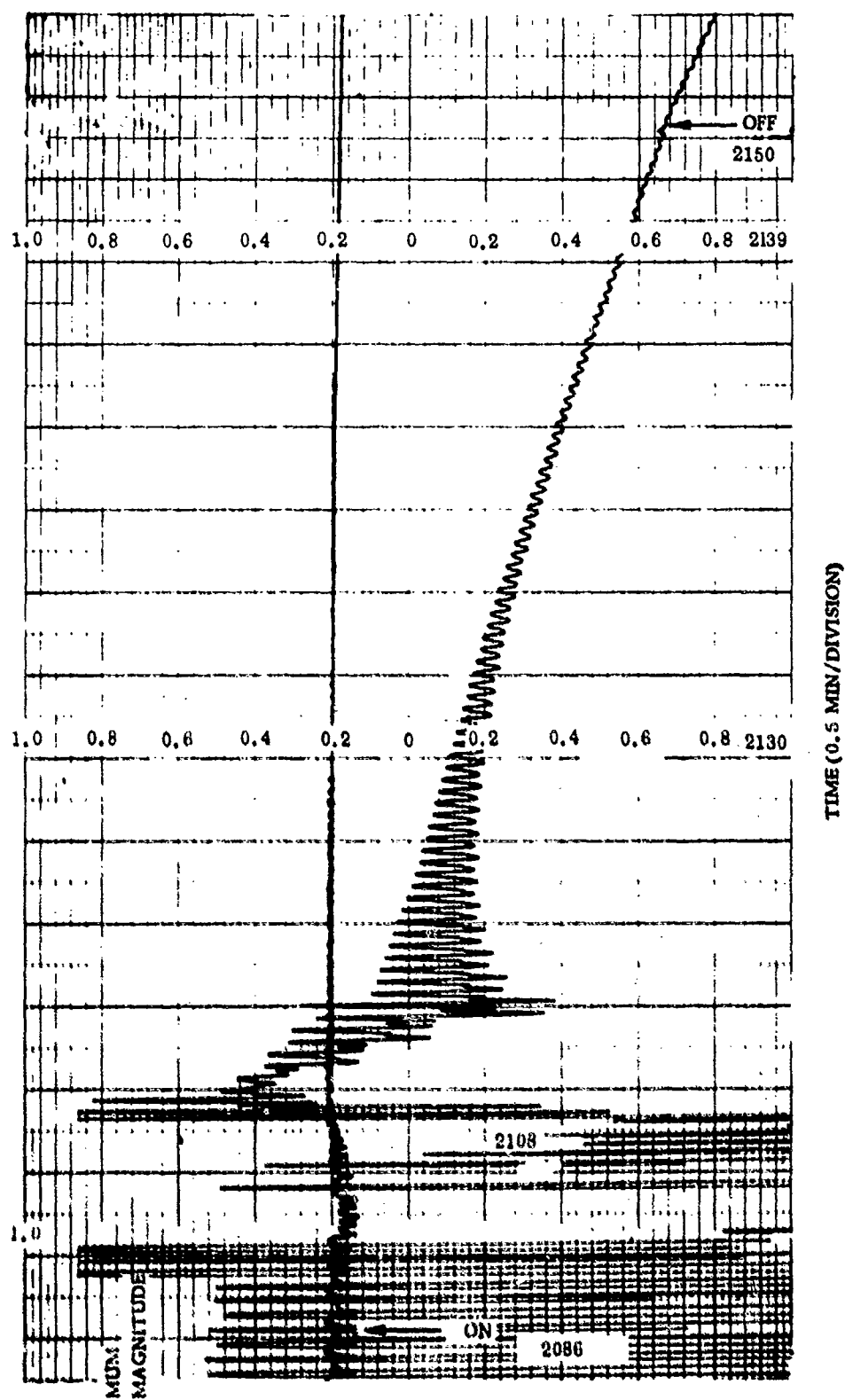


Figure 38. Small Angle Recorder Plot of Run 6, Gyro 58

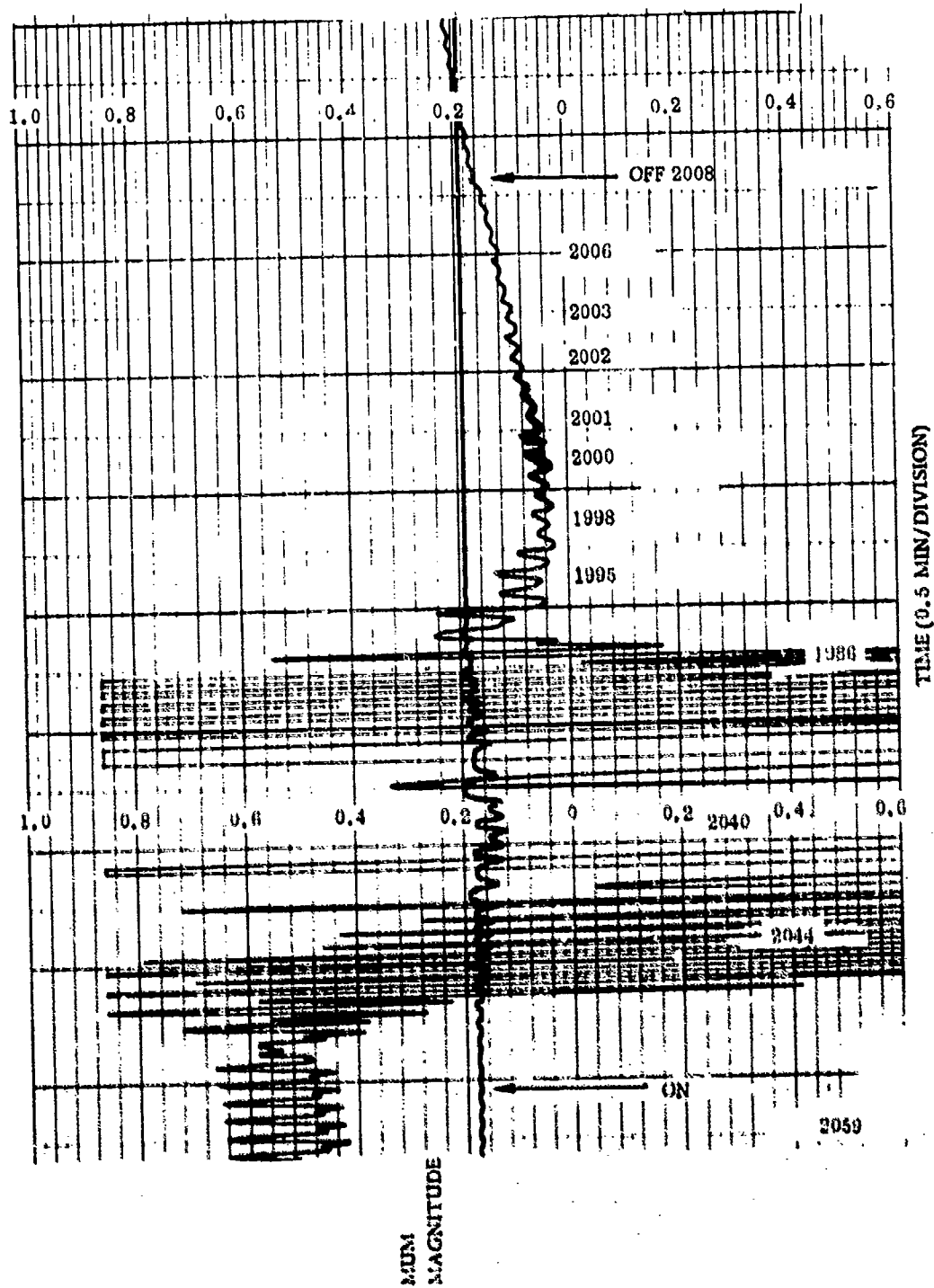


Figure 39. Small Angle Recorder Plot of Run 7, Gyro 68

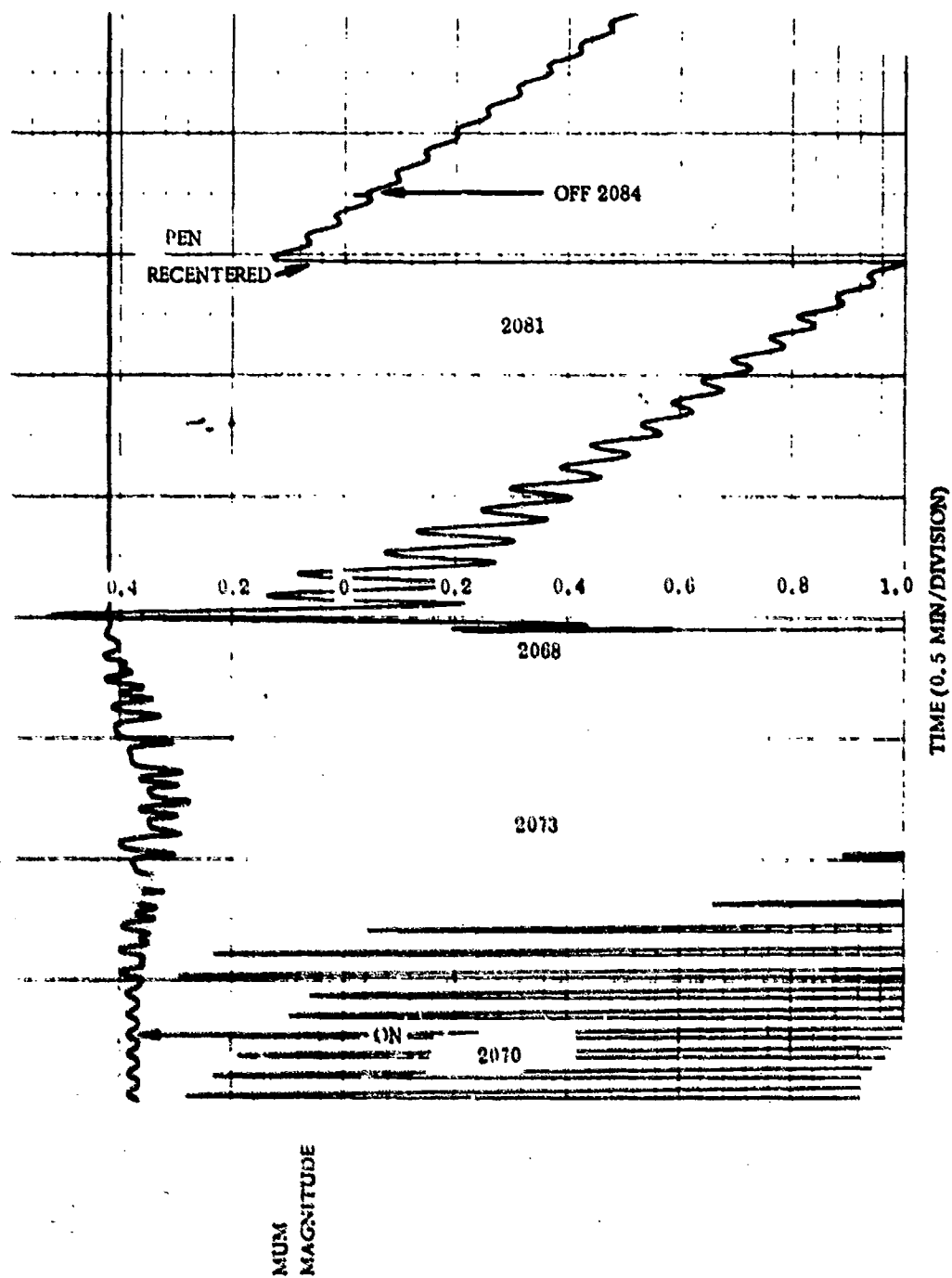


Figure 40. Small Angle Recorder Plot of Run 8, Gyro 68

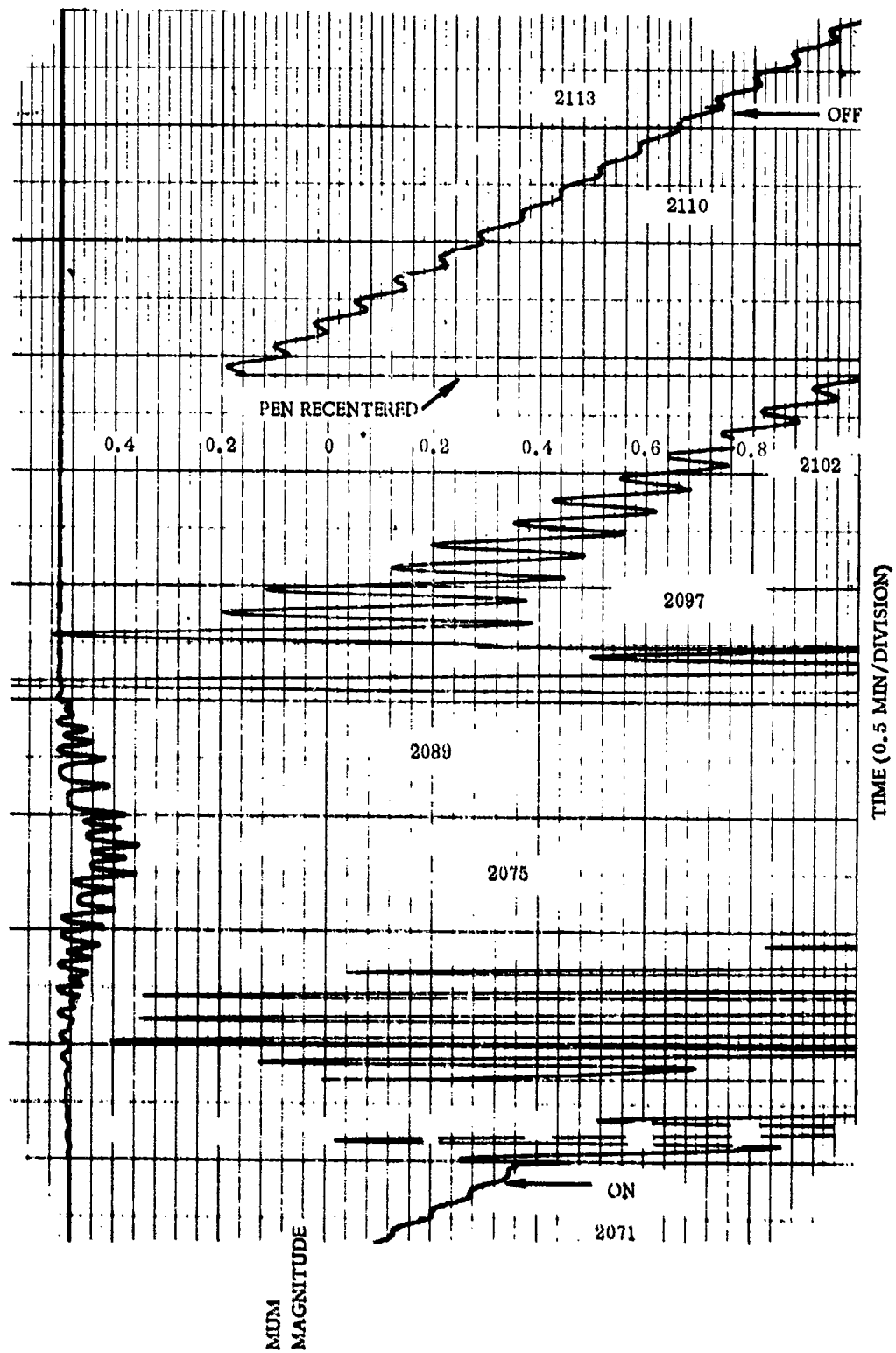


Figure 41. Small Angle Recorder Plot of Run 9, Gyro 68

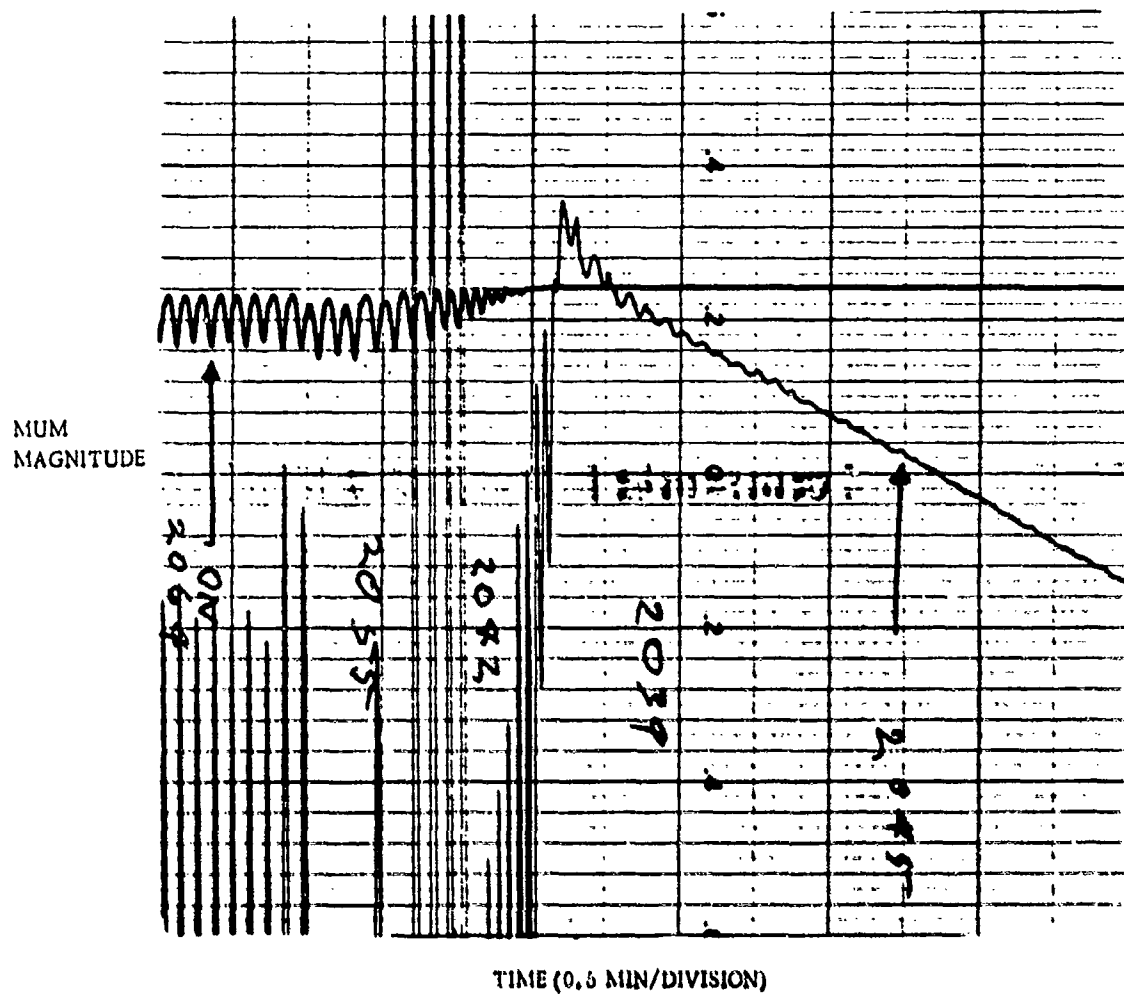


Figure 42. Small Angle Recorder Plot of Run 10, Gyro 68

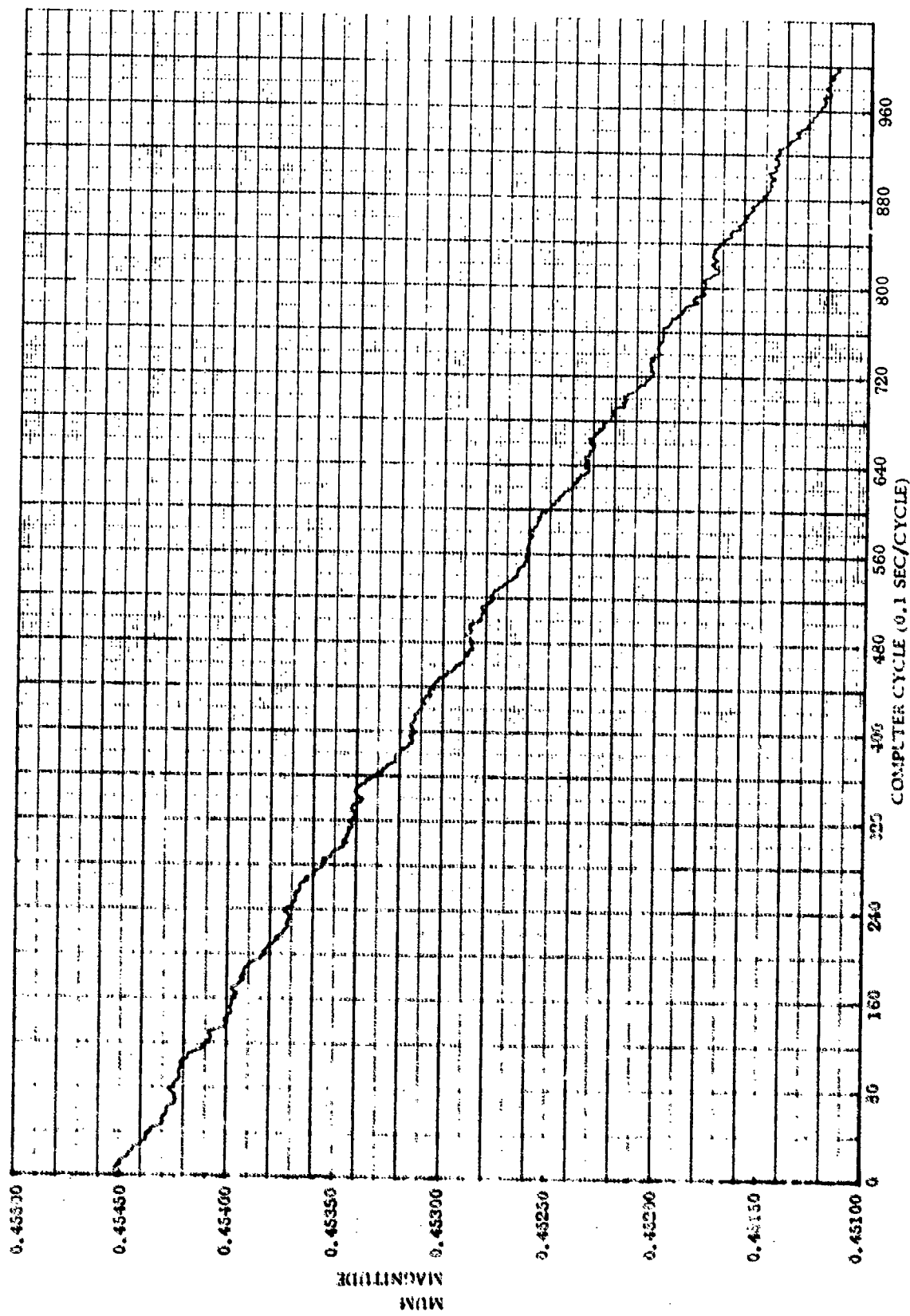


Figure 43. Polhode Motion Residual of Run 3, Gyro 59

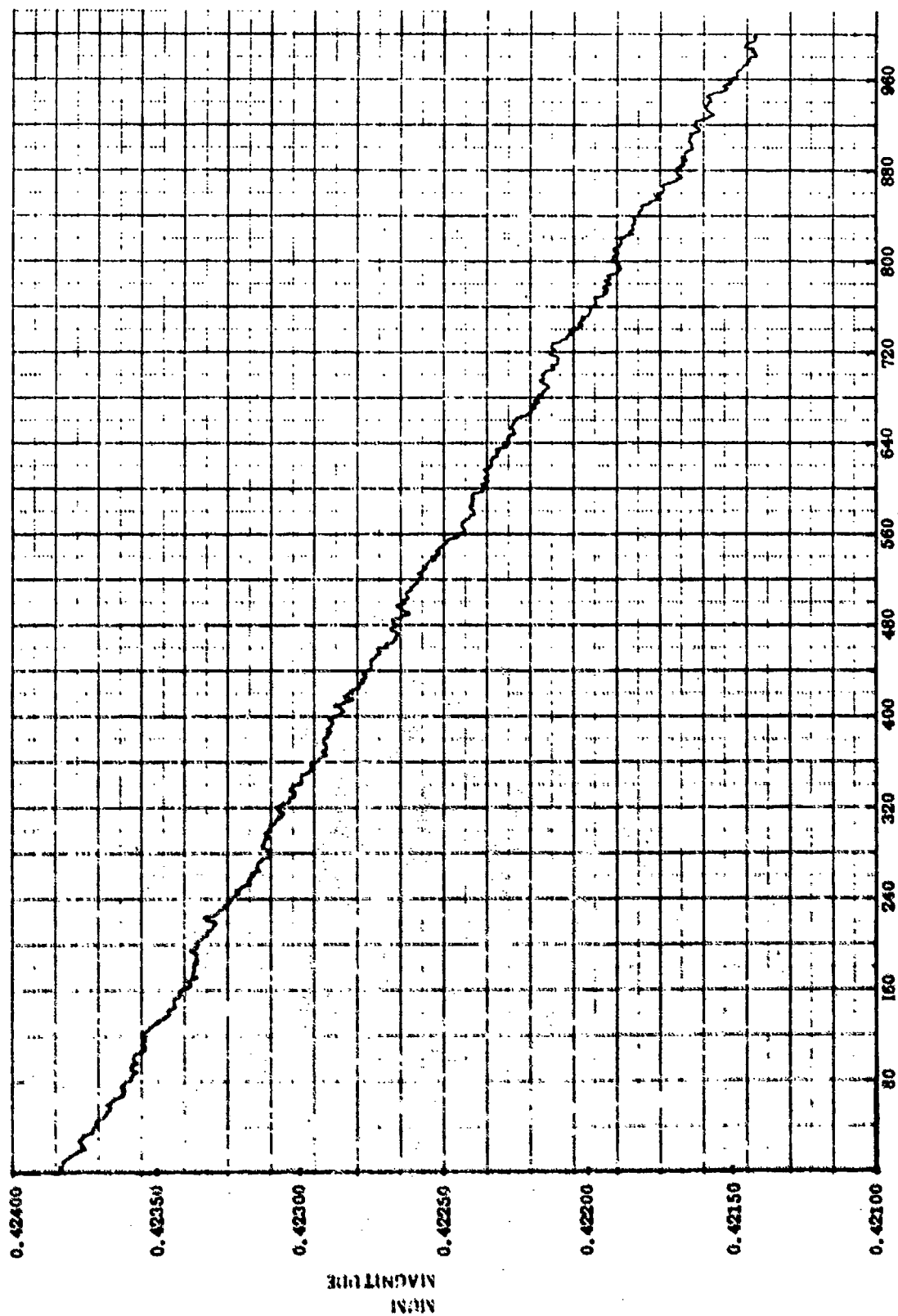


Figure 44. Polhode Motion Residual of Run 8, Gyro 68

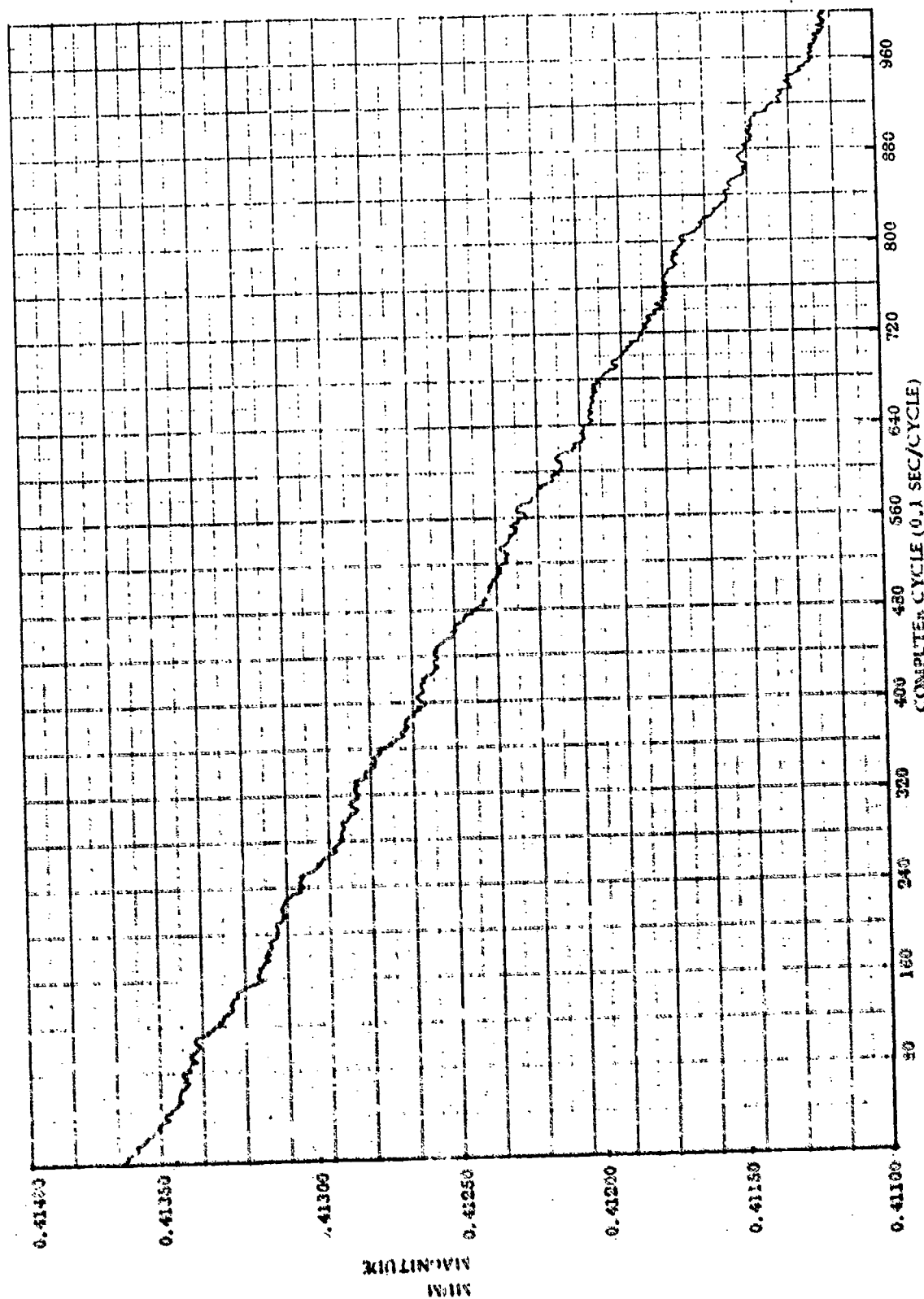


Figure 45. Polhode Motion Residual of Run 9, Gyro 68

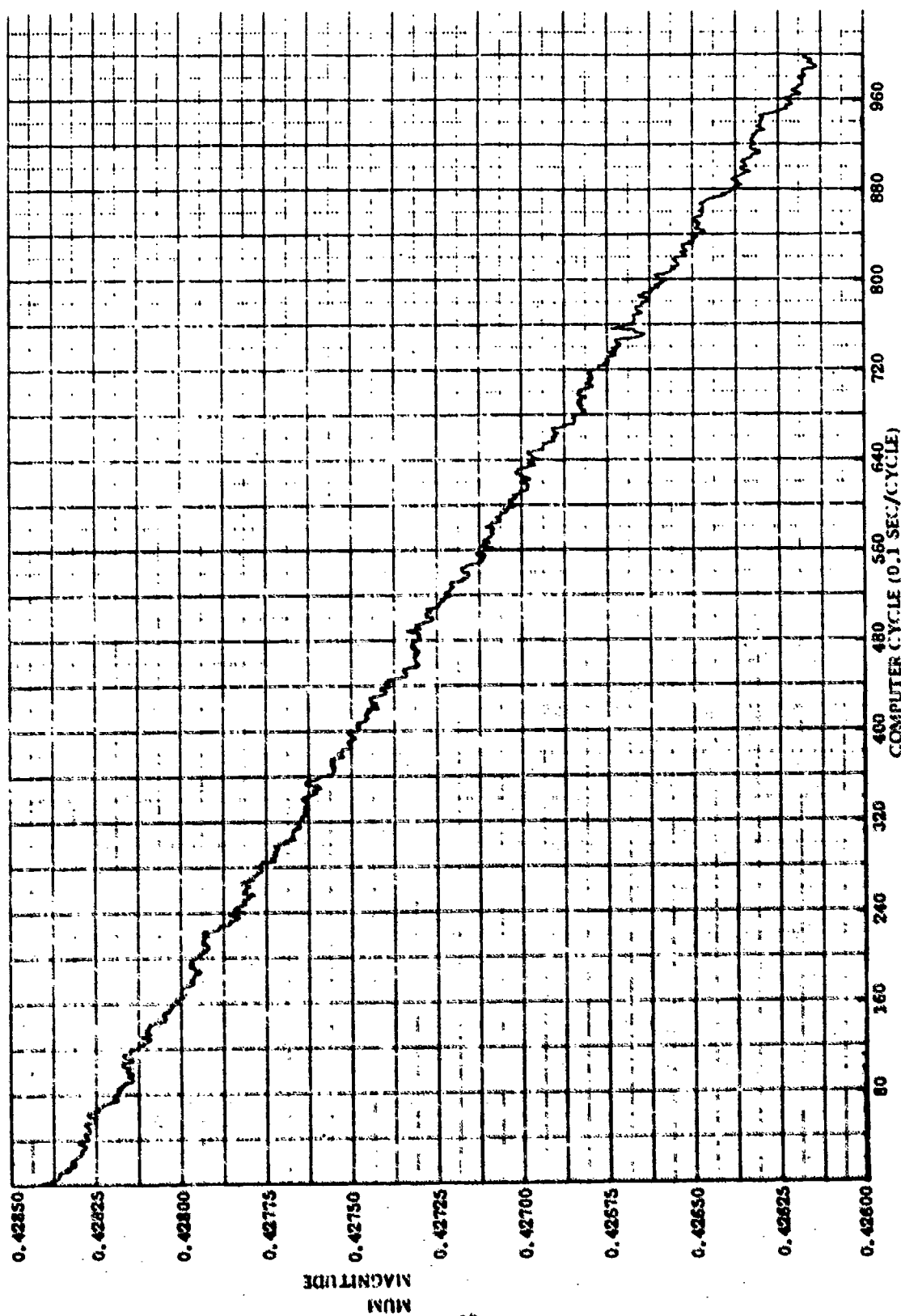


Figure 46. Polhode Motion Residual of Run 10, Gyro 68

SECTION IX

CONCLUSIONS

Polhode motion has been successfully damped ten times using two different gyros. Spin vector orientations were vertical and north which is the normal damping orientations for the N57A navigation system. There were no failures to damp. The program's ability to automatically recover from errors in damping and go on to complete the damping was demonstrated. Automatic damping parameters were taken from only one of the two gyros. The other gyro has never been calibrated.

The most important design goal in developing the automatic damping program is that it must successfully damp the rotor every time. Program efficiency and speed were also considered but were of secondary importance. Future effort to reduce the logic and make the program more efficient would be very fruitful. The major portions of the mathematical computations are now programed in assembly language using fixed point arithmetic.

The longest damping time, excluding run 6 which is a special case, is 9.3 min. This is damping from the A axis, out to C, and back to A which is the worst case. Between 2.5 and 5 min was spent in terminal control. Damping time is directly related to polhode period. A reduced polhode period and a corresponding increase in torque will reduce damping time proportionately. Normalizing on the polhode period near the A axis gives maximum damping time of 56 polhode periods and terminal control time of 26 polhode periods. Additional torquing capability alone would reduce the time. However, since automatic damping information is only obtained one or two times per polhode period, reducing the number of polhode periods to damp could reduce the damping efficiency. The terminal control time is not limited by torquing capability.

A fast reaction goal of the MICRON system is to damp two gyros in one minute. Several changes in the current design will be required to meet this goal.

1. Approximately 50 percent more torquing capability per polhode period is required to reduce the maximum time to damp into the terminal control region from 30 polhode periods to 20 polhode periods or less. This requires 22 percent more current in the motor coils.
2. Fast damping can be accomplished by designing rotors with much shorter polhode periods. Polhode period near the A axis of one sec or less appears ideal. The position of the separating polhode is also a factor effecting time. Polhode motion starting from the A axis requires the longest damping time with a 45 deg separating polhode. The separating polhode latitude could be increased so that the damping time from either C or A is equal. Unfortunately this also increases the polhode period near the A axis, T_A , relative to the polhode period near the C axis, T_C , as shown in Eq (9). T_A has far greater impact on damping time than the separating polhode latitude has. Therefore separating polhode latitude should not be increased unless T_A is made as small as practical (less than 1 sec).

When the polhode period is increased, the computer solution rate must also be increased proportionally to 1/64 sec per computational cycle, and torquing capability must be increased to maintain a constant torque angle per polhode period.

3. Calibration of the terminal control gain for each gyro will allow higher gains for terminal control and consequently faster damping. The navigation program already has a large number of angle readout and drift rate compensation parameters so adding two more per gyro will not be a severe penalty.
4. The damping should be performed at full rotor speed which makes the electrostatic forcing at rotor frequency negligible. This eliminates the coupling of rotor speed changes to MUM magnitude changes and terminal control can be applied on every polhode period instead of alternate polhode periods as was done in the tests reported here. The same result can be achieved by operating at a low rotor frequency such as 400 Hz. However, the polhode period is much longer at 400 Hz rotor frequency. The new quasi square wave pin motor control electronics will be capable of operating at full rotor speed while the current electronics were not.

Rotor speed changes by as much as 114 Hz occurred during damping. This may be due to motor coil axis misalignment and gain variations, but it has not been investigated. Linearity and dc offsets in the electronics were measured and do not appear large enough to cause these effects. Uncompensated angle readout errors as large as one deg occur and may contribute to rotor speed errors.

Rotor speed must be controlled to stay in the notch for minimum electro-static suspension forcing. The spin motor control electronics can be periodically switched to a rotor spin mode and the rotor speed adjusted.

5. If two gyros are to be damped with the same spin motor control electronics faster reaction time can be achieved by time sharing the electronics in the terminal control mode. Each gyro would have to be sequentially brought into the terminal control region. However since the torquing duty cycle is very low in terminal control the electronics could be time shared with little loss of efficiency.

The fastest damping time can be achieved by using separate spin motor control electronics for each gyro and damping both gyros simultaneously.

With the above modifications the one minute automatic damping requirement can be budgeted

Damp Gyro No. 1 up to terminal control	20 sec
Damp Gyro No. 2 up to terminal control	20 sec
Simultaneously apply terminal control to No. 1 and 2	10 sec

which leaves a 10 sec safety factor. Motor current must be increased by a factor of 3.3 which is approximately 600 ma. One amp is planned for use in fast warmup. The current requirements could be reduced if dual spin motor control electronics were used and both gyros damped simultaneously.

The residual polhode motion after automatic damping varied between 2.3 and 0.4 mrad with a termination threshold of 0.0001. The residual polhode motion is about the same or a little worse than that achieved by manual damping. The residual polhode motion appears adequate to meet the navigation requirements. The termination threshold is dependent on the noise level in the MUM data.

Rotor heating during polhode damping must be anticipated during fast warmup so that the rotor is not over heated. Fast rotor heating is applied before spinup and polhode damping. Rotor temperature is left sufficiently low so that the rotor is still under temperature after polhode damping. Rotor heating to achieve thermal stabilization is performed after polhode damping.

APPENDIX A

MUM SIGNAL WITH ELECTROSTATIC SUSPENSION FORCING AT ROTOR FREQUENCY

The geometry of the rotor is shown in Figure A-1. Electrostatic forcing acts on the center of geometry. The vector force, F_S , applied by the suspension is

$$F_S = -G \Phi M \quad (A1)$$

where G is scalar gain at rotor frequency, M is MUM vector, and Φ is (3 x 3) matrix

$$\Phi = I \cos \phi + \frac{\tilde{\omega}}{|\omega|} \sin \phi \quad (A2)$$

ϕ is scalar phase shift of electrostatic suspension at rotor frequency, ω is rotor frequency and $\tilde{\omega}$ is (3 x 3) skew symmetric "cross product" matrix

$$\tilde{\omega} = \begin{bmatrix} 0 & -\omega_Z & \omega_Y \\ \omega_Z & 0 & -\omega_X \\ -\omega_Y & \omega_X & 0 \end{bmatrix} \quad (A3)$$

The centrifugal force, F_A , is

$$F_A = -M \tilde{\omega}^2 R \quad (A4)$$

where M is rotor mass and R is the vector radius of the mass center orbit. Summing the forces

$$F_S + F_A = -M \tilde{\omega}^2 (P + M) - G \Phi M = 0 \quad (A5)$$

Solving for MUM, M ,

$$M = \left[I - \frac{G}{M |\omega|^2} \Phi \right]^{-1} \frac{\tilde{\omega}^2}{|\omega|^2} P \quad (A6)$$

This can be put in a more convenient form by defining a quadrature pendulosity vector, P_Q ,

$$P_Q = \frac{\tilde{\omega}}{|\omega|} P \quad (A7)$$

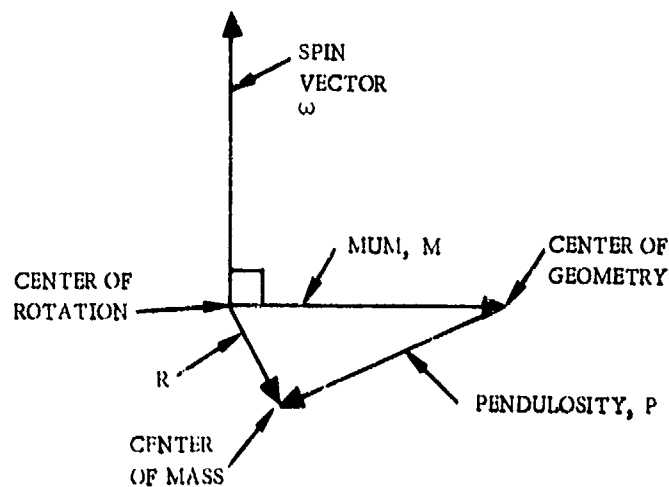


Figure A-1. Rotor Geometry

and quadrature MUM vector, M_Q ,

$$M_Q = \frac{\tilde{\omega}}{|\omega|} M \quad (A8)$$

Equation (A6) can be written

$$\left(1 - \frac{G}{M|\omega|^2} \cos \phi\right) M - \left(\frac{G}{M|\omega|^2} \sin \phi\right) M_Q = \frac{\tilde{\omega}^2}{|\omega|^2} P. \quad (A9)$$

Multiplying Eq (A9) by $\tilde{\omega}/|\omega|$ gives

$$\left(\frac{G}{M|\omega|^2} \sin \phi\right) M + \left(1 - \frac{G}{M|\omega|^2} \cos \phi\right) M_Q = -P_Q \quad (A10)$$

Solving for M and M_Q

$$M = \frac{1}{\Delta} \left[\left(1 - \frac{G}{M|\omega|^2} \cos \phi\right) \frac{\tilde{\omega}^2}{|\omega|^2} P + \left(\frac{G}{M|\omega|^2} \sin \phi\right) P_Q \right] \quad (A11)$$

$$M_Q = \frac{1}{\Delta} \left[\left(1 - \frac{G}{M|\omega|^2} \cos \phi\right) P_Q - \left(\frac{G}{M|\omega|^2} \sin \phi\right) \frac{\tilde{\omega}^2}{|\omega|^2} P \right] \quad (A12)$$

$$\Delta = 1 + \left(\frac{G}{M|\omega|^2} \right)^2 - \frac{2G}{M|\omega|^2} \cos \phi. \quad (A13)$$

Equations A11-A13 show the electrostatic forcing at rotor frequency introduces amplification and phase shift of the MUM single relative to its zero forcing value. However the amplification and phase shift is not dependent on position of the spin vector on the rotor. The MUM magnitude is now frequency dependent since forcing gain and phase are frequency dependent. The relative forcing gain as a function of rotor frequency is shown in Figure A-2 for the N57A.

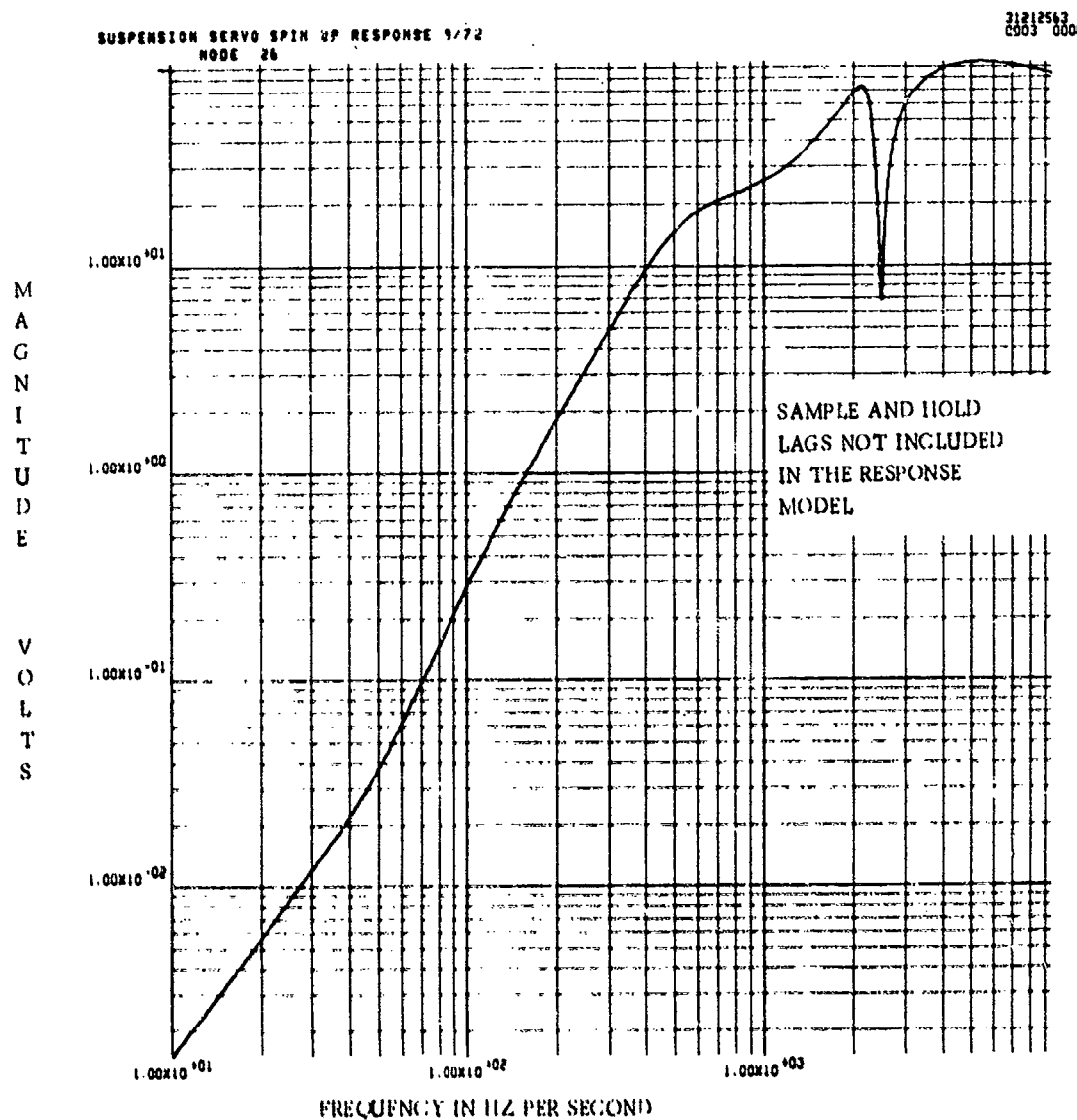


Figure A-2. Suspension Forcing vs Rotor Frequency

APPENDIX B

FOURIER ANALYSIS PHASE TRACKING

The polhode phase variable is based on a constant frequency per polhode period. Sine and cosine of polhode phase are generated and the first and second harmonic Fourier coefficients of MUM magnitude are computed from the sinusoids. A sampled data phase locked loop is constructed to maintain polhode phase lock by nulling second harmonic sine Fourier coefficient. The 180-deg phase uncertainty is resolved by requiring the first harmonic cosine Fourier coefficient to be positive.

The MUM magnitude sine and cosine first and second harmonic and average value are plotted vs polhode latitude in Figures B-1 through B-3, for $\theta_s = 45$ deg and 1 percent pendulosity vector along -A. Sine first and second harmonic are zero.

The same variables are also plotted for 1 percent pendulosity on -A and 10 percent pendulosity on -B in Figures B-4 through B-8. All of the curves have either a dip or peak at 45 deg latitude since the frequency goes to zero at this latitude. The point at 45 deg is not plotted since it is a singularity and the nearest point plotted is 0.5 deg from the singularity.

Fourier analysis sensitivities to frequency errors and errors due to not taking an integer number of samples per polhode period were computed. Considering the dynamic range of the Fourier coefficients it was decided to compute the Fourier coefficients with a least squares filter to avoid some of the numerical problems. The five state least squares filter used second harmonic sine and cosine, first harmonic cosine, average value, and ramp. The ramp state was added to describe MUM magnitude variation while torquing. The filter is initialized once per polhode period at 270-deg phase which is near the -B axis.

A sampled data phase locked loop was used to track polhode frequency and maintain phase lock. The frequency and phase outputs of the phase locked loop are used to correct the sine, cosine signals used as the reference to compute the Fourier coefficients for the next sample. The error signal, ϕ , to the phase locked loop is

$$\frac{1}{2} \tan^{-1} \left(\frac{S_2}{C_2} \right) \quad (B1)$$

where S_2 and C_2 are the Fourier coefficients of second harmonic sine and cosine, respectively. A block diagram of the phase locked loop is shown in Figure B-9. The sampling period is T which is also the polhode period. The effective sampling time is the midpoint of the data collection interval since the best fit criterion of least squares measures the average phase error in the presence of changing frequency. The lag of half a sampling period is introduced since the data are not available until the end of the data taking interval. Using modified Z transforms (Ref 2) system response is computed.

$$\delta\omega(Z) = \frac{K_2 (Z-1) \delta\phi(Z)}{Z^2 - Z(2-K_1-K_2T) + (1-K_1)} \quad (B2)$$

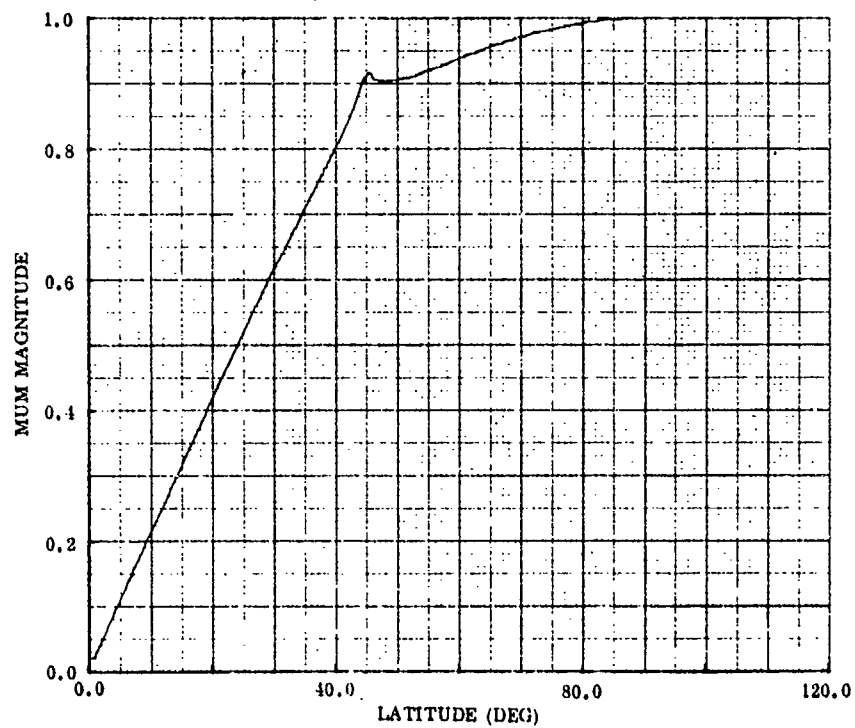


Figure B-1. Average MUM Magnitude for Pendulosity on -A Axis of 1 Percent ($\theta_g = 45$ deg)

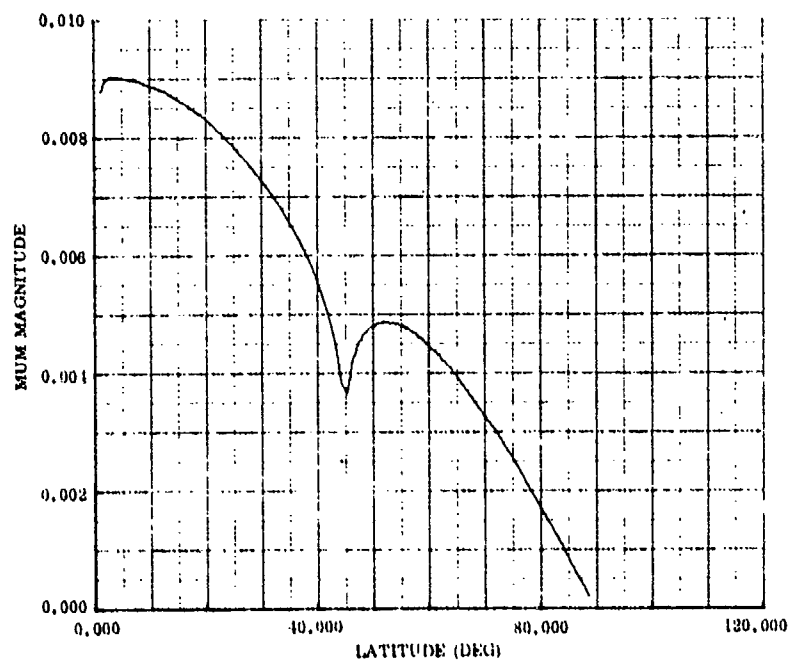


Figure B-2. First Harmonic Cosine of MUM Magnitude for Pendulosity on -A Axis of 1 Percent ($\theta_g = 45$ deg)

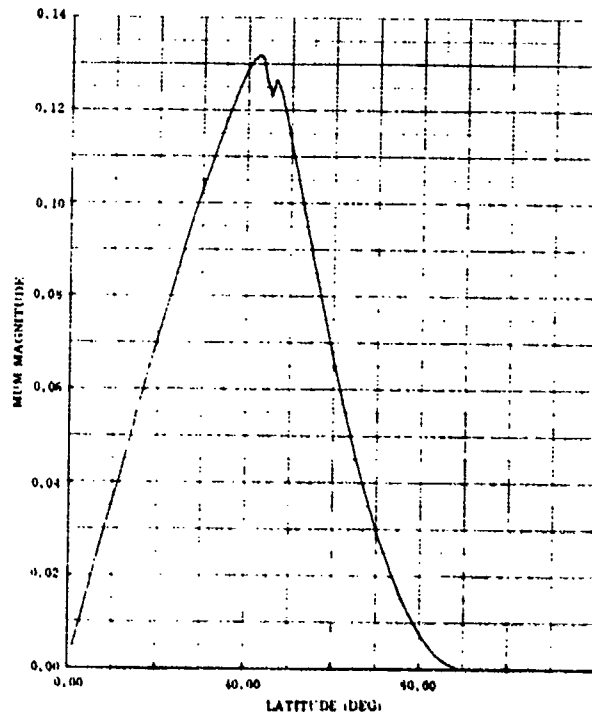


Figure B-3. Minus Second Harmonic Cosine of MUM Magnitude for Pendulosity on -A Axis of 1 Percent ($\theta_s = 45$ deg)

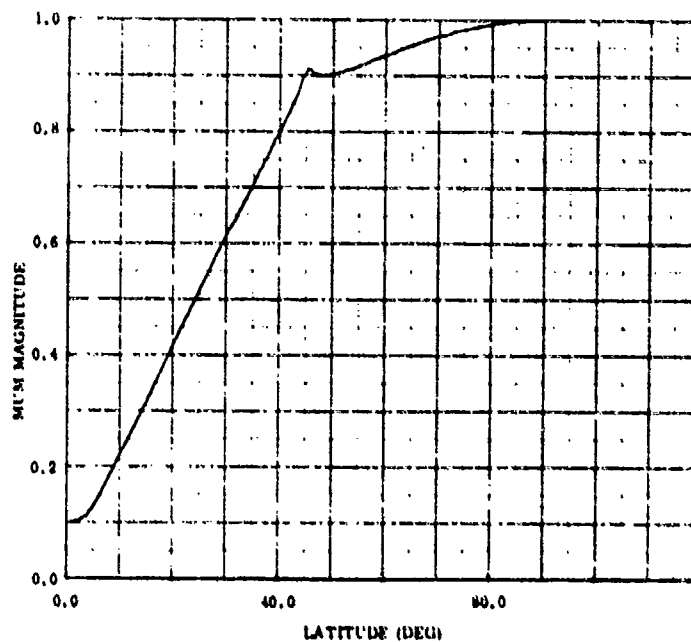


Figure B-4. Average MUM Magnitude for Pendulosity on -A, -B Axes of 1 and 10 Percent, Respectively ($\theta_s = 45$ deg)

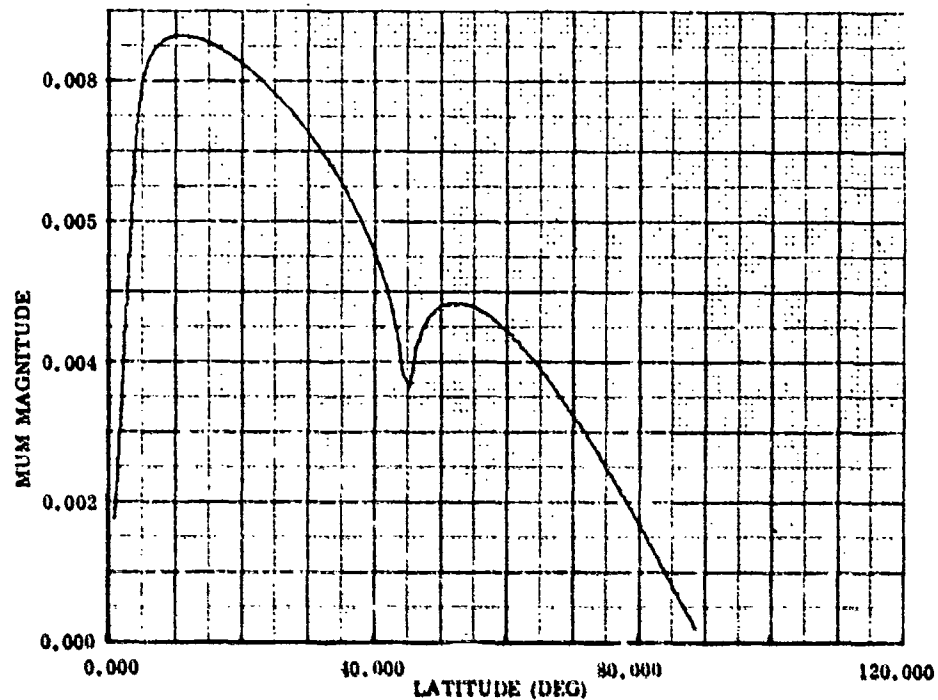


Figure B-5. First Harmonic Cosine of MUM Magnitude for Pendulosity on -A, -B Axes of 1 and 10 Percent, Respectively ($\theta_s = 45$ deg)

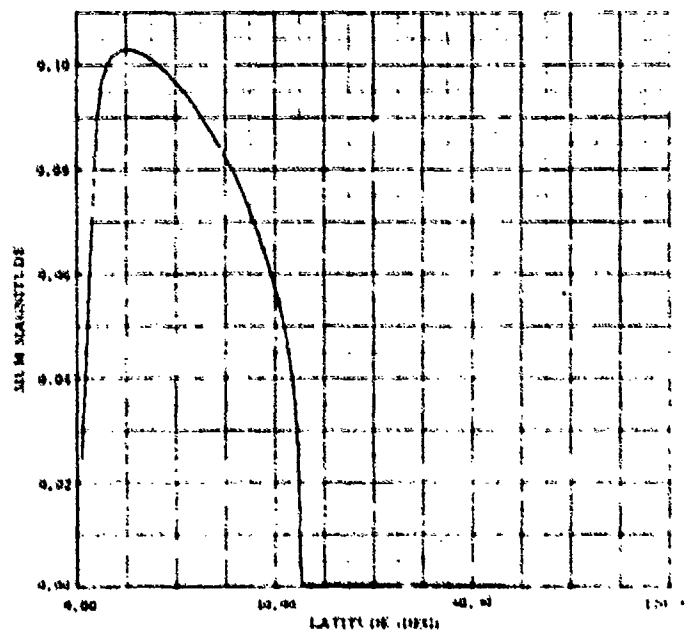


Figure B-6. Minus First Harmonic Sine of MUM Magnitude for Pendulosity on -A, -B Axes of 1 and 10 Percent ($\theta_s = 45$ deg)

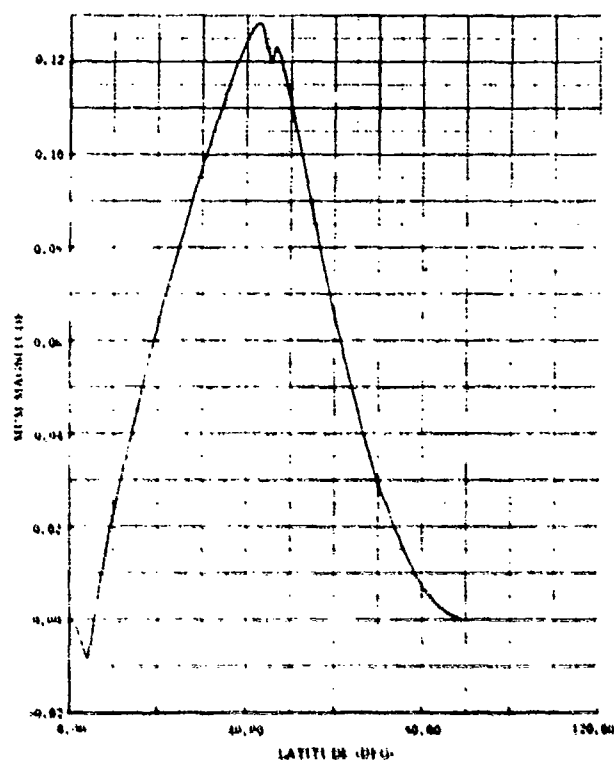


Figure B-7. Minus Second Harmonic Cosine of MUM Magnitude for Pendulosity on -A, -B Axes of 1 and 10 Percent, Respectively ($\theta_g = 45$ deg)

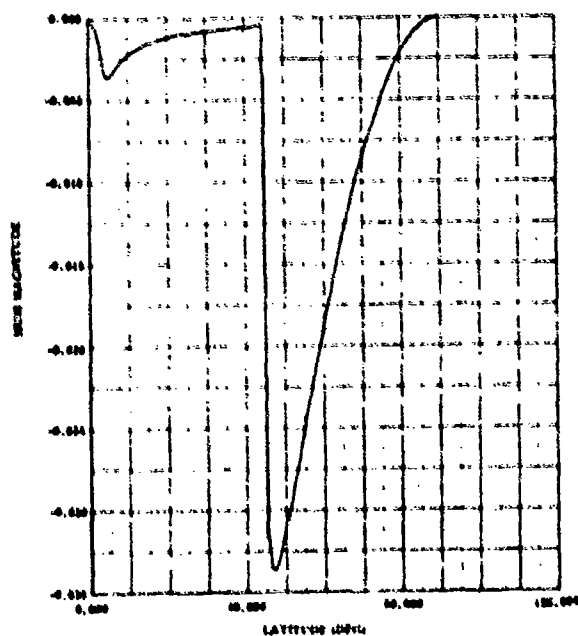


Figure B-8. Minus Second Harmonic Sine of MUM Magnitude for Pendulosity on -A, -B of 1 and 10 Percent, Respectively ($\theta_g = 45$ deg)

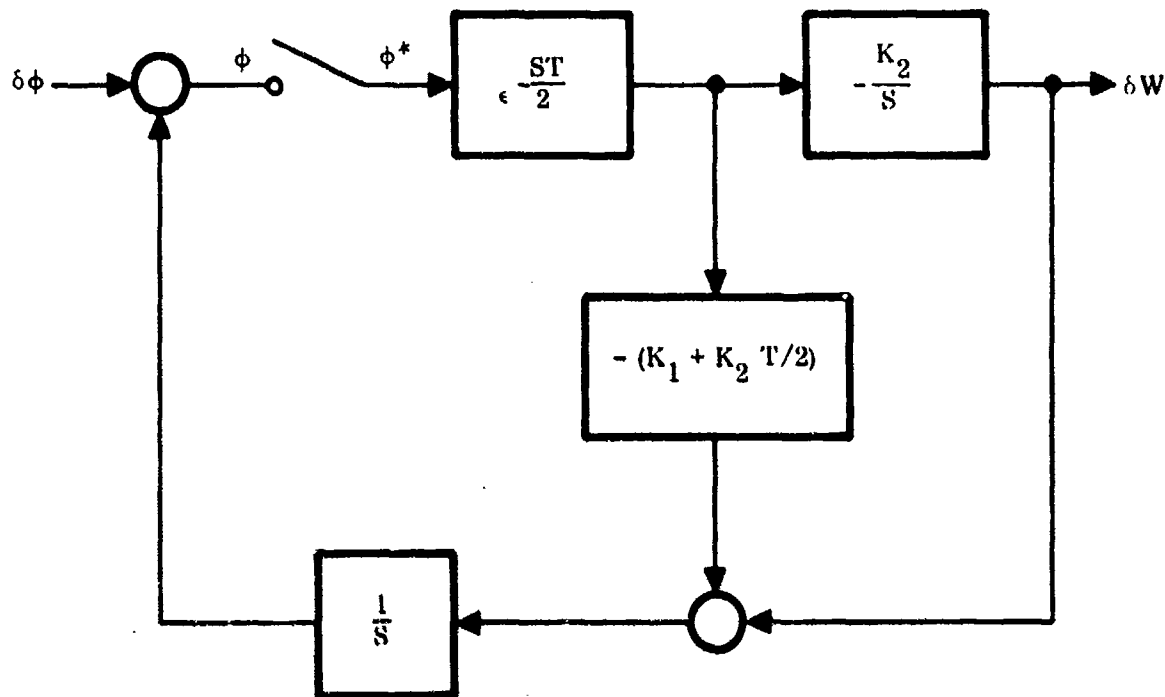


Figure B-9. Phase Locked Loop Block Diagram

For a time constant $\tau = T$ and a damping ratio of 0.7, the phase locked loop gains are

$$K_1 = 0.865$$

$$K_2 = 0.735/T.$$

(B3)

Polhode frequency varies with polhode latitude as shown in Figure 2 and since torquing changes polhode latitude, it is of interest to determine how polhode frequency varies with torquing to determine whether or not phase lock can be maintained. A control law must be assumed to establish these relationships. Therefore, it is assumed the torque is always applied normal to the trajectory which is the unit vector.

$$u_N = \pm \frac{\omega \times \dot{\omega}}{|\omega \times \dot{\omega}|}$$

(B4)

The torque vector, T_Q , will be defined in units of precession rate as

$$T_Q = \frac{1}{\omega_0} \begin{bmatrix} Q_A/A \\ Q_B/B \\ Q_C/C \end{bmatrix}$$

(B5)

where (Q_A, Q_B, Q_C) is the physical torque vector defined in Eq (2) and ω_0 is the magnitude of rotor angular rate when in the A-C plane. The change in polhode latitude introduced by a unit torque impulse at time t is

$$\text{Torque Efficiency} = \frac{\partial \theta}{\partial \omega} \omega \quad (\text{B6})$$

where θ is polhode latitude. This function is a measure of torquing efficiency vs polhode phase and latitude. The function is plotted in Figure 16 vs polhode phase for several polhode latitudes. The average torquing efficiency is computed by averaging

$\frac{\partial \theta}{\partial \omega} \omega$ over the polhode period which will be called $\overline{\frac{\partial \theta}{\partial \omega}} \omega$. For an infinitesimal torque,

dT_Q , acting over the entire period, T_P ,

$$d\theta = \overline{\frac{\partial \theta}{\partial \omega}} T_P dT_Q \quad (\text{B7})$$

To obtain a quick answer for these preliminary relationships, it will be assumed that

$$T_P dT_Q = T_Q dt \quad (\text{B8})$$

The result of the above approximation is that relationships will be computed for an ensemble of trajectories with starting phase uniformly distributed $(0, 2\pi)$ instead of the desired single trajectory with starting phase of zero degree. Equation (B7) can be integrated as

$$\int_{\theta_1}^{\theta_2} \frac{1}{\left(\frac{\partial \theta}{\partial \omega} \omega\right) T_P} d\theta = T_Q \quad (\text{B9})$$

so given a starting latitude θ_1 , the final latitude, θ_2 , after one polhode period can be computed from the above equation. The average frequency over the polhode period can be computed

$$f_{\text{NEW}}(\theta_1) = \frac{1}{\theta_2 - \theta_1} \int_{\theta_1}^{\theta_2} f(\theta) d\theta \quad (\text{B10})$$

as well as the average frequency over the previous polhode period

$$f_{\text{OLD}}(\theta_1) = \frac{1}{\theta_1 - \theta_0} \int_{\theta_0}^{\theta_1} f(\theta) d\theta \quad (\text{B11})$$

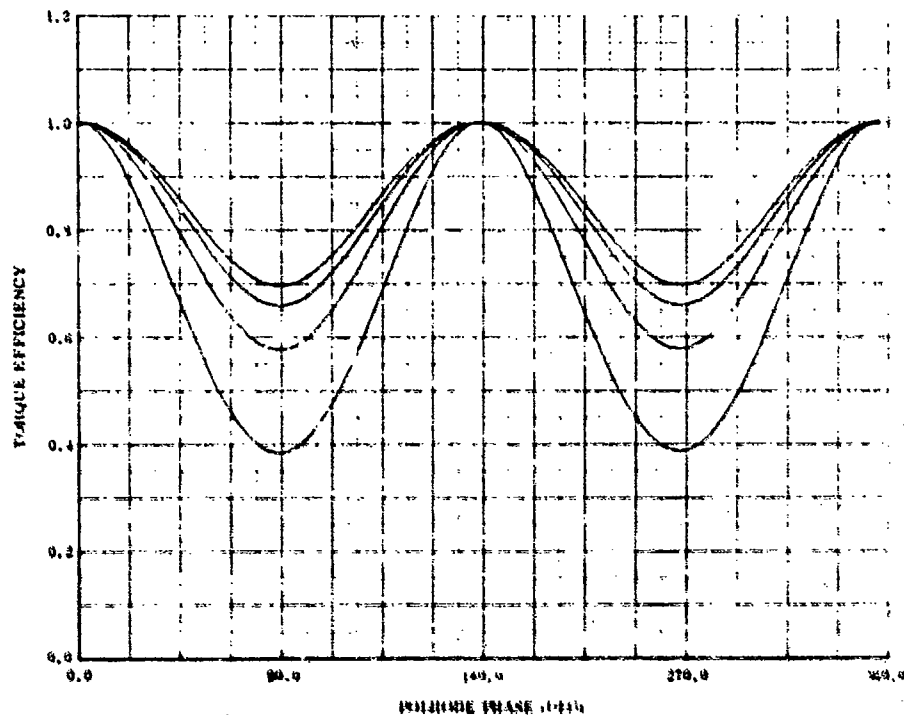


Figure B-10. Torque Efficiency

Figure B-11 shows f_{OLD} plotted vs f_{NEW} and Figure B-12 shows $(f_{NEW} - f_{OLD})$ plotted vs f_{OLD} assuming a torquing rate of 0.01 rad/sec and rotor parameters $T_A = 2.83$ sec and $\theta_s = 45$ deg.

If the frequency used for phase tracking is only based on the measured frequency of the previous polhode period, the resulting phase error will be

$$\text{Phase Error} = ((f_{NEW} - f_{OLD})/f_{NEW}) (360 \text{ deg})$$

The phase error is plotted in Figure B-13. A means of frequency prediction is clearly required. The frequency prediction approach used is to curve fit Figure B-12. Two functions are required since the curve is double valued. The curve fit was performed by weighted least squares to yield for the -A and C families (bottom segment of curve)

$$(f_{NEW} - f_{OLD}) = \frac{0.6604 \times 10^{-4} (0.1116 - f_{OLD})}{(f_{OLD} - 0.1163)((0.1677 - f_{OLD})^2 + 0.794 \times 10^{-3})} \quad (B12)$$

and for the +A family (top segment of curve)

$$(f_{NEW} - f_{OLD}) = \frac{0.1837 \times 10^{-2} (f_{OLD} - 0.1201)}{((0.1111 - f_{OLD})^2 + 0.3779 \times 10^{-4})} \quad (B13)$$

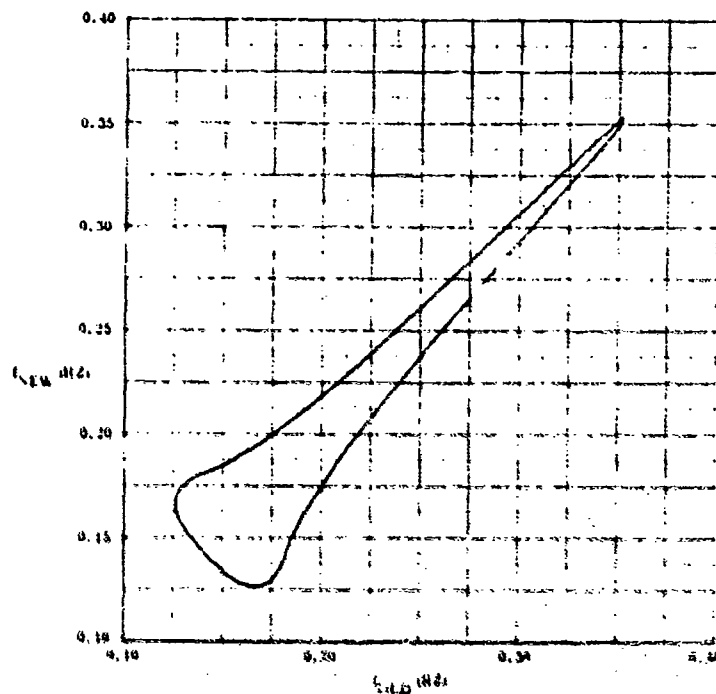


Figure B-11. Pollhede Frequency (f_{NEW}) vs Previous Pollhede Frequency (f_{OLD}) for Torquing Rate of 0.01 Rad/Sec ($\theta_s = 45$ deg, $T_A = 2.83$ sec)

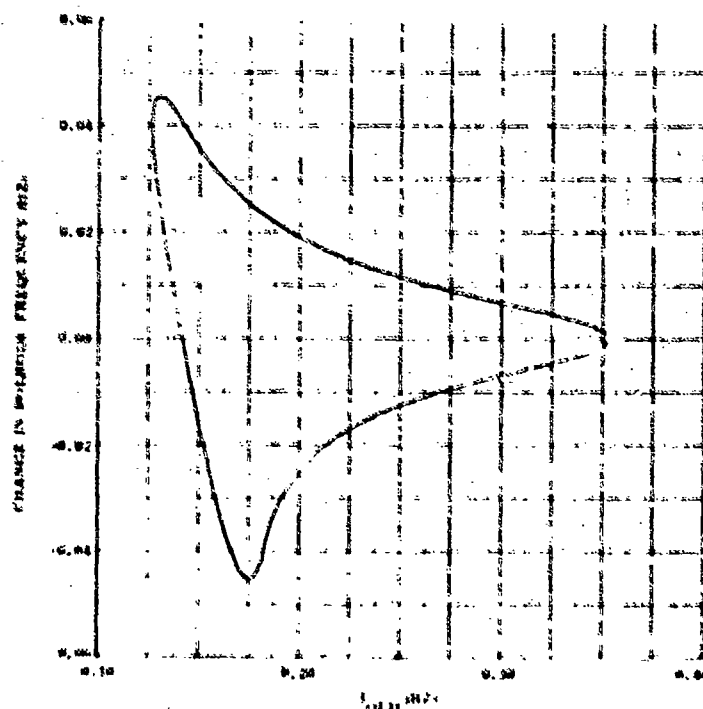


Figure B-12. Change in Pollhede Frequency vs Previous Pollhede Frequency (f_{OLD}) for Torquing Rate of 0.01 Rad/Sec ($\theta_s = 45$ deg, $T_A = 2.83$ sec)

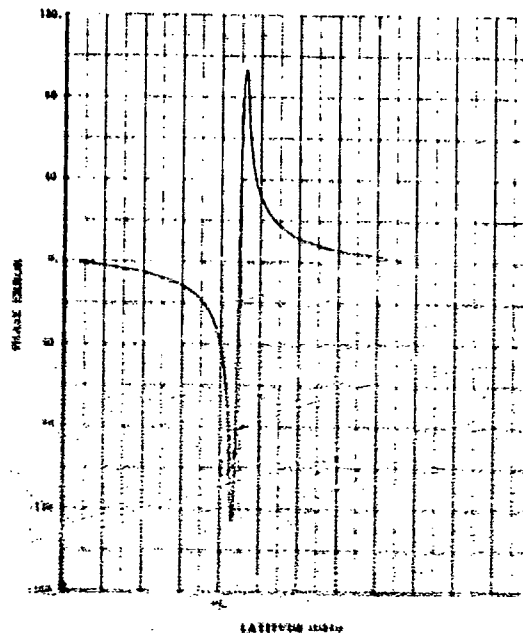


Figure B-13. Phase Error Without Frequency Prediction for Torquing Rate of 0.01 Rad/Sec ($\theta_g = 45$ deg. $T_A = 2.83$ sec)

The phase error using the curve fit frequency prediction is less than 9 deg. The curve fit could be improved with minor modification.

At this point one should notice that the Fourier analysis mechanization is evolving into a form that has many of the objections of the simulation mechanization. The primary concern is the heavy dependence on rotor and torque parameters for frequency prediction. The sensitivity to the major parameters θ_g , T_A , and magnitude of T_Q was computed. The problem to be analyzed can be stated as given

$$\Delta F(\theta, P) = f_{\text{NEW}} - f_{\text{OLD}} \quad (\text{B14})$$

Find the change in ΔF for a change in parameter, P , for a given value of f_{OLD} . The sensitivity is

$$\frac{d\Delta F}{dP} = \frac{\partial \Delta F}{\partial P} = \frac{\partial \Delta F}{\partial \theta} \frac{\partial f_{\text{OLD}}}{\partial P} + \frac{\partial f_{\text{OLD}}}{\partial \theta} \quad (\text{B15})$$

and the phase error sensitivity is

$$\text{Phase Error Sensitivity} = \frac{1}{f_{\text{NEW}}} \frac{d\Delta F}{dP} \quad (\text{deg}) \quad (\text{B16})$$

The computed phase sensitivities are plotted in Figures B-14 through B-16 for parameters $d\theta_s$, $(d T_A/T_A)$, and $(d|T_Q|/|T_Q|)$, respectively vs polhode latitude at the beginning of the polhode period. The sensitivities only predict phase error changes for infinitesimal parameter changes. Because of the large singularity at the separating polhode, the results cannot be extended to large parameter changes in this region.

The Fourier mechanization with prediction was simulated in spite of the sensitivity results. The simulation used the A family, $\pm C$ family, and transition control laws. The only difficulty encountered was in crossing the separating polhode. It was not possible to maintain phase lock if the separating polhode was crossed near the B axis which is where the singularity exists. This is due in part to the assumption made in computing the predicted frequency as stated by Eq (B8). There is also a feedback coupling from control to estimation since the frequency change over a polhode period is related to torquing efficiency. Torquing efficiency in turn is degraded if the estimation mechanization has phase errors. Under certain conditions this can be a positive feedback loop.

The problems listed in the above paragraph are not insurmountable. However, it is becoming clear that the computer mechanization will be complex and this is therefore an undesirable solution. The difficulty is completely related to the singularity on the B axis and a mechanization that avoids the singularity is preferable to one that attempts to compensate for it.

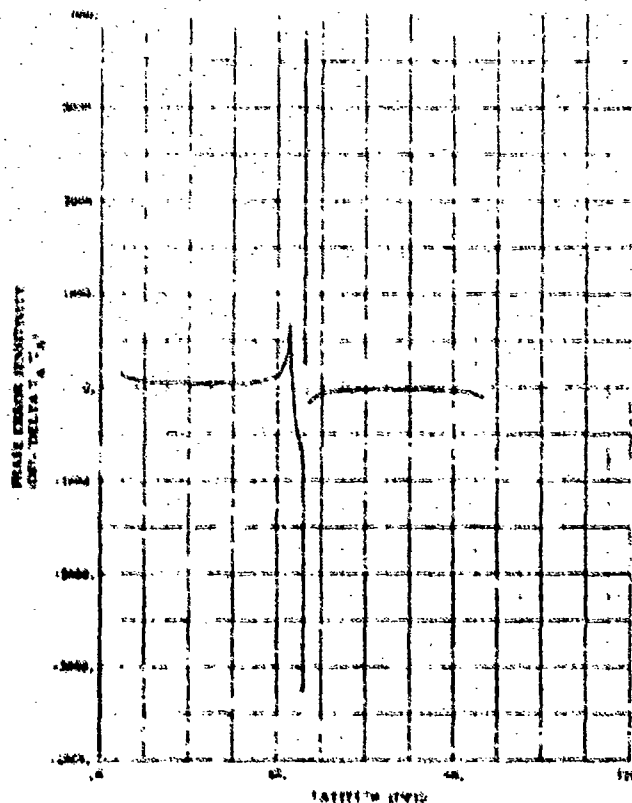


Figure B-14. Frequency Prediction Phase Error Sensitivity to Normalized A Axis Polhode Period ($\Delta T_A/T_A$). ($\theta_B = 45$ deg, $T_A = 2.83$ sec, Torque = 0.01 rad/sec)

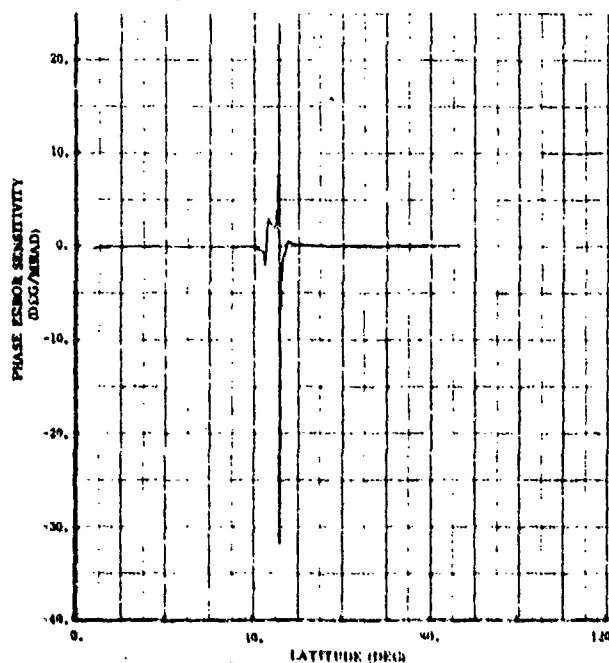


Figure B-15. Frequency Prediction Phase Error Sensitivity to Separating Polhode Latitude ($\theta_B = 45$ deg, $T_A = 2.83$ sec, Torque = 0.01 rad/sec)

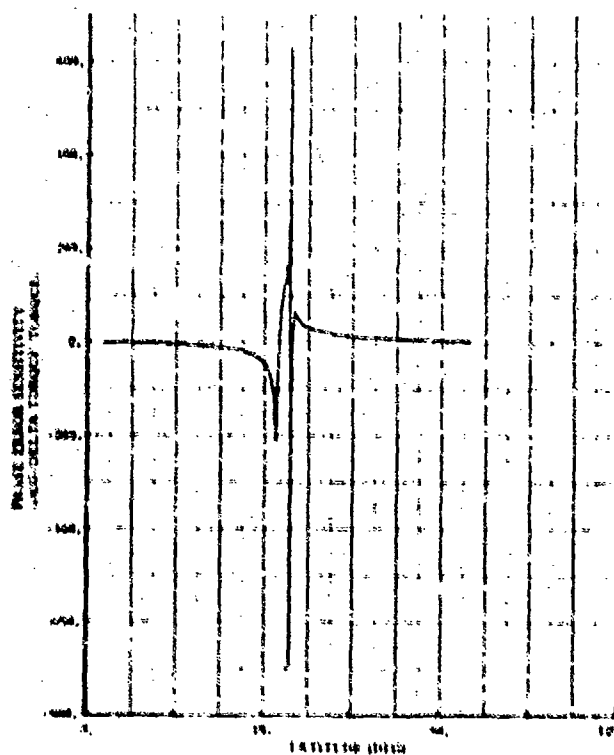


Figure B-16. Frequency Prediction Phase Error Sensitivity to Normalized Torque Magnitude (Delta Torque/Torque). ($\theta_B = 45$ deg, $T_A = 2.83$ sec, Torque = 0.01 rad/sec)

APPENDIX C

AUTOMATIC POLHODE DAMPING MECHANIZATION

The mechanization described here has been programmed in Fortran and assembly language on the IBM 1130 computer and operated successfully. A listing of Fortran subroutine CNTLR, is presented in Appendix D. The operation of the subroutine directly corresponds to the discussion presented here. The subroutine is an example of one possible implementation of the mechanization equations. All of the details of implementing automatic damping logic are presented in the subroutine listing. The text will concentrate more on the functional description of the logic.

The principal variables used in automatic polhode damping are listed in Table C1 and the constants used are listed in Table CIL

The automatic damping routine attempts to locate the spin vector on the rotor so that an appropriate control law can be applied. It is only necessary to locate the spin vector in one of five possible regions of the rotor and determine the phase of the polhode motion. The five regions, which do not have sharp boundaries, are

1. C Nbhnd - a small region about the $\pm C$ axes that does not enclose the pendulosity vector
2. C Family - the central part of the total $\pm C$ families
3. Transition Zone - a band about the separating polhode containing both the C and A families
4. A Family - the central part of the total $\pm A$ families
5. ANbhnd - a small region about the $\pm A$ axes

1. READ MUM DATA

The MUM data is read from the A/D converter exactly as is done in the navigation computations. Two three element vectors, σ_{ui} , β_{ui} , are obtained for each gyro, $i = 1, 2$. Apply dc offset correction and compute γ_{ai} for the gyro being damped.

$$\left. \begin{aligned} \sigma_{oi} &= \sigma_{ui} - \sigma_{oi} \\ \beta_{oi} &= \beta_{ui} - \beta_{oi} \\ \gamma_{oi} &= \sigma_{oi} \times \beta_{oi} \end{aligned} \right\} \quad (3 \times 1) \text{ vectors}$$

$i = 1 \text{ or } 2$

σ_{oi} , β_{oi} = previously stored dc offset compensation vectors.

Table C-1. Principal Variables Used in Automatic Polhode Damping

Variable	Definition
AMM	Current value of MUM magnitude
AMPK	Latest max or min value of AMM found in max/min search
PEAKX	Latest max value of AMM
PEAKN	Latest min value of AMM
PP	Difference between latest max and min value of AMM
TP	Latest observed polhode period (0.1 sec steps)
PTNO	Time of occurrence of latest min value of AMM (0.1 sec steps)
PTO	Time of occurrence of min 360 deg back in polhode phase from latest min (0.1 sec steps)
AMNO	Value of min 360 deg back in polhode phase from latest min
AMXO	Value of max 360 deg back in polhode phase from latest max
AMXI	Value of max 180 deg back in polhode phase from latest max
SMAX	Slope of max values
SMIN	Slope of min values
DMAX	Difference between high and low max
NMIN	Number of minima per polhode period
FE	Phase variable extrapolation frequency (rad/step)
CT, ST	Cos, sin of phase variable
AMMAX	Value of max threshold
CMAX	Value of threshold for C Nbd control law
DNANG	Maximum torquing angle for ANbd control law
TORK ₁ , TORK ₂	Control law commands
SGN	Sign of C family (+ 1)
PP _N	Normalized PP = PP/PEAKX

Table C-1 (Cont)

Variable	Description
IFAM	<p>Region of polhode motion</p> <ol style="list-style-type: none"> 1. C Nbhd 2. C Family 3. Transition zone 4. A Family 5. A Nbhd 6. Undefined Region
IFRZ	<p>Phase variable extrapolation control</p> <ol style="list-style-type: none"> 1. Extrapolate 2. Do not extrapolate 3. Do not extrapolate, check max threshold
IPHAS	Flag - 1 indicates -A axis has been identified
IDMAX	Flag - 1 indicates value of DMAX is valid
ISMAX	Flag - 1 indicates value of SMAX is valid
ISMIN	Flag - 1 indicates value of SMIN is valid

Table C-2. Constants Used in Automatic Polhode Damping

Constant	Description
TMAX	TP threshold for transition zone
TA1	TP threshold for NMIN change from 1 to 2 in ANbhd
TA2	TP threshold for NMIN change from 2 to 1 in ANbhd
TC1	TP threshold for NMIN change from 1 to 2 in CNbhd
TC2	TP threshold for NMIN change from 2 to 1 in CNbhd
AMAP	PP threshold for ANbhd and CNbhd
AMAX	PEAKX threshold for A, C family logics
EPDS	Threshold for testing DMAX for zero
EPDMC	Threshold for testing SMAX for nonzero
EPDMA	Threshold for testing SMAX for zero
EPSCN	Threshold for testing SMIN for large positive value
EPSAN	Threshold for testing SMIN for large negative value
TPO	Maximum period of extrapolation frequency, FE
ϕ_T	Change in phase variable from max to max threshold
GPAN2	ANbhd proportional control gain
PPT	PP threshold for damping termination

Compute MUM magnitude, AM, and normalize α_{oi} , β_{oi} , γ_{oi} .

$$AM = (\sqrt{\alpha_{oi} \cdot \alpha_{oi}} + \sqrt{\beta_{oi} \cdot \beta_{oi}}) / 2$$

$$\left. \begin{aligned} \alpha_N &= \alpha_{oi} / \sqrt{\alpha_{oi} \cdot \alpha_{oi}} \\ \beta_N &= \beta_{oi} / \sqrt{\beta_{oi} \cdot \beta_{oi}} \\ \gamma_N &= \gamma_{oi} / \sqrt{\gamma_{oi} \cdot \gamma_{oi}} \end{aligned} \right\} \quad (3 \times 1) \text{ vectors}$$

$$i = 1 \text{ or } 2$$

AM is filtered by

$$AMM = AMM + (2^{-p})(AM - AMM)$$

where p is a program variable with value $p=1$ everywhere except the ANbhd where it has values $p=4$ or 5 . MUM data is read four times per computer cycle (0.1 sec). AMM is the sole piece of information used for automatic damping estimation. α_N , β_N , γ_N are used in spin motor control electronics outputs.

2. PHASE TRACKING

The purpose of phase tracking is to maintain phase lock with the polhode motion. The sin and cos of the phase variable is computed. Phase lock is maintained by requiring the phase variable to be at quadrature values at max or min points in MUM magnitude. The MUM magnitude data is continuously examined for local maxima and minima. Phase variable is extrapolated between max and min points based on previous observations of polhode period. Logical operations are performed to decide whether to extrapolate the phase variable, freeze it, or reinitialize it.

a. Maximum/Minimum Search

The max/min search is based on a moving window least squares filter using 17 data points. The data are fit to a quadratic function in time

$$\begin{aligned} f(n) &= A - 2Bn + Cn^2 \\ &= C(n - B/C)^2 + (A - B^2/C) \end{aligned}$$

$$-8 \leq n \leq 8$$

where the midpoint of the window is taken as time zero. A max or min event occurs only if the point of zero slope, n_0 , of $f(n)$ falls in the range

$$0 < n_0 = B/C < 8$$

The point of zero slope is allowed to move to the leading edge of the window so that the broad max as shown in Figures 7 and 18 can always be recognized. The best estimate of the max or min parameters is obtained when the point of zero slope is at the midpoint of the window and so the last recognition of the max or min is when it is nearest the midpoint. Usually a max or min event will be recognized on 7 or 8 successive cycles.

The window size should be approximately half the distance between min near the A or C axis or 1/4 the polhode period. It will be seen later that a minor simplification occurs if the window size, $2N+1$, is such that $N(2N-1)/3$ is an integer.

Sometimes in the ANbhd an additive slope must be removed from the data before the max or min can be recognized. The quadratic fit is performed on

$$AMM_n = (n) (ISLOP) + A + (2B + ISLOP)n + Cn^2$$

where ISLOP is the slope to be removed. Therefore a max or min event occurs only if

$$0 < \frac{B + ISLOP/2}{C} < 8$$

The least squares computations for $2N+1$ window size ($N = 8$) is

$$D1 = \sum_{i=-N}^N AMM_i$$

$$D2 = \sum_{i=-N}^N i AMM_i$$

$$D3 = \sum_{i=-N}^N i^2 (AMM_i - D1/2N + 1)$$

This can be reduced to a recursive form.

$$D1' = D1 - AMM_{OLD}$$

$$D2' = D2 - D1' + (N) AMM_{OLD}$$

$$D3^+ = D3^- - (2) D2' - D1' + \frac{N(2N-1)}{3} (AMM_{NEW} - AMM_{OLD})$$

$$D2^+ = D2' + (N) AMM_{NEW}$$

$$D1^+ = D1' + AMM_{NEW}$$

where AMM_{OLD} is the old data that fell inside the window on the previous computation cycle but falls outside the window on the current computation cycle and AMM_{NEW} is the new data obtained on the current computation cycle. The least squares solution is

$$C = \left[\frac{45}{N(N+1)(2N+1)(2N+3)(2N-1)} \right] D3$$

$$B = \left[\frac{1.5}{N(N+1)(2N+1)} \right] D2$$

$$A = \left[\frac{1}{2N+1} \right] D1 - \left[\frac{N(N+1)}{3} \right] C$$

A min event occurs if

$$0 < \frac{B + ISLOP/2}{C} < 8$$

and $C > 0$.

Set flag IDPT = -1.

A max event occurs if

$$0 < \frac{B + ISLOP/2}{C} < 8$$

and $C < 0$

Set flag IDPT = 1

Otherwise no event occurs and set flag IDPT = 0. The peak value, AMPK, and time of the event, PTNO, are computed for max or min events

$$AMPK = A - B^2/C$$

$$PTNO = IDATA - 8 + \frac{B + ISLOP/2}{C} - LAG$$

where IDATA is the time that the last data point was obtained and LAG is the lag introduced by the filter of section 1.

For one min per polhode period in the ANbhd the data window is only half as wide as it should be for maximum noise rejection. The window is widened by skipping the least squares filter on alternate computation cycles.

b. Phase Tracking Logic

The phase tracking logic must freeze the phase variable after the maximum point until MUM magnitude drops by 10 percent of the peak-to-peak value. Then the phase variable is reinitialized and extrapolation is begun. The angle from trajectory normal to MUM vector at the max, min, and 90 percent max points are shown in Figure C-1 for 0.03 and 0.07 percent pendulosity and A and B axes respectively and 45 deg separating polhode. The phase at the 90 percent max points are approximately 20 deg from the corresponding max points. The phase variable must

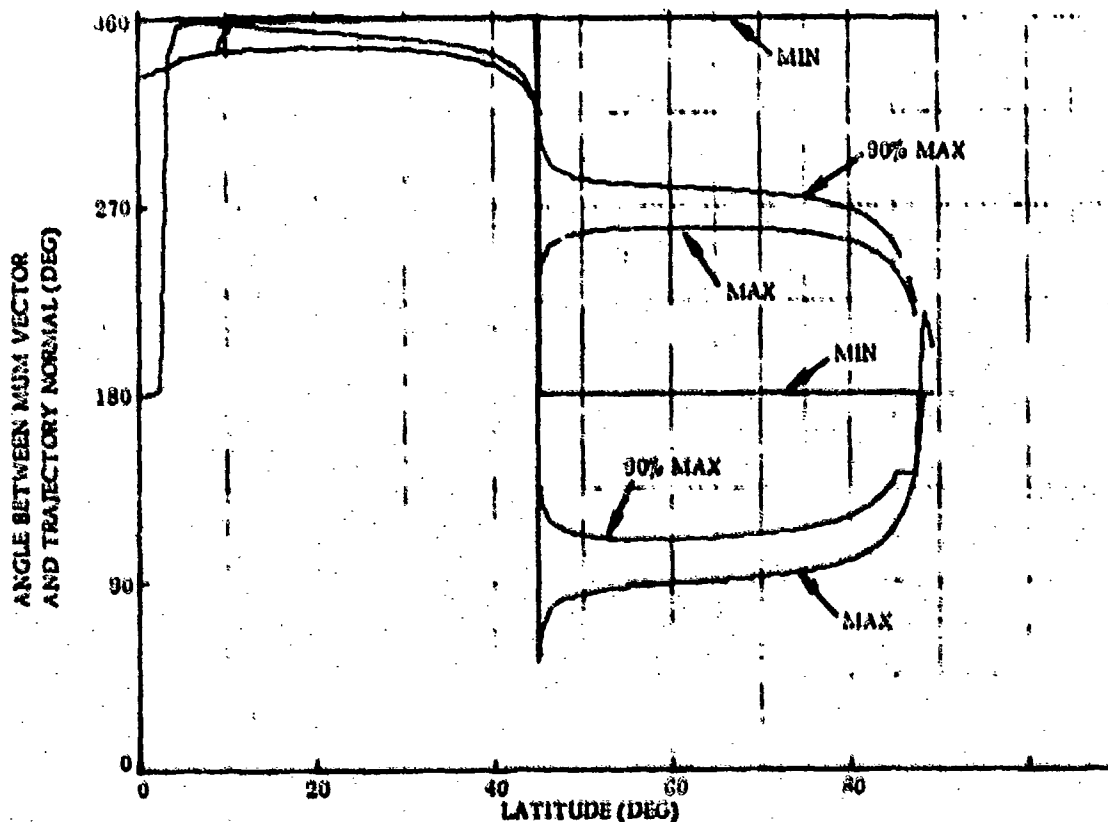


Figure C-1. Angle Between MUM Vector and Trajectory Normal at Min, Max and 90% Max Points in +C and +A Families (45 deg Separating Polhode, 0.03, 0.07 Pendulosity on A and B Axes Respectively)

be extrapolated 70 deg from the 90 percent max point to the min point. The extrapolation frequency is shown in Figure C-2 plotted against the polhode frequency. Also drawn on the figure is an approximation to the extrapolation frequency, F_{Extrap} , which is defined by:

$$F_{\text{Extrap}} = 1/T_p, \text{ if } 1/T_p > 0.0549$$

$$= 0.142, \text{ if } 1/T_p < 0.0549$$

A flow diagram of the phase tracking mechanization is shown in Figure C-3.

(1) MIN Event (IDPT -1)

All of the basic computations are performed at the min event. The max event is primarily used for data collection. This is because the minimum is always well behaved while the maximum can be quite broad and ill-defined and its position on the polhode trajectory varies when near the A axis as shown in Figure C-1.

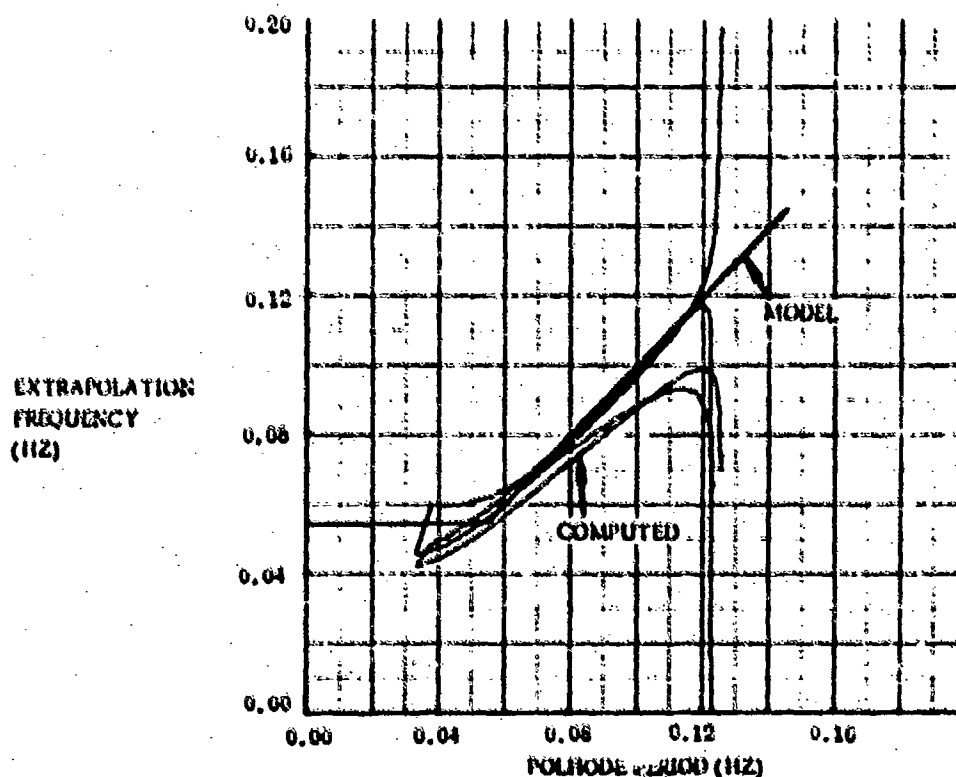


Figure C-2. Extrapolation Frequency vs Polhode Frequency
(45 deg separating Polhode, 0.03, 0.07 Pendulosity
on A and B Axes Respectively, 7.96 sec Polhode
Period Near A and C Axes)

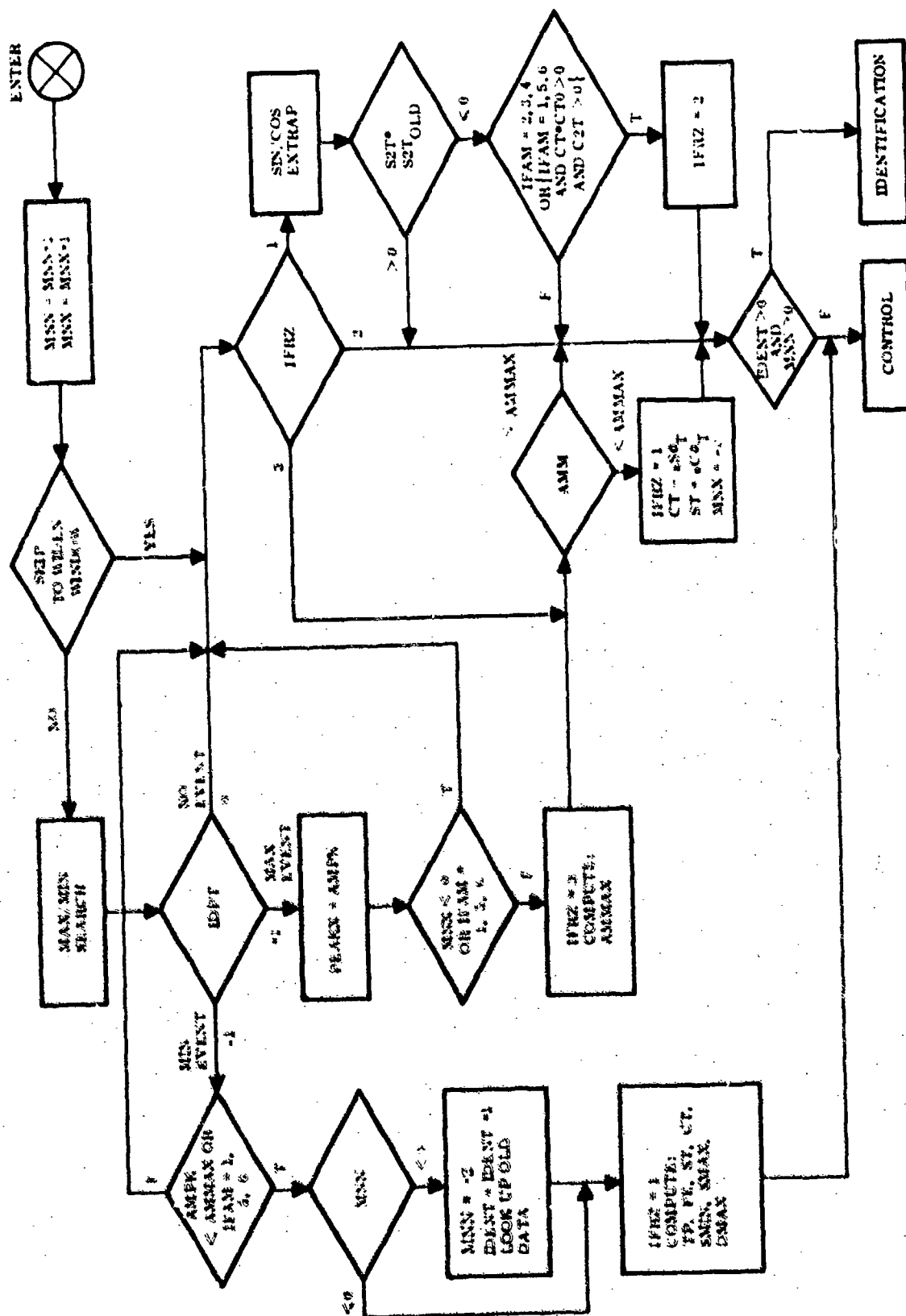


Figure C-3. Phase Tracking Flow Diagram

Data on the previous two min and max amplitudes and the time of the previous two min events must be saved. The old data must be identified as that which occurred 360 deg back in polhode phase from the most recent data and is called

PTO = time of old min event.

AMXO = amplitude of old max.

AMNO = amplitude of old min.

Also the amplitude of the maximum that occurred 180 deg back in polhode phase from the most recent data is identified (AMXI).

The number of minima per polhode period is stored by variable NMIN which can have value 1 or 2. Choosing the right value for NMIN is an identification function.

Phase lock is accomplished by remembering the sign of cos phase variable CT at the previous min. This is called CTO which can have value ± 1 . For NMIN=2 CTO reverses sign at every min. For NMIN=1 CTO keeps its same sign for every min. As an added protection against phase loss in the terminal control mode only, the sign of CTO with NMIN=1 is remembered and thereafter CTO must have the same sign whenever NMIN=1.

Compute polhode period, TP, and extrapolation frequency, FE,

$$TP = PTNO - PTO$$

$$FE = 2 \pi / TP, TP < TPO$$

$$= 2 \pi / TPO, TP \geq TPO$$

where TPO is a program constant.

Initialize the sin and cos of the phase variable

$$TH = (IDATA - PTNO) (FE)$$

$$ST = \sin (TH) CTO$$

$$CT^+ = \cos (TH) CTO$$

$$S2T = (CT) (ST)$$

Compute peak to peak MUM, PP,

$$PP = PEAKX - PEAKN$$

where PEAKX is the last observed max amplitude and PEAKN is the min amplitude.

In the ANbhd with large slopes a more accurate peak-to-peak computation is

$$PPAN = PEAKX - 1/2 (PEAKN + AMNO)$$

if the rotor was not torqued during the last polhode period.

Compute the change in max and min values over 360 deg which is used to represent the slope of the max and min

$$SMAX = PEAKX - AMXO$$

$$SMIN = PEAKN - AMNO$$

The difference between the two maxima, DMAX, must be computed both with and without torquing so the slope is removed from the data

$$DMAX = PEAKX - 2(AMXO) + AMXO$$

When no torque has been applied during the data taking interval the slope does not have to be removed so

$$DMAX = 2 (PEAKX - AMXO).$$

DMAX is twice Δ max presented in Figure 9.

To avoid false minima in the transition zone, the amplitude of the minima must be below the previous max threshold (AMMAX). However, the test cannot be performed in the A or CNbhd's since the high minima may not be below the threshold value. In the C or ANbhd's large torques produce significant relative change in the MUM amplitude and can result in false minima at the initiation of torque. Therefore, apparent min events that occur within 17 cycles after initiation of torque in A or CNbhd's are rejected. The sin/cos extrapolation is restarted at a min event by setting flag IFRZ = 1.

A minimum will be recognized on several cycles for the same min event. Due to noise the min may not be recognized on consecutive cycles. A series of minimum recognitions will be assumed to compose the same event if they are not separated by more than 3 cycles with no minimum recognized.

(2) Maximum Event

At the maximum event the maximum value, AMPK, is saved as PEAKX.

If the maximum threshold (AMMAX) has not been passed and polhode motion is not in the A or C Nbhd's, the phase variable is frozen at its current value by setting flag IFRZ = 3. The maximum threshold is computed

$$AMMAX = PEAKX - 0.05 (PEAKX - PEAKN)$$

where PEAKN is the previous minimum amplitude. Then if the current MUM amplitude is less than the maximum threshold (AMMAX) initialize the phase variable at $\phi_T + 90$ or $\phi_T + 270$ deg whichever is closest and restart sin/cos extrapolation by setting flag IFRZ = 1. ϕ_T is 20 deg as shown in Figure C-1.

(3) No Event

At times during which neither a maximum nor minimum event occurs, phase tracking is concerned with extrapolating the phase variable and determining whether a quadrature point was crossed. Extrapolation is not performed when it is frozen as determined by flag IFRZ. For IFRZ = 3 the MUM magnitude is compared to maximum threshold. AMMAX, as described in Para C.2.b(2). For IFRZ = 2 no computation is performed. For IFRZ = 1 the phase variable is extrapolated by

$$ST^+ = (ST^-) \cos (FE) + (CT) \sin (FE)$$

$$CT^+ = (CT^-) \cos (FE) - (ST^-) \sin (FE)$$

$$S2T = (ST) (CT)$$

$$C2T = (CT)^2 - .5$$

A quadrature point has been crossed by the phase variable if S2T reverses sign during the extrapolation. Freeze the extrapolation (IFRZ = 2) if a quadrature point is crossed and if either:

1. Polhode motion is not in A or C Nbhds, or
2. Polhode motion is in A or C Nbhds, and the quadrature point is 0 or 180 deg (min event), and it has been 360 deg since the last minimum event was recognized.

The reason for special treatment of the A and C Nbhds is that the maximum events do not always occur near quadrature points. When there is only one minimum per polhode period, the phase variable can only be frozen 360 deg after the minimum event.

After completion of phase tracking, the program always transfers to the control function except after a sequence of minimum events. Then the program transfers to identification for one pass. After initialization, identification cannot proceed until sufficient data base is built up by phase tracking to compute DMAX.

(4) Singularities

Polhode motion has six singular positions which are spin vector along the $\pm A$, $\pm B$, and $\pm C$ axes. The occurrence of one of these events has zero probability, however, an operational damping mechanization should be able to handle them. If neither maximum or minimum event has been found for a long time, PTMAX computation cycles, a singularity is assumed to exist. If spin vector was last estimated to be in the ANbhd with $\pm A$ axis identified damping is complete. Otherwise reinitialize automatic damping and apply C family torque for 3/8 of a CNbhd polhode period.

3. IDENTIFICATION

The data generated in phase tracking which consists of:

PEAKN = minimum value

PEAKX = maximum value

PP = peak-to-peak value

DMAX = 2 times difference between high and low maximum

SMIN = slope of minimum

SMAX = slope of maximum

TP = polhode period

is examined by the identification routine to select the appropriate control law. Variables DMAX, SMIN, and SMAX are not always valid, so logical variables IDMAX, ISMIN, and ISMAX are established to indicate when the data is valid. The conditions that invalidate the data are listed in Table CIII together with the data that is invalidated. The concern is that changes in the control law produce changes in slope and hence invalidate some of the data.

Table CIII Conditions Under Which Identification Data Are Invalid

Condition that invalidates data	Data invalidated	Number of Polhode cycles data are not valid
No torquing	SMIN SMAX	0.5 1.0
Initiate torquing	DMAX	1.5
Initiate torquing with polhode motion in transition zone	SMIN	1.0
Reverse C Family control	DMAX SMIN SMAX	1.5 1.5 1.5
Reverse A Family control	SMIN	2.5

The primary purpose of identification is to select one of five possible regions of the rotor that contains the spin vector. The regions are assigned numerical code, called IFAM:

1. CNbhd
2. C Family
3. Transition Zone
4. A Family
5. ANbhd
6. Undetermined region (no torque applied)

The sixth mode indicates identification has not taken place and is used for initialization. The A and CNbhd regions can have either 1 or 2 minima. Identification must determine the number of minima called NMIN.

Identification is performed by comparing data to threshold values to make decisions. The threshold values are listed in Table CII together with a brief description. The principals used in establishing the logic are briefly listed:

1. The transition zone is a symmetric band about the separating polhode. Since both PP and TP are approximately symmetric about the separating polhode, they are used to define the transition zone.
2. Both the A and CNbhd are identified by small PP values. The PP value is always small when NMIN = 1. A and CNbhd are differentiated by the magnitude of PEAKX.
3. A change in NMIN is identified by the conditions of the A or CNbhd plus an observed polhode period, T_p , that is either too large or too small.
4. The A and C families consist of the leftover regions. A portion of the C families is identified by small value of PEAKX. Near the transition zone this is unreliable and identification is based on DMAX. If DMAX is not valid identification is based on the previous family identification.

A flow chart of this portion of the identification problem is shown in Figure C-4. The only computation involved is that necessary to change NMIN. When NMIN changes from 1 to 2 a new minima has just appeared on the MUM waveform and there is no past history on the minima so identification is skipped. The polhode period, T_p , is doubled and the extrapolation frequency is recomputed. The sign of the phase locking variable, CTO, is reversed. When NMIN changes from 2 to 1 the previous minimum data is 360 deg old. The phase tracking data is recomputed on this basis as described in Para C. 2. b. (1). Identification is then repeated with NMIN = 1.

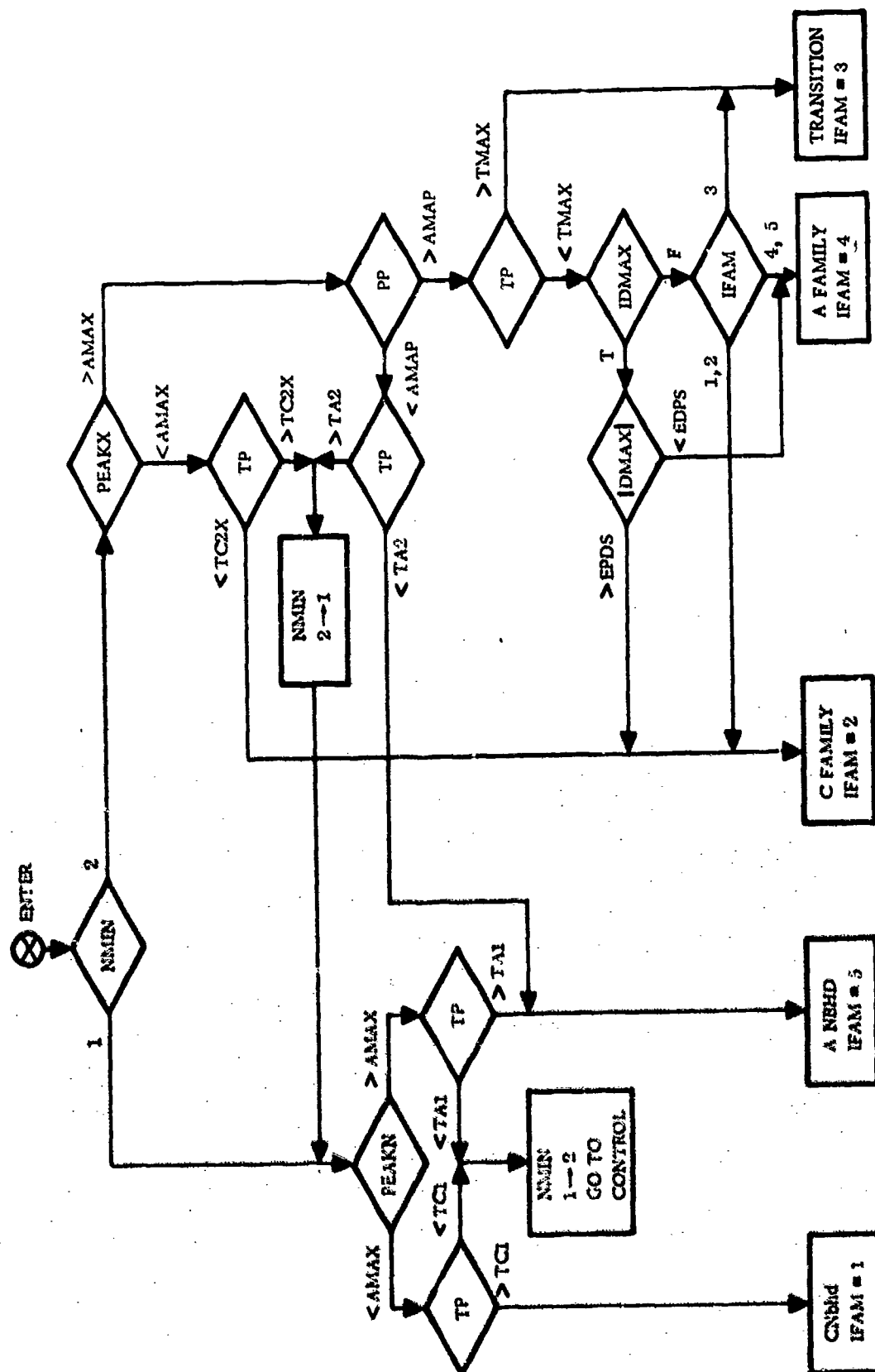


Figure C-4. Identification 1 Flow Diagram

The number of min can remain at one very deep into the C family for large pendulosity components on A and B axes. A constant TP threshold for recognizing the change of NMIN from one to two is not adequate as can be seen from the frequency plot of Figure 2. Therefore the threshold for changing NMIN from one to two in the C family, TC2X, is based on approximate polhode latitude as given by

$$TC2X = TC2 (1 + 0.25 \frac{PEAKX}{AMAX})$$

The polhode period near the A axis varies significantly with rotor temperature. Thresholds TA1 and TA2 should roughly obey the relationship

$$TA1 = (0.75) ATP$$

$$TA2 = (1.25) ATP$$

where ATP is the polhode period near the A axis. ATP is computed by the program

$$ATP = ATP - (0.3935) (TP - ATP)$$

which is a low pass filter with a time constant of two identification cycles. ATP is only allowed to have values in a limited range of ± 25 percent of nominal polhode period near A axis. Figure C-5 illustrates the NMIN switching logic.

After the basic identification is completed several special cases must be resolved. A flow chart of these special cases is shown in Figure C-6.

a. Identify +A Axis

The +A axis is implicitly identified by resolving the 180 deg uncertainty in the phase variable. The 180 deg uncertainty can only be resolved in the C family (IFAM = 2). SGN is a variable (± 1) indicating the estimated sign of the C family. The algorithm is:

1. (DMAX) (SGN) > 0
The phase variable is near 0 deg.

$$CT^+ = |CT^-|$$

$$ST^+ = |ST^-|$$

$$CTO = 1$$
2. (DMAX) (SGN) < 0
The phase variable is near 180 deg.

$$CT^+ = -|CT^-|$$

$$ST^+ = -|ST^-|$$

$$CTO = -1$$

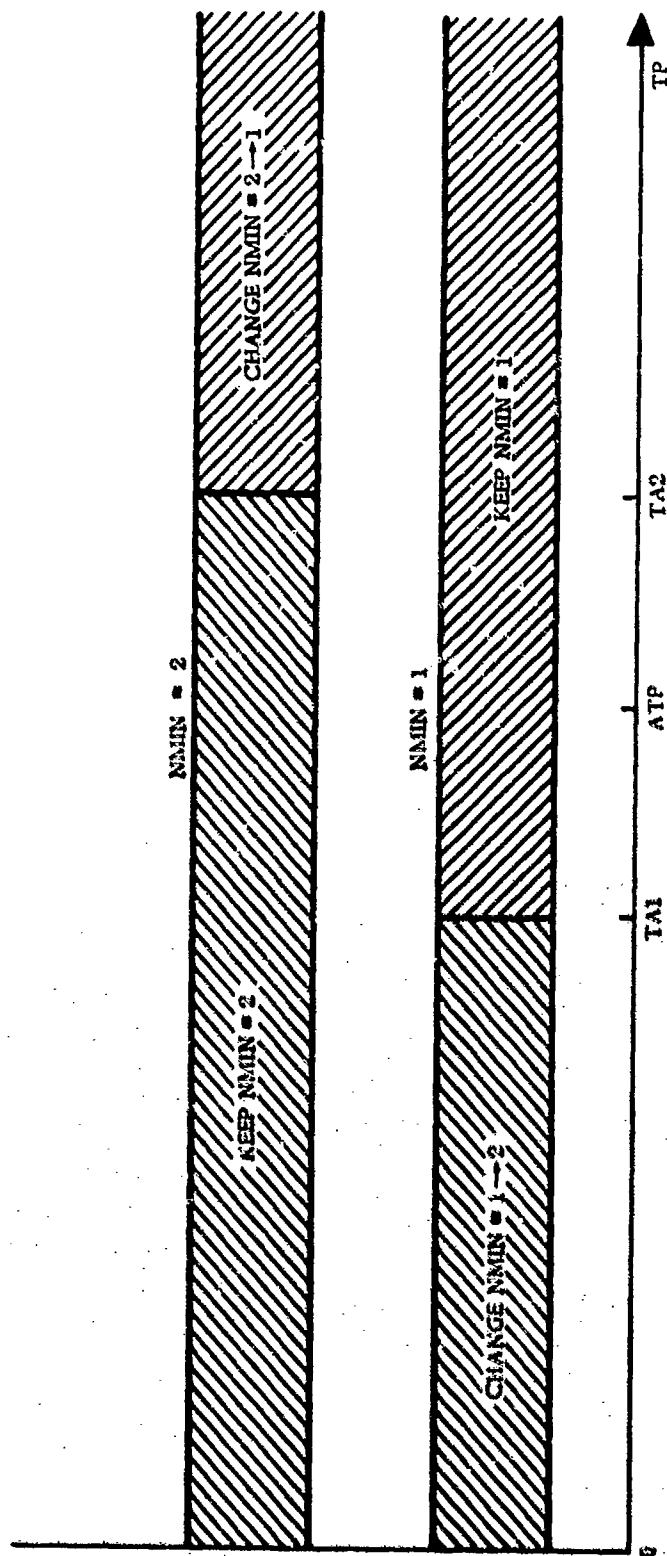


Figure C-5. NMN Switching Logic

After the +A axis is identified a flag, IPHAS, is set

$$\text{IPHAS} = 1.$$

b. Identify +C or -C Family

The C family control law should always torque to move out of the C family. If the sign of the C family (SGN) is assumed wrong it will torque into the C axis as indicated by a negative SMIN. However, in the C Nbd the polhode trajectories that do not enclose the pendulosity vector have a negative SMIN when moving away from C as can be seen in Figure 8. Under these conditions the sign of the C family must be determined by the slope of the max, SMAX. If SMIN and SMAX have the same sign, the polhode trajectory encloses the pendulosity vector and the more efficient C control law can be used.

If the first identification of automatic damping locates polhode motion in the C family the ANbd control law is used until the C family sign is resolved. The correct SGN always results in a large positive SMIN or SMAX so an incorrect SGN is indicated by

$$\text{SMIN} < \text{EPSCN} \text{ or } \text{SMAX} < \text{EPSCN}.$$

Since SGN was previously involved in determining the +A axis the phase variable is in error by 180 deg and must be corrected whenever SGN is reversed.

When automatic damping is operating correctly, SGN should not be wrong after the first identification of +C family. If a later change in SGN is required, the automatic damping has gotten lost and should be restarted.

c. Torque Out of A Family

If the +A axis has not been identified (IPHAS = 0) and polhode motion is in the A family, the spin vector must be torqued into the C family. Therefore, 180 deg shifts in the phase variable are introduced to keep

$$\text{SMIN} < \text{EPSAN}.$$

d. Prevent Phase Loss in A Nbd

Once the polhode motion has been placed in the A family with the +A axis defined it should not be allowed to leave the family due to automatic damping malfunction resulting in phase loss. Therefore, 180 deg shifts in the phase variable are introduced to keep

$$\text{SMIN} > -\text{EPSAN}.$$

The phase loss may have been caused by terminal control gain that was too high. If this mode is entered the terminal control gain is reduced by one half.

e. Detect Crossing off the Separating Polhode

In the transition zone there are two cases based on the polhode region (IFAM) of the previous identification cycle that must be considered.

(1) Previous IFAM $\neq 6$

After the separating polhode has been crossed there is no longer a need to apply the transition control law which is only half as efficient as the C and A family control laws. The slope of the max, SMAX, is zero in the A family and nonzero in the C family. When crossing from C to A families IPHAS is 1 and a crossing is detected when

$$|S_{MAX}| < EPSMA.$$

When crossing from A to C families IPHAS is 0 and a crossing is detected when

$$|S_{MAX}| > EPSMC.$$

After entering the C family, torquing is stopped for one polhode period to obtain data to identify the +A axis. The C family sign, SGN, is reversed to prepare for torquing out of C family after +A axis is identified.

(2) Previous IFAM = 6.

If polhode motion is on the C side of the transition zone after a period of no torquing, the +A axis can be identified before torquing starts. Polhode motion is on the C side of the transition zone if

$$|D_{MAX}| > EPDS.$$

f. Terminal Control Functions

Terminal control is used when the spin vector is in the ANbhd and the +A axis has been identified. It is concerned with precisely computing the peak-to-peak amplitude for use in proportional control, computing the control angle, and determining when damping is complete.

The peak-to-peak amplitude, PP, must be corrected for slope effects due to rotor speed changes. When the peak-to-peak signal is large relative to slope the correction is based on average SMAX, ASMAX, computed

$$ASMAX = SMAX + (0.3935) (SMAX - SMAX).$$

The corrected peak-to-peak amplitude is

$$PP = PP + (ASMAX) (TP)/(2 NMN)$$

For small peak-to-peak MUM signal the corrected PP value can only be obtained after a complete polhode period of no torquing in which case the PPAN computed in paragraph C. 2. b. (1) is the correct value for PP. For small PP values the

untorqued slope must be given to the least squares max/min search as ISLOP in paragraph C.2. a.

$$\text{ISLOP} = \text{SMIN}/\text{TP}$$

if no torque has been applied for one polhode period.

If the +A axis has been identified proportional control is used. The desired angle to be torqued, NANG, is computed once per polhode period. Maximum torque is applied immediately after identification and continues until the desired angular change is introduced. No further torque is applied until the next identification.

Angle to be torqued, NANG, is based on the estimated polhode colatitude. Polhode colatitude is related to peak-to-peak MUM, PP, as shown in Figure C-7 for pendulosity components on A and B axes of one percent and 45 deg separating polhode. Gain variations and pendulosity length variations from gyro-to-gyro can be eliminated in these computations if normalized peak-to-peak amplitude is used

$$\text{PP}_N = \text{PP}/\text{PEAKX}.$$

Figure C-8 shows the A-C plane cross section of a polhode trajectory with colatitude $\Delta\theta$ and pendulosity component on A axis of $\sin \theta_0$. The figure is drawn for

$$\Delta\theta < \theta_0$$

so that NMIN = 1. The peak-to-peak amplitude is then

$$\begin{aligned}\text{PP}_N &= \cos(\theta_0 - \Delta\theta) - \cos(\theta_0 + \Delta\theta) \\ &= (2\theta_0) \Delta\theta.\end{aligned}$$

When

$$\Delta\theta > \theta_0$$

so that NMIN = 2, the peak-to-peak amplitude is

$$\begin{aligned}\text{PP}_N &= 1 - \cos(\Delta\theta \pm \theta_0) \\ &= \frac{(\Delta\theta \pm \theta_0)^2}{2}\end{aligned}$$

The colatitude at which NMIN changes from 2 to 1 is

$$\Delta\theta = \theta_0$$

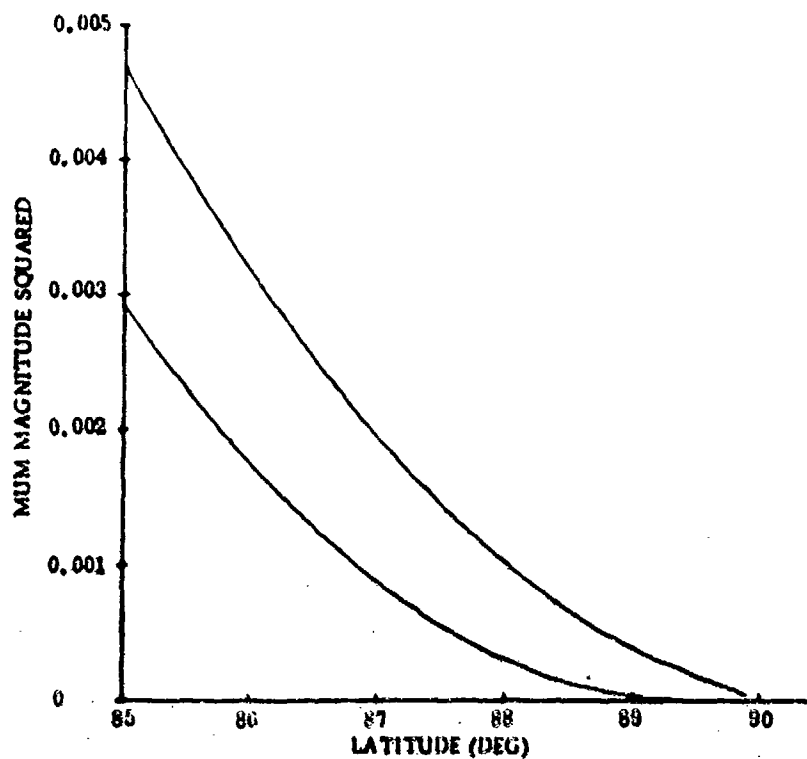


Figure C-7. Peak-to-Peak MUM Magnitude in ANbhd (45 deg separating polhode, 1 percent pendulosity on A and B)

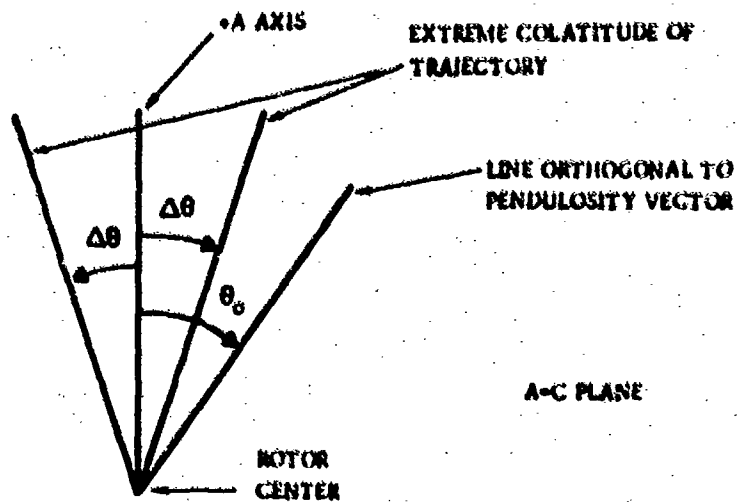


Figure C-8. Geometry of Peak-to-Peak MUM Amplitude in ANbhd

and the peak-to-peak amplitude is

$$PP_N = 2 \theta_0^2.$$

Angle θ_0 is not controlled in the manufacturing process and will vary considerably from rotor-to-rotor. On a perfect rotor $\theta_0 = 0$. However, for $NMIN = 2$

$$0 \leq \sqrt{PP_N} \leq \sqrt{2\Delta\theta}$$

so that control angle, $\Delta\theta_c$, is

$$\Delta\theta_c = \frac{G}{\sqrt{2}} \sqrt{PP_N}$$

where G is the control gain. Maximum control is applied just before $NMIN$ changes from 2 to 1. ANbhd control is initiated when the spin vector is nearest the B axis. In this region torquing efficiency is 70 percent for 45 deg separating polhode. Therefore, G can be unity without danger of applying more than 100 percent control. Just before $NMIN$ changes from 2 to 1 the peak-to-peak amplitude PP_{N2} is approximately described

$$\theta_0 = \frac{1}{\sqrt{2}} \sqrt{PP_{N2}}$$

However PP_{N2} is not known precisely because in general uncontrolled slopes due to rotor speed changes corrupted the data. Since the last $NMIN = 2$ point is not recognized until the first $NMIN = 1$ point is obtained, PP_{N1} , an accurate peak-to-peak value of PP_{N1} can be obtained by applying no torque for one polhode period. The problem now is to obtain θ_0 in terms of PP_{N1} . The control angle used to go from PP_{N2} to PP_{N1} is saved as $\Delta\theta_{C2}$. Therefore

$$\theta_0 - \Delta\theta_{C2} = PP_{N1}/2\theta_0$$

and solving for θ_0

$$\theta_0 = 1/2 (\Delta\theta_{C2} + \sqrt{\Delta\theta_{C2}^2 + 2 PP_{N1}})$$

so that the control angle for $NMIN = 1$

$$\Delta\theta_c = \left[\frac{G}{\Delta\theta_{C2} + \sqrt{\Delta\theta_{C2}^2 + 2 PP_{N1}}} \right] PP_N$$

This mechanization is adaptive in that the gain is automatically adjusted for θ_0 without requiring θ_0 to be input as a calibration parameter.

The control angle is normalized on unit torque angle which on tests presented here is

$$\delta\theta = \text{unit torque angle} = 1/8 \text{ (max torque) (0.1 sec)}$$

The normalized control angle, NANG, is

$$\text{NANG} = \Delta\theta_C / \delta\theta$$

The proportional control mechanization can be reduced to three equations. For NMIN = 2

$$\text{NANG} = (\text{GPAN2}) \sqrt{\text{PP}_N}$$

On the first NMIN = 1 compute PP_{N1} so that

$$\text{GPAN1} = \frac{(\text{GPAN2}) \sqrt{2}}{\Delta\theta_{C2} + \sqrt{\Delta\theta_{C2}^2 + 2 \text{PP}_{N1}}}$$

where

$$\Delta\theta_{C2} = \frac{1}{\sqrt{2}} (\text{NANGO}) / \text{GPAN2}$$

and NANGO is the previous value of NANG used to go from PP_{N2} to PP_{N1} . For NMIN = 1

$$\text{NANG} = (\text{GPAN1}) \text{PP}_N$$

GPAN2 is a hardware parameter and is defined

$$\text{GPAN2} = \frac{G}{\sqrt{2} \delta\theta}$$

The net control gain as defined by $\Delta\theta_{CT} / \Delta\theta$ where $\Delta\theta_{CT}$ is the total control angle over one polhode period and $\Delta\theta$ is polhode colatitude at the beginning of the period will be computed. First for NMIN = 2 the first control angle is

$$\begin{aligned} \Delta\theta_{C1} &= (\eta G / 2) \sqrt{\text{PP}_1} \\ &= (\eta G / 2) (\Delta\theta \pm \theta_0) \end{aligned}$$

where η is the torque efficiency as shown in Figure 14. Assuming the control is accomplished before the second min occurs which is at colatitude $\Delta\theta_1$

$$\Delta\theta_1 = \Delta\theta - \Delta\theta_{C1}$$

the second control angle is

$$\begin{aligned}\Delta\theta_{C2} &= (\eta G/\sqrt{2}) \sqrt{PP_2} \\ &= (\eta G/2) (\Delta\theta - \Delta\theta_{C1} \mp \theta_0)\end{aligned}$$

The total control angle $\Delta\theta_{CT}$ is then

$$\begin{aligned}\Delta\theta_{CT} &= \Delta\theta_{C1} + \Delta\theta_{C2} \\ &= (\eta G/2) [\Delta\theta(2 - \eta G/2) \mp \theta_0 \eta G/2]\end{aligned}$$

which is valid for $\Delta\theta > \theta_0$. For $NMIN = 1$ $\Delta\theta \geq \theta_0$ the gain is frozen at the last $NMIN = 2$ value. Figure C-9 presents the input-output plot showing the range of possible gains that can occur for $\eta G = 1$ and the large variation from run to run. In practice smaller values of ηG must be used since η is unpredictable due to its phase dependence.

The phase variable extrapolation during terminal control torquing is unstable. The phase variable is used to direct the torque vector and track the polhode motion. If the phase variable leads the polhode motion a torque vector component will point in a direction to slow down the polhode motion thus increasing the phase variable error. The effect occurs throughout the A family however the extrapolation period is so short and the polhode motion is so much stronger than the torque that the effect is negligible except for a small region about the A axis. The problem was briefly investigated to determine if any real danger of phase loss exists. Starting with the differential equations of polhode motion, Equation (2), the motion in the ANbhd where ω_A is essentially constant is

$$\omega_B = -K_B \omega_C + T_B$$

$$\omega_C = K_C \omega_B + T_C$$

where

$$K_B = \frac{A - C}{C} \omega_A$$

$$K_C = \frac{A - B}{C} \omega_A$$

and torque defined by the A control law

$$T_B = T \cos \hat{\phi}$$

$$T_C = T \sin \hat{\phi}$$

$$\hat{\phi} = \text{phase variable.}$$

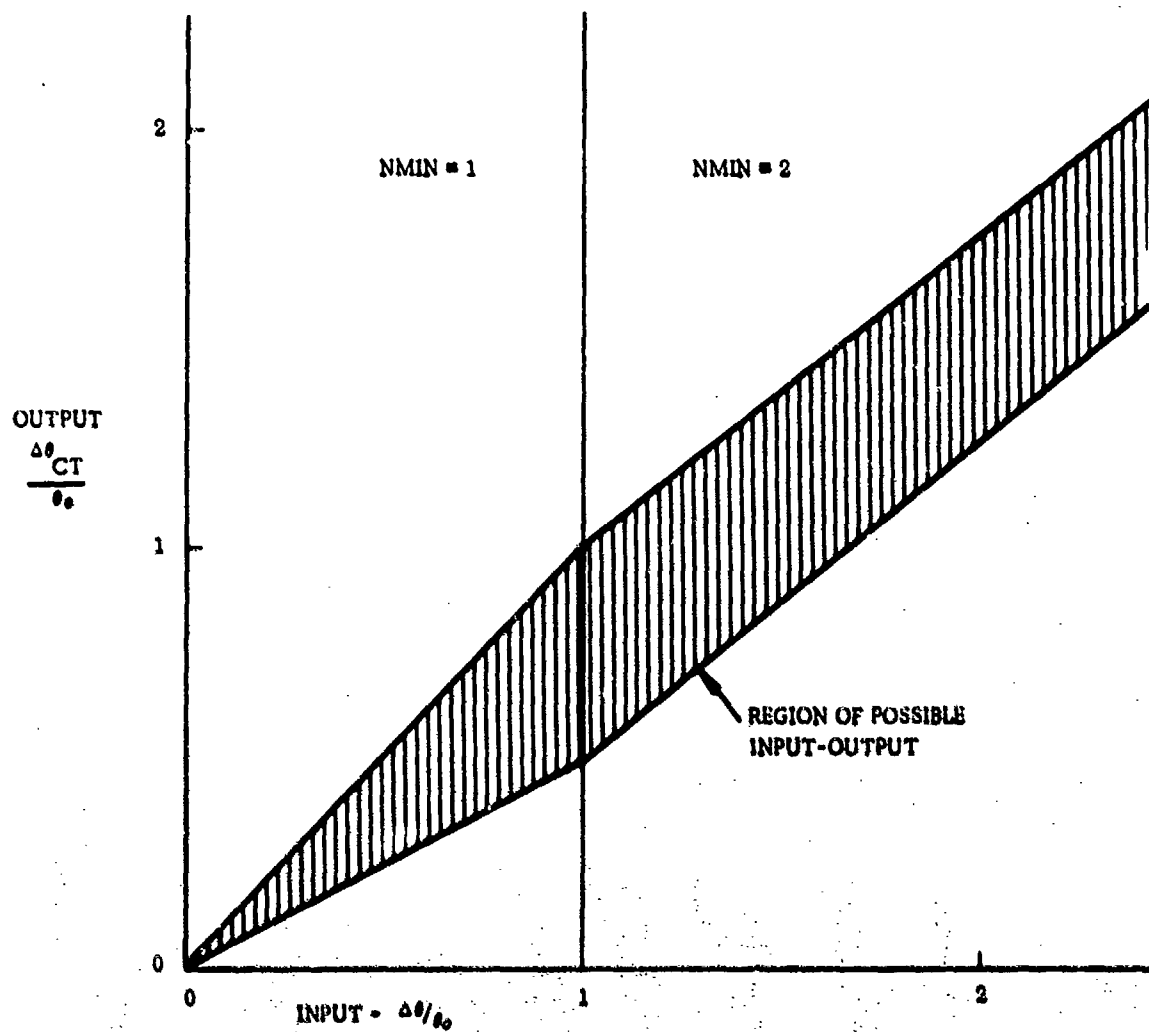


Figure C-9. Terminal Control Input-Output Relationship
($\eta G = 1$)

Transforming into an elliptical coordinate frame with

$$\omega_B = \frac{1}{\sqrt{K_C}} r \cos \phi$$

$$\omega_C = \frac{1}{\sqrt{K_B}} r \sin \phi$$

gives

$$\dot{\phi} = J + \frac{TR(\hat{\phi})}{r} \sin(\phi - \hat{\phi})$$

$$\dot{r} = -R(\hat{\phi}) \cos(\phi - \hat{\phi})$$

where

$$J = \sqrt{K_B K_C}$$

$$R(\hat{\phi}) = \frac{1}{\sqrt{\cos^2 \hat{\phi} \frac{K_B}{K_C} + \sin^2 \phi}}$$

Phase variable $\hat{\phi}$ is extrapolated by

$$\dot{\hat{\phi}} = \hat{J}$$

The phase variable error during extrapolation and control, $\delta\phi$, is given by

$$\delta\dot{\phi} = \delta J + \frac{TR(\hat{\phi})}{r} \sin(\delta\phi)$$

$$\delta J = J - \hat{J}$$

It can be seen that $\delta\phi$ has an unstable equilibrium at zero and a stable equilibrium at 180 deg which supports the intuitive observation made earlier. $\delta\phi$ has been evaluated numerically for various conditions of initial phase error, $\delta\phi(0)$, frequency error, δJ , initial distance from A, $r(0)$, and torque magnitude, T . The number of degrees of freedom were further reduced in the numerical evaluation by normalization. The largest error at the end of the control period was 90 deg which was caused by an extrapolation frequency error of 0.3 rad/control period plus a 20 deg initial phase error and applying 100 percent of estimated control. As an added precaution control is not applied if the phase variable has been extrapolated more than 270 deg.

Termination of polhode damping is based solely on the peak-to-peak MUM amplitude. A threshold is set that is just above the noise level. The peak-to-peak amplitude must be under the threshold for two consecutive polhode periods.

4. CONTROL

The control function involves computing the appropriate control law and commanding the appropriate motor currents in the spin motor control electronics. The control law commands 2 degrees of freedom, the amplitude of torque and direction of torque in a plane orthogonal to the spin vector. The control law computes three scalar quantities

$$\text{TORQ}_1 = \cos \theta$$

$$\text{TORQ}_2 = \sin \theta$$

$$\text{FLUX} = \sqrt{\frac{\text{Desired Torque}}{\text{Max Torque}}}$$

where Amplitude is the desired torque amplitude and θ is the angle from MUM vector to torque vector measured about spin vector.

a. C Family Control Law

The C family control law applies maximum torque along \pm MUM vector.

$$\text{TORQ}_1 = -\text{SGN}$$

$$\text{TORQ}_2 = 0$$

$$\text{FLUX} = 1$$

b. CNbhd Control Law

The basic control law is the same as the C family control law except torque is not applied continuously under all conditions. Polhode trajectories very close to the C axis do not enclose the pendulosity vector and so torquing can only be performed near the max value of MUM magnitude. If the sign of the C family is wrong, continuous torquing will slave the spin vector to be collinear with the pendulosity vector. Both difficulties can be overcome with a simple mechanization. At each identification compute threshold

$$\text{CMAX} = \text{PEAKX}_{\text{old}} - 0.25 (\text{PEAKX}_{\text{old}} - \text{PEAKN})$$

where PEAKN is the value of MUM min last observed and $\text{PEAKX}_{\text{old}}$ is the value of MUM max two observations ago. When initially starting up CMAX is the value to be observed on the next max event reduced by 25 percent of the peak-to-peak value. Start torquing and continue to torque as long as

$$\text{AMM} > \text{CMAX}.$$

If after torquing has been initiated the above inequality fails, further torquing is prohibited by setting

$$C_{MAX} = 1$$

until the next identification period. This prevents limit cycling that might otherwise occur. If the C family sign (SGN) is wrong the inequality will fail after torquing for 1/16 sec. Subsequent identification will resolve the SGN error.

c. A Family Control Law

The A family control law applies maximum torque while rotating the torque vector with respect to MUM.

$$TORQ_1 = CT$$

$$TORQ_2 = ST$$

$$FLUX = 1$$

d. Transition Zone Control Law

The transition zone control law must be compatible with either C or A family polhode motion. When CT and SGN are of opposite sign

$$TORQ_1 = (CT - SGN) (5/8 - 1/8 CT)$$

$$TORQ_2 = (ST) (5/8 - 1/8 CT)$$

$$FLUX = 1$$

and when CT and SGN are of same sign

$$TORQ_1 = TORQ_2 = 0.$$

e. ANbhd Control Law

If the +A axis has not been identified the ANbhd control law is identical to the A family control law. Control is only applied for half a polhode period.

When the +A axis has been identified control is applied as in the A control law except the duration of torque is adjusted to correspond to the control angle command, NANG.

f. Rate Limited Torque

The rate of change of torque is limited to avoid large transients in the magnetic flux field. Torque is quantized by the unit torque which is 1/8 the maximum torque. Torque is raised and lowered by one step change per computational cycle.

This mechanization does not appear to be necessary.

g. Spin Motor Control Electronics Commands

Spin motor control commands consist of three vectors α_s , β_s , γ_s where

$$\alpha_s = \left[(\text{TORK}_1) \alpha'_N + (\text{TORK}_2) \beta'_N \right] \text{ FLUX}$$

$$\beta_s = \left[(\text{TORK}_1) \beta'_N - (\text{TORK}_2) \alpha'_N \right] \text{ FLUX}$$

$$\gamma_s = \left[\gamma_N \right] \text{ FLUX}$$

and α'_N , β'_N , γ'_N corresponds to vectors α_N , β_N , γ_N computed in Para C.1 with no phase shifts introduced by the electronics. The net phase shift introduced by both MUM readout electronics and spin motor control electronics is compensated by

$$\alpha'_N = \cos \phi \alpha_N + \sin \phi \beta_N$$

$$\beta'_N = \sin \phi \alpha_N + \cos \phi \beta_N$$

where ϕ is the nominal phase shift inherent in the electronic design.

If the x, y, and z gyro motor coils exhibit a scale factor unbalance or axis misalignment they can be compensated by a (3x3) matrix, C_T . The spin motor commands would consist of vectors α'_s , β'_s , γ'_s where

$$\alpha'_s = C_T \alpha_s$$

$$\beta'_s = C_T \beta_s$$

$$\gamma'_s = C_T \gamma_s$$

If this compensation is used it would only be a nominal compensation based on an ensemble of gyros. Individual calibration of the motor coils is not intended. Motor coil compensation was not used in the tests reported here.

5. INITIALIZATION

Initialization of course is performed at the beginning of polhode damping. There are also two conditions under which reinitialization is performed. They are:

1. C family sign reversal occurred after the initial sign determination was made. Automatic damping is lost. Reverse the C family sign and reinitialize. (Para C.3. b.)

2. The separating polhode was crossed from A to C and the +A axis has not been identified. Reverse the C family sign and reinitialize. (Para C. 3. 3. (1).

After reinitialization data is taken for one complete period before identification and further torquing. After the original initialization, data is taken until three minima are found before identification and initiation of torquing. The original initialization must accumulate 17 data points before the maximum/minimum search can begin.

APPENDIX D

AUTOMATIC POLHODE DAMPING SUBROUTINE LISTING

The IBM 1130 Fortran subroutine CNTLR listed here is called from an executive routine 10 times per second based on an interrupt clock. MUM data is read and MUM magnitude, AMM, is computed by the executive before calling CNTLR. CNTLR specifies direction, TORQ(1) and TORQ(2), and magnitude, NTQ, of torque to the executive. The executive sends the torque commands to the spin motor control electronics.

Other variables used to communicate with executive are:

- (1) PARAM = a general parameter list 25 elements long. Each of the elements is defined in the listing. The values used for the automatic damping tests are:

PARAM	(1)	96.
	(2)	0.0001
	(3)	0.34
	(4)	3056.
	(5)	0.015
	(6)	0.3935
	(7)	80.
	(8)	0.1
	(9)	8.
	(10)	0.
	(11)	0.02
	(12)	0.008
	(13)	2.
	(14)	0.004
	(15)	0.002
	(16)	0.3935
	(17)	0.
	(18)	2.5
	(19)	2.5
	(20)	2.
	(21)	64.
	(22)	106.
	(23)	19.
	(24)	57.
	(25)	20.

- (2) JGAIN specifies the MUM filter time constant.

- (3) JMODE specifies special test modes

JMODE = 2, MUM Phase calibration mode
= 4, No Torque is applied
= 5, Normal mode.

(4) **MODE** specifies automatic damping modes

- MODE** = 1, Initialization
- = 2, Normal Damping Mode
- = 3, Damping Complete
- = 4, Print automatic damping data after damping complete
- = 5, Stop torquing
- = 6, Undamp from an equilibrium point.

Two assembly language subroutines are called from **CNTRLR**.

(1) **LSTSQ** (**ISLOP**, **IBOC**, **IPK**, **JPk**, **IDPK**)

LSTSQ mechanizes the max/min search of Para C.2.a where

$$\text{IBOC} = (B + .5 \text{ ISLOP})/C$$

$$\text{AMFK} = \text{IPK} (6.4 \times 10^{-5}) + \text{JPk} (19.7 \times 10^{-10})$$

LSINT is the initialization entry for **LSTSQ**

(2) **SICOS** (**ITH**, **ISIN**, **ICOS**)

SICOS is a sin/cos routine where

$$\text{ITH} = 0 \quad 2^{15}/\pi \text{ (input)}$$

$$\text{ISIN} = \sin(\theta) \quad 2^{14} \text{ (output)}$$

$$\text{ICOS} = \cos(\theta) \quad 2^{14} \text{ (output)}$$

One Fortran function routine called from **CNTRLR** is

$$\text{FE} = \text{FXTRP}(\text{TP}, \text{FEO})$$

where

TP is the polhode period

FE is the phase variable extrapolation frequency

FEO is dummy variable not used.

The computation for **FE** in Para C.2.b.(1). is mechanized.

Copy available to DDC does not
 permit fully legible reproduction

```
// FOR
*LIST SOURCE PROGRAM
*ONE WORD INTEGERS
  SUBROUTINE CRTL2
    REAL LAG
    DIMENSION IDAT(9,150),FIDAT( 7,150)
    DIMENSION PTVX(2),AMX(2),AMX(2)
    COMMON TORQ(2),NTQ,      PARAM(25),AMX,JGAIN,MODE,JMODE
    DATA PKYST,PXLST/6.4499484E-5,19.883680422E-10/
    DATA P15,R14/10430.37835,6.10351583E-5/
    DATA CSLOP/106954752./
    DATA R10                                     /9.765625E-4/
    DATA DPK,THX,PPC./0.05,20.0,0.25/
C   TIME LAG FOR NEW MAX / MIN
    DATA VMAX,VMAXC/-2,-8/
C   FILTER THRESHOLD
    DATA PPFLT/0.002/
C
    PARAM(17)=-1
    GO TO (101,200,200,340,700,199),MODE
C   SHUT DOWN MODE
    700 NTQ=0
    IDATA=IDATA+1
    GO TO 190
C   MODE 6 - UNDAVE FROM EQUILIBRIUM POINT
    199 IF (IDATA-IDATS) 195,196,196
    195 IDATA=IDATA+1
    GO TO 800
C
C   INITIALIZATION
C
    101 CONTINUE
    TVAX=PARAM(1)
    PPF=PARAM(2)
    AVAX=PARAM(3)
    GPAR2=PARAM(4)
    AMAP=PARAM(5)
    GSLOP=PARAM(6)
    MANG=PARAM(7)+.5
    AMTP=PARAM(8)
    NTQVX=PARAM(9)+.5
```

PAGE 2

```
PHASE=PARAM(10)
EPDS=PARAM(11)
EPDMA=PARAM(12)
GPHAS=PARAM(13)
EPSCN=PARAM(14)
EPSAN=PARAM(15)
GTP=PARAM(16)
ID2=PARAM(18)
IDC=PARAM(19)
NPR NT=PARAM(20)
TA10=PARAM(21)
TA20=PARAM(22)
TC1=PARAM(23)
TC2=PARAM(24)
PTMAX=PARAM(25)
MODEC=2
IDAT1=C
NMIN2=0
ATP=TA10/.75
IPT=0
NPT=0
NTQD=0
NWIND=17
CALL LSINT
GO TO (161,162),IDC
161 CT=1.
   CTO=1.
   SGN=-1.
   GO TO 163
162 CT=-1.
   CTO=-1.
   CT1=CTO
   SGN=1.
163 CONTINUE
   ST=0.
   PTMN(1)=0.
   PTMN(2)=0.
   DS=0.
   DC=1.
   FE=0.
```

PAGE 3

```
FED=0.
CX= SIN(THVX*.0174533)
SVX= COS(THVX*.0174533)
SPVX=-2.*CX*SVX
CV=1
VX=1
IFRZ=7
ICATA=0
ID=1
AF2=1
ATC=0
106  XODE=7
    JGAIN=12
    LAG=.5
    IDENT=-1
    IFXOD=2
    ICAT2=ICATA+NX*IND
    PTN1=ICATA+PTMAX
    JVAX=0
    CVAX=0
150  SGV=-SGV
    IFAV=6
    XANGO=C
    ISIGN=C
    INIDE=0
    XSLOP=0
    TA1=TA10
    TA2=TA20
    IDENT=IDENT-1
    ASVAX=C
    IGPAN=1
    CVIN=2
    IDVAX=1
    KDVAX=2
    ISVAX=0
    ASVAX=1
    ISVIN=0
    ASVIN=0
    IPHAS=0
    GO TO (901,902),ID2
```


PAGE 4

901 IPHAS=1
902 CONTINUE
GO TO 791

C

C PHASE TRACKING

200 CONTINUE
IF (IDATA-PTN1) 190,190,191

C NO MIN CAN BE FOUND

191 IF (IPHAS) 192,192,193
193 IF (IFAV-5) 192,194,192
192 MODE=6

IDATS=IDATA+TC1*.5

IFAN=7

GO TO 800

C DAMPING COMPLETE

194 MODE = 3

GO TO 400

190 CONTINUE

IF (JMODE-5) 110,111,111

110 ISMAX=0

ISMIN=0

111 CONTINUE

IDATA=IDATA+1

MAX=MAX+1

MIN=MIN+1

ISLOP=NSLOP

ISKIP=IWIDE*MOD(IDATA,2)

IF (ISKIP) 302,302,202

302 CALL LSTSQ(ISLOP, IHOC, IPK, JPK, IOPT)

IF (IWIDE) 303,303,305

305 IHOC=IHOC+IHOC

JGAIN=16

LAG=8.5

303 IF (IOPT) 201,204,203

C NONE

204 CONTINUE

202 GO TO (205,250,206),IFRZ

205 CONTINUE

C SIN/COS UPDATE

STO=ST

PAGE 5

```
S2T0=S2T
ST=ST*DC+CT*DS
CT=CT*DC-ST0*DS
S2T= ST*CT
C2T=CT*CT-.5
IF (S2T*S2T0) 207,207,250
C A/C NBHD LOGIC
207 CONTINUE
GO TO (208,210,210,210,208,208),IFAM
208 IF (C2T) 253,253,209
209 IF (CT*CT0) 250,250,210
210 IFRZ=2
PARAM(17)=0.
C LIMIT TORQUE FOR 270 DEG - A NBHD
253 IF (ST*CT0) 254,254,250
254 NANG=0
250 CONTINUE
IF (IDENT*(1-ISKIP)) 800,800,251
251 IF (MNX) 800,800,252
252 IDENT=0
GO TO 400
C
C
206 IF (AMM-AMMAX) 214,214,250
C MAX THREASHOLD
214 IFRZ=1
MNX=MNX0
CT=-CMX*CT0
ST=SMX*CT0
S2T=S2MX
PARAM(17)=1.5
GO TO 250
C MAX POINT
203 PEAKX=IPK*PKNST+JPK*PKLST
JMAX=1
STX=ST
IF (MNX) 202,220,220
220 GO TO (202,221,221,221,202,202),IFAM
221 CONTINUE
IF ( (IFRZ-3)) 752,753,752
```

PAGE 6

```
752 PARAM(17)=1.5
753 CONTINUE
    IFRZ=3
    CT=0.
    ST=CTO
    AMMAX=PEAKX-DPK*(PEAKX-PEAKN)
    GO TO 206
```

C MIN POINT

```
201 PEAKN=IPK*PKMST+JPK*PKLST
    GO TO (230,301,301,301,230,230),IFAM
301 IF (PEAKN-AMMAX) 230,230,202
230 IF (MNN) 232,232,231
231 IF (IDATA-IDAT2) 202,202,233
233 CONTINUE
    TPOLD=TP
    IDENT=IDENT+1
    ID1=ID
    ID=MOD(ID,2)+1
    IDO=MOD(ID-NMIN+1,2)+1
    IF (IFAM-6) 261,262,261
262 AMMX(IDO)=PEAKX
261 CONTINUE
    IF (NMIN-1) 263,263,264
264 CTO=-CTO
269 CONTINUE
    PTO=PTNR(IDO)
    AMXO=AMMX(IDO)
    AMNO=AMMN(IDO)
    AMX1=AMMX(ID1)
    AMMX(ID)=PEAKX
    PARAM(17)=1.5
    IMAX=JMAX
    KMAX=KMAX+JMAX
    JMAX=0
232 IFRZ=1
    IDAT2=IDATA+NWIND
    MNN=MNNO
    PTNO=IDATA-IROC*R10-LAG
    PTN1=PTNO+PTMAX
    TP=PTNO-PTO
```

PAGE 7

```
FE=FXTRP(TP,FE0)
IFE=FE*P15
CALL SICOS(IFE,ISIN,ICOS)
DS=ISIN*R14
DC=ICOS*R14
ITH=(IDATA-PTNO)*IFE
CALL SICOS(ITH,ISIN,ICOS)
ST=ISIN*R14*CTO
CT=ICOS*R14*CTO
S2T= ST*CT
PP=PEAKX-PEAKN
PPAN=PEAKX-(PEAKX+AMXO)*.5
SMAX=PEAKX-AMXO
SMIN=PEAKN-AMNO
DMAX=PEAKX-AMX1-AMX1+AMXO
PTMN(ID)=PTNO
AMN(ID)=PEAKN
GO TO 800
```

```
C
C
C IDENTIFICATION
C
C FAMILY IDENTIFICATION
C 400 CONTINUE
C
C PHASE ADJUST MODE
C JMODE = 2
  IF (JMODE=2) 401,402,401
402 PHASE=PHASE-GPHAS*SMIN
  TORQ(1)=SIN(PHASE)
  TORQ(2)=-COS(PHASE)
  NTQD=NTOMX
  IPT=IPT+1
  FIDNT(1,IPT)=PHASE
  FIDNT(2,IPT)=SMIN
  IF(IPT=150) 403,405,405
403 MODE=3
403 GO TO 890
401 CONTINUE
C
```

PAGE 8

IF (6-IFAM+KMAX) 491,192,491
491 CONTINUE
SMINP=SMIN
IDAT2=IDATA

C
PPN=PP/PEAKX
GO TO (511,510),NMIN
511 IF (PEAKN-AMAX) 512,513,513
512 IF (TP-TC1) 514,514,515
513 IF (TP-TA1) 514,514,516

C CHANGE NMIN 1 TO 2
514 NMIN=2
NMIN2=1
CTO=-CTO
CT=-CT
ST=-ST
TP=TPOLD
FE=FXTRP(TP,FEO)
IFE=FE*P15
CALL SICOS(IFE,ISIN,ICOS)
DS=ISIN*R14
DC=ICOS*R14
IDMAX=0
ISMAX=0
NANG=0
GO TO 471

C
510 IF (PEAKX-AMAX) 521,521,522
521 GO TO 524
524 TC2X=TC2+TC2*.25*PEAKX/AMAX
IF (TP-TC2X) 523,525,525
522 IF (PPN-AMAP) 526,526,627
627 IF (TP-TMAX) 527,504,504
526 IF (TP-TA2) 516,525,525
527 IF (IDMAX) 529,529,528
528 IF (ABS(DMAX)-EPOS) 530,530,523
529 GO TO (529,529,504,530,530,528),IFAM

C
C CHANGE NMIN 2 TO 1
525 NMIN=1

PAGE 9

```

TP=PTNG-PTMX(ID1)
FE=FXTRP(TP,FEQ)
IF (NIN2*IPHAS) 625,625,626
625 CTO=-CTO
626 IFE=FE*P15
CALL SICUS(IFE,ISIN,ICOS)
DS=ISIN*R14
DC=ICOS*R14
ITH=(IDATA-PTNG)*IFE
CALL SICUS(ITH,ISIN,ICOS)
ST=ISIN*R14*CTO
CT=ICOS*R14*CTO
MPAX=PEAKX=(PEAK+(AX-4*(ID1))*5
SVI=PEAKI=APX(ID1)
SMAX=PEAKX=APX(ID1)
GO TO 511

```

C IDENTIFY SPECIAL CASES

C TRANSITION ZONE

```

504 CONTINUE
IFAY6=IFAY-6
IFA=3
IIDE=3
ISLOP=1
IF (IFAY6) 442,545,442
442 IF (ISMAX) 444,444,443

```

C DETECT CROSSING OF THE SEPARATING POLYHED

```

443 IF (IDPHAS) 543,543,544
543 IF (ABS(SMAX)-EPDS) 444,444,150
544 IF (ABS(SMAX)-EPDVA) 530,530,444

```

C TRANSITION REGION

```

545 KSVIN=1
IF (ABS(SMAX)-EPDS) 444,444,234
444 CONTINUE
IF (IDPHAS) 460,460,450

```

C C-LOOP

515 IFAY=1

PAGE 10

DMAX=1.
SMIN=SMAX
GO TO 616

C
C C FAMILY
523 IFAM=2
C
C LOCATE +A AXIS
C C NBHD LOGIC
616 IDC=MOD(ID+NMIN,2)+1
CMAX=AMMX(IDC)-(AMMX(IDC)-PEAKN)*PPCN
IWIDE=0
NSLOP=0
IF (ISIGN) 617,617,618
617 IFAM=1
GO TO 621
618 IF (SMINP-EPSCN) 621,620,620
620 IFAM=2
SMIN=SMINP
621 IF (IDMAX) 450,450,234
C RESOLVE 180 DEG UNCERTAINTY
234 IF (IDMAX *SGN) 235,235,236
C LOW MAX (PHASE = 180 DEG)
235 CT=-ABS(CT)
ST=-ABS(ST)
CTO=-1
GO TO 237
C HIGH MAX (PHASE = 0 DEG)
236 CT=ABS(CT)
ST=ABS(ST)
CTO=1
237 IPHAS=1
STX=-CT
450 CONTINUE
C
C IDENTIFY +C OR -C FAMILY
IF (ISMIN) 470,470,451
451 IF (SMIN-EPSCN) 452,452,453
452 IF (ISIGN) 454,454,150
454 SGN=-SGN

Copy available to DDC does not
permit fully legible reproduction.

PAGE 11

CTO=-CTO

CT=-CT

ST=-ST

STX=-STX

IDMAX=0

KDMAX=2

ISMAX=0

KSMAX=2

ISMIN=0

KSMIN=2

453 ISIGN=1

GO TO 470

C

C

C A NHD

516 IFAY=5

IF (IDMAX) 946,946,947

946 NALG=NTGX*TP/2

GO TO 460

947 NPP=PP

PP=PP+AS*AX*TP/(2*IDMAX)

C

C *****

IF (PP) 265,266,266

265 PP=0.

GO TO 927

266 CONTINUE

IF (INVIN-1) 927,927,928

927 INVID=1

928 CONTINUE

PPK=PP/PEAKA

C

C PROPORTIONAL CONTROL GAINS

IF (INVID=ISPAK) 921,945,972

922 RPP=SQRT(PPK)

NALG =GPAK2*RPP

CT1=CTO

GO TO 923

945 IGPAK=3

DTNC=NALGGO/(2.*GPAK2)

PAGE 12

```
GPAN1=0.
921 NANG =GPAN1*PPN
    IF (NMIN-1) 943,943,923
943 CTO=CT1
923 CONTINUE
C *****
C
    IF (IMAX) 938,938,941
941 IF (NANG-NANG) 936,939,939
936 IF (PTNO-IDAT1-TP) 938,937,937
938 NANG=0
    GO TO 940
939 ASMAX=ASMAX+GSLOP*(SMAX/TP-ASMAX)
    PP=PPO+ASMAX*TP/(2*NMIN)
    NSLOP=0
    GO TO 942
937 ASMAX=SMIN/TP
    PP=PPAN
    NSLOP=ASMAX*CSLOP
    IF (GPAN1) 944,944,942
944 GPAN1=GPAN2/(DTHC+SQRT(DTHC*DTHC+PP/PEAKX))
942 CONTINUE
C *****
C
    IF (PP) 1265,1266,1266
1265 PP=0.
    GO TO 1927
1266 CONTINUE
    IF (NMIN-1) 1927,1927,1928
1927 IWIDE=1
    NSLOP=NSLOP+NSLOP
1928 CONTINUE
    PPN=PP/PEAKX
C
C PROPORTIONAL CONTROL GAINS
    IF (NMIN-IGPAN) 1921,1921,1922
1922 RPP=SQRT(PPN)
    NANG =GPAN2*RPP
    GO TO 1923
C
```

PAGE 13

1921 NANG =GPAN1*PPN

1923 CONTINUE

C *****

C

NF1=NF2

NF2=1

IF ((PPN-PPF)*[PHAS] 930,931,931

930 NF2=0

931 IF(NMIN=1) 934,934,935

934 NF1=NF2

935 IF (NF1+NF2) 932,932,933

C DAMPING COMPLETE

932 MODE=MODEC

MODEC=3

GO TO 940

933 MODEC=2

940 CONTINUE

IDAT2=IDATA+NMIN

NANG=NANG

GO TO 460

C

C A FAMILY

530 IFAN=4

INIDE=0

NSLOP=0

C

C

460 IF (ISIN) 463,463,466

466 IF (IPHAS) 468,468,467

C TORQUE OUT OF A FAMILY

468 IF (ISIN+EPSAN) 463,462,462

C PREVENT PHASE LOSS IN A NBHD

467 IF (ISIN+EPSAN) 465,463,463

465 GPAR2=GPAN2*.5

GPAN1=GPAN1*.5

ISGAN=1

C 180 DEG PHASE SHIFT TO UNDAMP A

462 CT=-CT

ST=-ST

CTO=-CTO

PAGE 14

```
      ISMIN=0
      KSMIN=4
463 CONTINUE
C
470 CONTINUE
      NMIN2=0
471 CONTINUE
C SET TA1 AND TA2
      ATP=ATP+GTP*(TP-ATP)
      IF (ATP-TA20) 474,474,475
475 ATP=TA20
474 IF (ATP-TA10) 472,473,473
472 ATP=TA10
473 TA1=ATP*.75
      TA2=ATP*1.25
      IFAMO=IFAM
      IF (PP-PPFLT) 561,562,562
561 JGAIN=15
      LAG=4.5
      GO TO 563
562 JGAIN=12
      LAG=.5
563 CONTINUE
C SET FLAGS
      KDEL=3-NMIN
      IDMAX=0
      IF (KDMAX) 601,601,602
601 IDMAX=1
602 KDMAX=KDMAX-KDEL
      IF (KSMAX) 603,603,604
603 ISMAX=1
604 KSMAX=KSMAX-KDEL
      IF (KSMIN) 605,605,606
605 ISMIN=1
606 KSMIN=KSMIN-KDEL
C
C
C DUMP DATA
C
791 ISGN=SGN
```

PAGE 15

```
      ICTO=CTO
      ATORK=NANG
      ATORK=ATORK/NTQMX
      PSMAX=ASMAX*1000.
      IF (NPR.NT) 915,915,916
915  CONTINUE
      IF ((IFAM=5) 911,912,911
911  WRITE (1,3001) IDATA, IFAM, NMIN, IPHAS, IDMAX, ISMAX, ISMIN, ISGN, ICTO,
      X TP, PEAKN, PEAKX, PP, DMAX, SMAX, SMIN
3001  FORMAT(16,8I2,F8.2,10F8.5)
      GO TO 913
912  WRITE (1,3002) IDATA, IFAM, NMIN, IPHAS, IDMAX, ISMAX, ISMIN, ISGN, ICTO,
      X TP, PEAKN, PEAKX, PP, PSMAX, SMAX, SMIN, GPAN1, ATORK
3002  FORMAT(16,8I2,F8.2,2F8.5,E9.2,3F8.5,2E9.2)
      GO TO 913
916  IPT=IPT+1
      IF (IPT=150) 919,919,920
920  NPT=IPT
      IPT=1
919  CONTINUE
      ID NT(1,IPT)=IDATA
      ID NT(2,IPT)=IFA
      ID NT(3,IPT)=NMIN
      ID NT(4,IPT)=IPHAS
      ID NT(5,IPT)=IDMAX
      ID NT(6,IPT)=ISMAX
      ID NT(7,IPT)=SMIN
      ID NT(8,IPT)=ISGN
      ID NT(9,IPT)=ICTO
      FIDNT(1,IPT)=TP
      FIDNT(3,IPT)=PEAKX
      FIDNT(4,IPT)=PP
      FIDNT(6,IPT)=SMAX
      FIDNT(7,IPT)=SMIN
      IF ((IFAM=5) 917,918,917
917  FIDNT(2,IPT)=PEAKN
      FIDNT(5,IPT)=DMAX
      GO TO 913
918  FIDNT(2,IPT)=ATORK
      FIDNT(5,IPT)=PSMAX
```

PAGE 16

```
913 CONTINUE
C
C CONTROL
C
800 CONTINUE
    IF (JMODE-2) 881,890,881
881 CONTINUE
    NTQD=NTQMX
    CP=CT
    SP=ST
    GO TO (801,802,803,804,805,806),IFAM
C C NBHD
801 IF (AHH-CMAX) 806,811,811
811 IC=BD=1
C C FAMILY
802 TORQ(1)=-S GN
    TORQ(2)=0.
    GO TO 890
C TRANSITION
803 IF (SGN*STX) 806,806,813
813 TRAN=.625-.125*ABS(CP)
    TORQ(1)=(CP-SGN)*TRAN
    TORQ(2)=SP*TRAN
    GO TO 890
C A FAMILY
804 TORQ(1)=CP
    TORQ(2)=SP
    GO TO 890
C A NBHD
805 NDANG=ANG-(INTQ*(NTQ+1))/2
    NTQD=NTQ
    IF (NDANG) 816,817,818
816 NTQD=NTQD-1
    IDAT1=IDATA
    GO TO 817
818 IF (ADANG-NTQ) 817,819,819
819 IF (INTQ-NTQMX) 820,817,817
820 NTQD=NTQD+1
817 NANG=NANG-NTQD
    IF (NANG) 821,822,822
```

Copy available to DDC does not
permit fully legible reproduction

PAGE 17

```
821 NANG=0
822 TORQ(1)=CP
    TORQ(2)=SP
    GO TO 890
C  UNDETERMINED FAMILY
806 NTQD=0
    IF (ICNRD) 827,827,826
826 CMAX=1.
    ICNRD=0
    IDAT2=IDATA+NWIND
827 CONTINUE
    IF (IFAMU-3) 802,813,804
C  RATE LIMITED TORQUE
890 IF (TORQ(1)*TORQ1+TORQ(2)*TORQ2) 897,895,895
897 IF (NTQ) 894,895,894
894 TORQ(1)=-TORQ(1)
    TORQ(2)=-TORQ(2)
    NTQD=0
    GO TO 896
895 TORQ1=TORQ(1)
    TORQ2=TORQ(2)
896 IF (NTQ-NTQD) 891,892,893
891 NTQ=NTQ+1
    GO TO 892
893 ATQ=NTQ-1
892 CONTINUE
    RETURN
C
C  DUMP DATA
340 IF (NPT-IPT) 341,342,342
341 NPT=IPT
342 CONTINUE
    DO 350 I=1,NPT
    IF (JMODE-2) 343,344,343
344 WRITE(1,3004) FIDNT(1,I),FIDNT(2,I)
3004 FORMAT(2F8.5)
    GO TO 350
343 CONTINUE
    IF (ID NT(2,I)-5) 351,352,351
351 WRITE(1,3001)((ID NT(J,I),J=1,9),(FIDNT(K,I),K=1,7))
```

PAGE 18

```
GO TO 350
352 WRITE(1,3003)((ID NT(J,I),J=1,9),(FIDNT(K,I),K=1,7)
3003 FORMAT(16,8I2,FP,2,F8.3,F8.5,E9.2,4F8.5,2E9.2)
350 CONTINUE
WRITE (1,3005) IDATA
3005 FORMAT ('DAMPING TIME', 16)
RETURN
END
```

FEATURES SUPPORTED
ONE WORD INTEGERS

CORE REQUIREMENTS FOR CNTRL
CONVX 62 VARIABLES 3712 PROGRAM 3312

RELATIVE ENTRY POINT ADDRESS IS 0ED5 (HEX)

END OF COMPILATION

REFERENCES

1. C70-972/201, Micro-Electrostatically Suspended Gyro (MESG) Fast Reaction Study, August 1970, Unclassified.
2. Tou, Julius T., "Modern Control Theory," McGraw-Hill, Inc. New York, 1964.

DISTRIBUTION LIST

DD Center, Attn: 10C-10A 2 copies
Cameron Sta. Bldg 5
Alexandria, Va 22314

Commander 1 copy
Naval Elect. Lab Center
Attn: Library
San Diego, Ca 92152

AFAL 1 copy
Attn: AFAL/DOT, STINFO,
WPAFB, Oh 45433

Capt. R. R. Warzynski 1 copy
AFAL/NVA-666A
Wright-Patterson AFB, Ohio

Ofc Asst. Sec of the Army (R&D) 1 copy
Attn: Asst for Research
Room 3-E-379, The Pentagon
Washington, D.C. 20310

Hq DA (DAIRD-ARP/ 1 copy
Dr. R. Watson)
Washington, D.C. 20310

CG, U. S. Army Missile Command 1 copy
Redstone Scientific Info Center
Attn: Chief, Document Sec.
Redstone Arsenal, Ala 35809

Commanding Officer, 1 copy
Picatinny Arsenal,
Attn: SMUPA-TV1
Dover, N.J. 07801

Commanding General 2 copies
U. S. Army Electronic Command
Ft. Monmouth, N.J. 07703
Attn: AMSEL-MS-T1

A15ABE - Commanding General 4 copies
U. S. Army Electronic Command
Bldg 2504
Ft. Monmouth, N.J. 07703
Attn: AMSEL-VL-NS
Mr. Ray Clark

UNCLASSIFIED

SECURITY CLASSIFICATION OF THIS PAGE (When Data Entered)

REPORT DOCUMENTATION PAGE		READ INSTRUCTIONS BEFORE COMPLETING FORM
1. REPORT NUMBER ECOM-0230-F	2. GOVT ACCESSION NO	3. RECIPIENT'S CATALOG NUMBER
4. TITLE (and Subtitle) Automatic Polhode Damping Investigation for Micro Electrostatic Gyro		5. TYPE OF REPORT & PERIOD COVERED Final Technical Report 1 July 1972 through 23 May 1973
7. AUTHOR(s) John C. Wauer		6. PERFORMING ORG. REPORT NUMBER
9. PERFORMING ORGANIZATION NAME AND ADDRESS Rockwell International Autonetics Division, 3370 Miraloma Avenue Anaheim, California		8. CONTRACT OR GRANT NUMBER(s) DAA B07-72-C-0230
11. CONTROLLING OFFICE NAME AND ADDRESS Fort Monmouth Procurement Branch United States Army Electronics Command Fort Monmouth, New Jersey		10. PROGRAM ELEMENT, PROJECT, TASK AREA & WORK UNIT NUMBERS
14. MONITORING AGENCY NAME & ADDRESS (if different from Controlling Office)		12. REPORT DATE June 1973
		13. NUMBER OF PAGES 156
		15. SECURITY CLASS. (of this report) Unclassified
		15a. DECLASSIFICATION/DOWNGRADING SCHEDULE
16. DISTRIBUTION STATEMENT (of this Report) Distribution limited to U.S. Government agencies only. Test and evaluation, June 1973. Other requests for this document must be referred to Commanding General U.S. Army Electronics Command: Attn: AMSEL-VI-N-S, Ft. Monmouth, N.J. 07703.		
17. DISTRIBUTION STATEMENT (of the abstract entered in Block 20, if different from Report)		
18. SUPPLEMENTARY NOTES		
19. KEY WORDS (Continue on reverse side if necessary and identify by block number) Automatic Polhode Damping, Polhode Motion, Polhode Period, Electrostatically Suspended Gyro, Herpolhode, Conformal Mapping, Target Return		
20. ABSTRACT (Continue on reverse side if necessary and identify by block number) A computer program for automatically damping the polhode motion of the Micro-Electrostatically Suspended Gyro (MESG) is presented. Test results are presented that demonstrate successful automatic polhode damping on two gyros. The fundamental characteristics of polhode motion of the MESG rotor are summa- rized. The techniques for monitoring polhode motion using Mass Unbalance Modulation (MUM) are described. The polhode torquing equation is derived and the spin motor control electronics that implement the torquing equation are described.		